

**T.C.
ISTANBUL AYDIN UNIVERSITY
INSTITUTE OF GRADUATE STUDIES**



**CONTROL DIFFERENT ELECTRIC LOADS ON MORE ELECTRIC
AIRCRAFT**

THESIS

Abdel Rahman BEYROUTI

**Department of Electrical & Electronic Engineering
Electrical and Electronics Engineering Program**

June, 2020

T.C.
ISTANBUL AYDIN UNIVERSITY
INSTITUTE OF GRADUATE STUDIES



**ANALYSIS AND MITIGATION OF POWER QUALITY ISSUES IN
DISTRIBUTED GENERATION SYSTEMS USING CUSTOM POWER
DEVICES**

THESIS

Abdel Rahman Beyrouti

(Y1813.300027)

Department of Electrical & Electronic Engineering
Electrical and Electronics Engineering Program

Thesis Advisor: Prof. Dr Murtaza FARSADI

June, 2020

DEDICATION

I hereby declare that all information in this thesis document has been obtained and presented in accordance with academic rules and ethical conduct. I also declare that, as required by these rules and conduct, I have fully cited and referenced all material and results, which are not original to this thesis.

Abdel Rahman BEYROUTI



FOREWORD

I would first like to thank my family, my father Bilal, and mother Rima, who have always been supportive and encouraging; they raised me to become the right person and a positive member of society. They were patient with me through good and better days, and everything I have accomplished is because of their effort. I hope I can make them happy in return for all they have done for me and also my brother Souhayb and sister Sara for all the support and encouragement. I would like to thank my thesis advisor Prof. Dr Murtaza Frasadi, of the Electric and Electronic Engineering department at Istanbul Aydin University. The door to Prof. Murtaza Frasadi's office was always open whenever I ran into a trouble spot or had a question. I would like to thank all my teachers for having a significant influence on me, and I would also like to thank Department of Electric and Electronic Engineering and also Istanbul Aydin University and its library for providing me with access to all the books and articles that I needed to finish this work

June, 2020

Abdel Rahman BEYROUTI

CONTROL DIFFERENT ELECTRIC LOADS ON MORE ELECTRIC AIRCRAFT

ABSTRACT

In the development of technology in the last centuries, many scientists start to focus on developing an electrically powered system to boost the performance and reliability of tomorrow's aircraft. Utilising the MEA achieves numerous advantages such as high reliability. They also save weight since different systems can share the same computers and electronics; lower pressure translates into reducing fuel burn and higher payload capacity. At the same time, energy consumption is reduced by more carefully controlling the allocation of resources using artificial intelligence; these lead to cut maintenance costs and increase dispatch reliability because electrical systems are faster and easier to repair. Moreover, the MEA reduces the emission of air pollutant gases from the aircraft, which can contribute to solving the problem of climate change. However, the MEA put some difficulties on the aircraft's electrical system. The challenges could be either in the amount of the required Power or management of this Power. Most of these applications need fast and smart speed control system. This thesis aims to develop methods for the design and evaluation of future electric propulsion aircraft, to use artificial controllers instead of the traditional controller. One of the efficient artificial controllers that have been gaining popularity in recent years is Fuzzy logic controllers. Using a fuzzy logic controller shapes human decision processing with a set of fuzzy rules. Compared to other control methods, such as the proportional integral derivative (PID) controller with pulse width modulation (PWM), FLC has gained extraordinary interest both in academia and industry over the past decades. This is true essentially because FLC can be applied in many different processes. In this thesis, the FLC is used for the control of different electric loads on aircraft. The controller aims to minimise the error and achieved the desired results by reducing the output error (the difference between output and a reference wanted values).

Keywords: *More electric aircraft; fuzzy logic controller; robustness*

DAHA ELEKTRİKLİ UÇAKTA KONTROL FARKLI ELEKTRİK YÜKLERİ

ÖZET

Son yüzyıllarda teknolojinin geliştirilmesinde, birçok bilim adamı yarının uçaklarının performansını ve güvenilirliğini artırmak için elektrikle çalışan bir sistem geliştirmeye odaklanıyor. MEA'nın kullanılması, yüksek güvenilirlik gibi sayısız avantaj sağlar. Farklı sistemler aynı bilgisayarları ve elektroniği paylaşabildikleri için ağırlıktan da tasarruf ederler; düşük basınç yakıt yakımını azaltmaya ve daha yüksek taşıma kapasitesi anlamına gelir. Aynı zamanda, yapay zeka kullanarak kaynakların tahsisini daha dikkatli kontrol ederek enerji tüketimi azaltılır; bu da elektrik sistemlerinin onarımının daha hızlı ve kolay olması nedeniyle bakım maliyetlerini düşürür ve sevkiyat güvenilirliğini artırır. Ayrıca, MEA hava kirletici gazların hava taşıtlarından emisyonunu azaltır, bu da iklim değişikliği sorununun çözümüne katkıda bulunabilir. Bununla birlikte, MEA, uçağın elektrik sisteminde gerekli güç miktarında veya bu gücün işlenmesi ve yönetiminde bazı zorluklar ortaya koymuştur. Bu uygulamaların çoğunun hızlı ve akıllı hız kontrol sistemine ihtiyacı vardır. Bu tezin amacı, gelecekteki elektrikli sevk uçaklarının tasarımı ve değerlendirilmesi için yöntemler geliştirmek, geleneksel kontrolör yerine yapay kontrolörler kullanmaktır. Son yıllarda popülerlik kazanan verimli yapay kontrolörlerden biri Bulanık mantık kontrolörleri. Bulanık mantık denetleyicisi kullanmak, insan karar işlemeyi bir dizi bulanık kuralla şekillendirir. Darbe genişliği modülasyonlu (PWM) oransal integral türevi (PID) kontrolör gibi diğer kontrol yöntemleriyle karşılaştırıldığında FLC, son on yılda hem akademiye hem de endüstride olağanüstü ilgi gördü. Bu esasen doğrudur çünkü FLC birçok farklı işlemde uygulanabilir. Bu tezde, FLC, uçak üzerindeki farklı elektrik yüklerinin kontrolü için kullanılmaktadır. Kontrolör, hatayı en aza indirmeyi ve çıkış hatasını (çıkış ile referans istenen değerler arasındaki fark) azaltarak istenen sonuçları elde etmeyi amaçlar.

Anahtar Kelimeler: *daha elektrikli uçak; bulanık mantık denetleyicisi; sağlamlık.*

TABLE OF CONTENTS

| | |
|--|------------|
| FOREWORD | iv |
| ABSTRACT | v |
| ÖZET | vi |
| TABLE OF CONTENTS | vii |
| ABBREVIATIONS | ix |
| LIST OF TABLES | xi |
| LIST OF FIGURES | xii |
| I. INTRODUCTION | 1 |
| A. Difficulties And Challenges Designing MEA..... | 4 |
| B. Main Objectives | 4 |
| C. Structure Of Work..... | 5 |
| II. HISTORY OF MEA | 6 |
| A. Electric Flight In History | 6 |
| B. Design Methods Of Electric Propulsion Aircraft..... | 11 |
| III. ELECTRIC DESIGN OF MEA | 14 |
| A. Power Generation..... | 15 |
| 1. DC Power Generation | 15 |
| 2. AC Power Generation | 16 |
| 3. Producing Power In case of Emergency | 18 |
| 4. Power Generation Control | 21 |
| 5. Advanced AC Electrical Power Generation Types | 25 |
| B. Primary Power Distribution | 29 |
| 1. Different Components..... | 30 |
| 2. Electrical Power Transmission..... | 38 |
| C. Secondary Power Distribution | 43 |
| 1. Electric Motors..... | 47 |
| 2. Lighting | 56 |

| | |
|---------------------------------------|-----------|
| IV. PROPOSED MEA DESIGN..... | 58 |
| A. Generators | 58 |
| 1. Integrated Drives | 59 |
| 2. VSCF Cyclo-Converter..... | 59 |
| 3. VSCF DC Link..... | 61 |
| B. Primary Power Distribution | 61 |
| C. Secondary Power Distribution | 62 |
| D. Transformer Rectifier Unit..... | 63 |
| E. AC Pump..... | 64 |
| 1. Structure For PIFLC..... | 65 |
| 2. Design For PIFLC | 66 |
| 3. Membership Functions..... | 67 |
| 4. Scaling Factors | 67 |
| 5. The Rule Base | 68 |
| F. AC Lamps | 68 |
| G. Actuators | 69 |
| V. SIMULATION RESULTS | 71 |
| A. AC Pump..... | 71 |
| 1. PI Controller..... | 73 |
| 2. STFLPI Controller | 83 |
| B. Actuators | 89 |
| VI. CONCLUSION..... | 93 |
| A. Summary | 93 |
| B. Outlook..... | 93 |
| VII. References | 94 |
| RESUME..... | 98 |

ABBREVIATIONS

| | |
|--------------|---|
| AEA | : All Electric Aircraft |
| BMS | : Battery Management System |
| BPCU | : Bus Power Controller Unit |
| BTB | : Bus Tie Breakers |
| CCB | : Converter Control Breaker |
| CF | : Constant Frequency |
| CSD | : Constant Speed Drive |
| ECS | : Environmental Control System |
| ELMS | : Electrical Loads Management System |
| FLC | : Fuzzy Logic Controller |
| EPC | : External Power Contactor |
| ETOS | : Extended Twin Operation System |
| FADEC | : Full Authority Digital Engine Control |
| GCB | : Generator Controller Breaker |
| GCU | : Generator Controller Unit |
| HTS | : High Temperature Superconducting |
| IDG | : Integrated Motor Generator |
| MEA | : More Electric Aircraft |
| PMAD | : Power Management and Distribution |
| PMSM | : Permanent Magnet Synchronous Motor |
| PI | : Proportional Integral |
| PID | : proportional integral derivative |

STFLPIC : Self Tuning Proportional Integral Fuzzy Logic Controller
TRU : Transformer Rectifier Unit
VF : Variable Frequency
VSCF : Variable Speed Constant Frequency
WAI : Wing Anti-Icing



LIST OF TABLES

| | |
|---|----|
| Table 1: The Taurus” with “e-Genius” | 10 |
| Table 2: Recent civil & military aircraft power system developments..... | 28 |
| Table 3: Conductor Temperature Characteristics | 40 |
| Table 4: FLC Rules | 53 |
| Table 5: Scaling Factor α | 68 |
| Table 6: Induction Motor Parameters | 71 |
| Table 7: Five-Phase PMSM Parameters | 72 |
| Table 8: Speed Comparison Between Induction Motor And Five-Phase PMSM (PI Controller) | 77 |
| Table 9: Torque Comparison Between Induction Motor And Five-Phase PMSM (PI Controller) | 82 |
| Table 10: STFLPI Controller Parameters | 83 |
| Table 11: Speed Comparison Of Five-Phase PMSM between (PI Controller) And (STFLPI)..... | 87 |
| Table 12: Torque Comparison Of Five-Phase PMSM Between (PI Controller) And (STFLPI)..... | 88 |
| Table 13: Three-Phase PMSM Parameters | 90 |
| Table 14: PI Controller Parameters..... | 91 |
| Table 15: STFLPI Controller Parameters | 91 |

LIST OF FIGURES

| | |
|---|----|
| Figure 1: Power Systems On A Traditional Aircraft | 3 |
| Figure 2: "La France" | 6 |
| Figure 3: Hb-3 First Electric Aeroplane..... | 7 |
| Figure 4: Solair I | 7 |
| Figure 5: Antares 20e | 8 |
| Figure 6: The "Electraflyer." | 8 |
| Figure 7: "Taurus" (1st) | 9 |
| Figure 8: "E-Genius" (2nd)..... | 10 |
| Figure 9: "Voltair" Electric Aircraft..... | 13 |
| Figure 10: Ac Electrical System In The Aircraft | 14 |
| Figure 11: Shunt-Wound DC Generator | 15 |
| Figure 12: DC Voltage Regulator | 16 |
| Figure 13: The Improved AC Generator | 17 |
| Figure 14: Three-Phase Generator Connected In Star Configuration..... | 18 |
| Figure 15: RAT | 19 |
| Figure 16: RAT Employed On MEA..... | 19 |
| Figure 17: Three-Phase PMG With Converter..... | 21 |
| Figure 18: Boeing 777 PMG/PMA Complement..... | 21 |
| Figure 19: DC Generator Parallel Operation | 23 |
| Figure 20: AC Generator Parallel Operation | 24 |
| Figure 21: Electrical Power Generation Types | 25 |

| | |
|--|----|
| Figure 22: Constant Frequency / IDG Generation | 26 |
| Figure 23: Variable Frequency Power Generation..... | 27 |
| Figure 24: VSCF Power Generation | 27 |
| Figure 25: Power Contactor | 29 |
| Figure 26: ‘Smart Contactor..... | 30 |
| Figure 27: Basic Motor Inverter..... | 31 |
| Figure 28: Transformer Rectifier Unit (TRU) | 32 |
| Figure 29: Basic Battery Cell Schematic..... | 33 |
| Figure 30: Standard Potential And Density Of Electrode Elements [35]..... | 34 |
| Figure 31: C-Rate Effect On Discharge Characteristics [36]..... | 35 |
| Figure 32: Temperature Effect On Discharge Characteristics [36]..... | 36 |
| Figure 33: Cycle Durability Of A Li-Ion Cell [36]..... | 37 |
| Figure 34: Main heat sources of a battery cell, based on [36] | 37 |
| Figure 35: Single Line Conductor..... | 39 |
| Figure 36: Aluminium Cable Losses | 41 |
| Figure 37: Copper Cable Losses | 41 |
| Figure 38: HTS Cable Construction..... | 43 |
| Figure 39: IGBT Weight VS Power..... | 44 |
| Figure 40: Solid-State Switch Models [39]..... | 45 |
| Figure 41: IGBT Module | 45 |
| Figure 42: IGBT Voltage Drop U_{drop} VS Blocking Voltage U_{block} | 46 |
| Figure 43: Ideal Electric Motor Characteristics [39] | 47 |
| Figure 44: Speed Control Of The PMSM | 51 |
| Figure 45: FLC Structure | 52 |
| Figure 46: FLC Membership Function Of Fuzzy Logic Controller For E , CE , And ΔI_q | 53 |

| | |
|--|---|
| Figure 47: Schematic Diagram Of A Five-Phase Voltage Source Inverter | 55 |
| Figure 48: Fundamental Switching Voltage Vectors | 56 |
| Figure 49: Harmonic Switching Voltage Vectors | 56 |
| Figure 50: Typical MEA Design..... | Hata! Yer işareti tanımlanmamış. |
| Figure 51: Integrated Drive Generator | 59 |
| Figure 52: VSCF Cyclo-Converter System..... | 60 |
| Figure 53: VSCF Cyclo-Converter Generator | 60 |
| Figure 54: VSCF DC Link | 61 |
| Figure 55: AC/AC Inverter | 61 |
| Figure 56: GCU | 62 |
| Figure 57: Secondary Power Distribution..... | 63 |
| Figure 58: TRU System | 64 |
| Figure 59: Five-Phase PMSM System | 65 |
| Figure 60: Block Diagram Of STFLPI Controller | 67 |
| Figure 61: Membership Functions Of STFLPI Controller For α | 68 |
| Figure 62: AC Lamps..... | 69 |
| Figure 63: Primary Flight Control..... | 70 |
| Figure 64: Actuators..... | 70 |
| Figure 65: Speed Comparison Between Induction Motor And Five-phase PMSM... | 73 |
| Figure 66: First Stage Reference Speed $W^*=307$ | 74 |
| Figure 67: Second Stage Reference Speed $W^*=376$ | 75 |
| Figure 68: Third Stage Reference Speed $W^*=330$ | 75 |
| Figure 69: Fourth Stage Reference Speed $W^*=365$ | 76 |
| Figure 70: Fifth Stage Reference Speed $W^*=342$ | 77 |
| Figure 71: Torque Comparison Between Induction Motor And Five-Phase PMSM | 78 |
| Figure 72: First Stage Reference Torque $Te^*= 17$ nm..... | 78 |

| | |
|--|----|
| Figure 73: Second Stage Torque Reference $T_e^*= 21 \text{ nm}$ | 79 |
| Figure 74: Third Stage Torque Reference $T_e^*=18 \text{ Nm}$ | 80 |
| Figure 75: Fourth Stage Torque Reference 20 Nm | 80 |
| Figure 76: Fifth Stage Torque Reference 19 nm | 81 |
| Figure 77: Stator Current Comparison Between Induction Motor And Five-Phase PMSM | 83 |
| Figure 78: Flight Cycle On MEA Using STFLPI Controller..... | 84 |
| Figure 79: First Stage Reference Speed $W^*=307$ | 85 |
| Figure 80: Second Stage Reference speed $W^*=376$ | 85 |
| Figure 81: Third Stage Reference Speed $W^*=330$ | 86 |
| Figure 82: Fourth Stage Reference Speed $W^*=365$ | 86 |
| Figure 83: Fifth Stage Reference Speed $W^*=342$ | 86 |
| Figure 84: Torque Using STFLPI Controller..... | 87 |
| Figure 85: Consuming Current Using STFLPI Controller..... | 88 |
| Figure 86: Comparing Actuator Speed Using PI And STFLPI Controller | 91 |
| Figure 87: Comparing Actuator Speed Using PI And STFLPI Controller At Steady | 92 |

I. INTRODUCTION

As concerns about global warming continue, air transport industries are beginning to face many challenges. The industrialised countries began to search for ways to reduce the crisis of global warming by reducing toxic gas emissions. Therefore, the best solution is to develop renewable energy to get environmentally friendly energy sources. An example adopted by the European Union is the formation of the European air traffic within the European Union Emission Trading Scheme (European Commission, 23 April 2009). Consequently, the European flying manufacturers have accepted to decrease toxic emissions from aircraft, as described in ACARE 2020 and “Flightpath 2050” (Commission, 2011), which included reducing carbon dioxide emissions by 75% per passenger-km until the middle of this century. However, it is difficult to achieve this goal by improving the structures of aircraft and combustion engines. An alternative energy source must be adopted to achieve this goal admirably.

Another challenge that the aircraft industry faces is the cost of petroleum and its availability, primarily a source of Jet fuel. During earlier decades, the rate of crude oil consumption has increased. With political instability in the producing countries, it is difficult to predict the price of crude oil because the factors of economics affect its growing—some optimistic studies about oil prices in the long term 2030 estimated at 130\$ a barrel (S.A.S, 2013). In contrast, the International Monetary Fund, otherwise expected, assumes a fuel cost around 300 \$. Therefore, it will have a critical influence on airline company designs (Kumhof & Muir, 2012).

In the principle of aircraft, automobile manufacturing challenges many difficulties in the aviation industry since they engage in its dependence on fossil fuel combustion. To overcome these difficulties is to rely on hybrid and fully electric cars that work via the battery, and this leads to lower emissions during operation. The most significant example of adopting an electric vehicle is what the German government was taken by targeting a million electric cars in the streets by the end of the year 2020 (Bundesregierung, 2009). The resulting need is dependent on light batteries and highly

efficient electric motors that do not consume large amounts of energy. In this context, studies and research have increased to improve the performance of electric motors.

In these circumstances, the main question for the flying industry is: Can the performance of electric motors be improved through the support of artificial intelligence? Till now, the electric motors suffer from a high-performance deficiency due to their adoption of the traditional control. Consequently, the electric-powered planes are still facing some restrictions on the modest pilot and global flight implementation. Nevertheless, the increase under global laws demands to reduce emissions from air traffic. Therefore, the implementation of the electric aircraft applications will appear in the coming transportation emergency as an option that will be used in the shortest time.

In recent years, scientists have increased interest in improving and developing the aircraft industry either in civil or military sectors. The use of aircraft around the world is growing significantly. Some commercial aircraft operate with weights above 300,000 kg and can even fly up to 16,000 km per flight without stopping at a speed of 1,000 km per hour (AbdElhafez & Forsyth, May 2009). Passenger traffic has increased at an average of 5.9% per year between 1988 and 1997. It has happened despite a dip in 1991 caused by the Gulf War and subsequent terrorism threats (Provost, 2002). The aircraft is like any vehicle that requires auxiliary power to operate its windshield wipers, dome light, and electric windows. Four kinds of power are applied to operate on today's aircraft: pneumatic, mechanical, hydraulic, and electrical. They give the necessary ability for flight control to control energy generation by engines and generators. Also, it runs the aircraft configuration, such as the actuation of landing gears and brakes. Additionally, they work to secure traveller comfort and assistance that including to run the air-conditioning and pressurisation. (Moir & Seabridge, 2001).

The primary source of general aircraft is from the gas turbine engines, as shown in Figure 1. The hydraulic power is provided by the mechanical rotation produced by the engine gearbox using the hydraulic pumps. This power feeds many loads on the plan, covering the operations during the flight, such as the actuators that used for flight direction, braking the plane, landing gear extension/retraction, and open the doors. The pneumatic energy is derived from the engine compressors, which used to power the environmental control system (ECS) and provided hot air for Wing Anti-Icing (WAI).

The mechanical power is obtained by a driven shaft from the generator and distributed to a gearbox for operating the lubrication pumps, fuel pumps, and hydraulic pumps. The electrical powers used to power the avionics, cabin and aircraft lighting, galleys, and electric motors (Rosero, Ortega, & Romeral, march 2007).

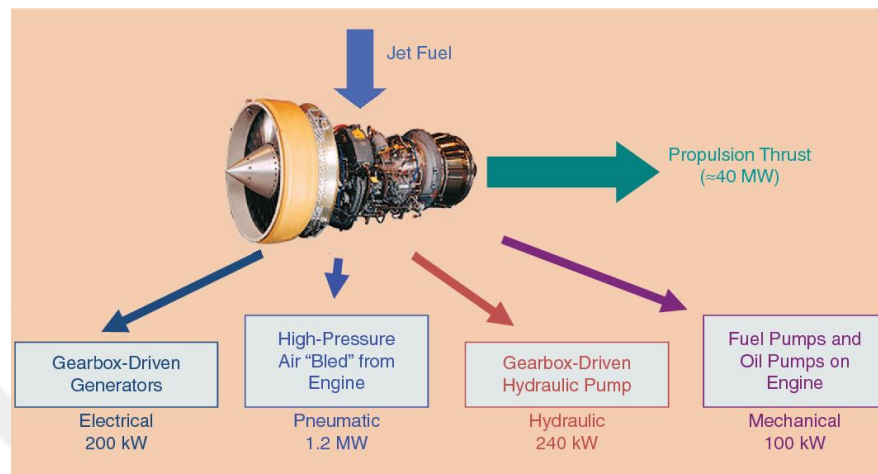


Figure 1: Power Systems On A Traditional Aircraft

When all these energies are combined into one system, this system becomes very complex and difficult to control well, and the interactions between the different parts impair performance and efficiency to the entire system. For example, any exposure to any slight leakage in the pneumatic or hydraulic system causes a network failure, and the aircraft operate not efficiently. Moreover, finding the leak is generally difficult to locate and repair since it cannot be reached easily. This exposure leads to either a flight delay or makes the aircraft out of control. Additional to that, The increased use of electrical and electronic features devices, passenger comfort and safety, has led to increasing the electrical loads in the aircraft. Some of these loads used to cool the generators, cables, motors, and navigation tools (Rajashekara, june 2014). In addition to that, the plane consumes much fuel, which will be executed over time. Therefore it leads to pollution of nature.

There has been significant progress in the use of more electric aircraft (MEA) to overcome these problems. The concept of electric aircraft production has been used for more than 30 years (Buticchi, Bozhko, Liserre, Wheeler, & Al-Haddad, 2018). The scientists and researchers have begun to replace some of the power generations, such

as hydraulic, mechanical, and pneumatic Power with electrical systems (Sarlioglu & Morris, June 2015). The research and studies have begun to increase to support the use of transport electrification. Many causes have driven this purpose, including the push for the decrease in pollution (often imposed by international agreements), the analysis for better performance, and the development of the technology. Furthermore, because of the sharp rise in fuel prices and its depletion with time, it was the main reason for this transformation.

A. Difficulties And Challenges Designing MEA

Aircraft configuration is defined by a relationship connecting the primary sources to operate the aircraft with the required efficiency. Moreover, to accomplish the most suitable performance, every region optimised concerning the overall performance of the aircraft. With the addition of the electric propulsion system, it led to significant challenges related to the methodology for designing the first aircraft.

Electric Propulsion additionally influences the operational characteristics of a plane. Turbines that work by gas consume fuel with oxygen, and that pollute the natural. They transform the production power into an extremely Brayton cycle. (The Brayton cycle means a thermodynamic period that defined behind GeorgeiBrayton, which explains the processes of a constant-pressure heat engine).

B. Main Objectives

This thesis aims to address the structural issues and introduce new systems of control and implementation in the plane by taking into consideration the prospects and challenges of the aircraft that is powered by electric energy in the following steps:

1. The adoption of electric aircraft in the place of a conventional plane

Mostly mentioned in the preceding section, the traditional plane layout is challenging to replace with electrical systems. The framework of this thesis is to discuss these problems and provide solutions to them

2. Discover and analyse the electrical systems and the plane's control mechanism

Electrical systems consist of several essential components for operating the aircraft, such as the generator, distributor, and loads. In this thesis, each part will be clarified with the adoption of new methods of control.

3. Discover future aircraft based on expected technological improvement

With the development of science and research in this field significantly, the plane of the future will be studied the first levels based on technological progress, which will achieve impressive results in the coming decades.

C. Structure Of Work

The objects as described are being performed, also arranging the structure of the thesis by the following steps:

1. Discuss the findings of research and studies on the electric plane

After a review of the history of the application of electric aircraft, the results of the research will describe. The results are compared with their predecessors.

2. Outline of modelling techniques for electric drive systems

Inside this part, particularly various types, including components of propulsion systems on the aircraft, will be described.

3. Explanation of components that operate in electrical systems

Electrical parts will explain in detail on the aircraft, such as storage, transmission, conversion, cooling, and switching taking with consideration new types of controller.

4. Comparison of traditional and proposed controllers

The traditional controllers and proposed controllers are compared in detail.

II. HISTORY OF MEA

Inside the chapter shows the past of some use of the electric plane and examined various aspects of electrical propulsion systems. After study and analysis, gaps in the design of electric aircraft are identified, and solutions indicated.

A. Electric Flight In History

Three years later, there was a 10 km race in France between Villacoublay and Medon, where the electric plane won against its steam-powered competitors. The airship “La France that worked with a nine electrical motor including a battery with 435 kg. The plan did not allow anyone to beat her, reaching the highest velocity around 19 km/h (Boucher, 1984) (Masson P. , 1906).

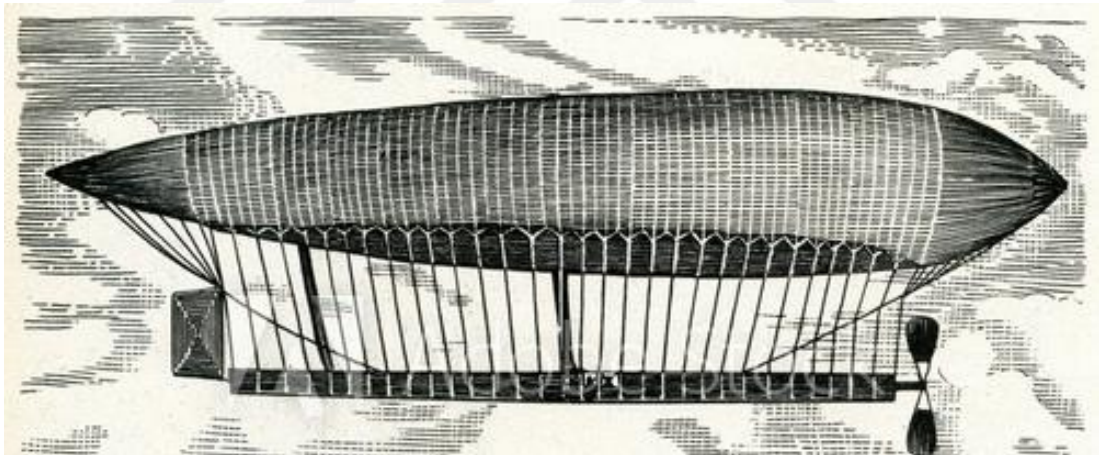


Figure 2: “La France”

The electric drive was no more valuable because of the enormous energy from fluid hydrocarbon combustibles, was not enough for the improvements toward the design of light capable generators. It took until 1973 until the Austrian light aircraft manufacturer “HBFlugtechnik” built an HB-3 glider with an electric

motor by Fred Milky. On the plane used a Bosch 10-kilowatt motor and rechargeable Varta batteries of nickel and cadmium (Moulton, 1973).



Figure 3: Hb-3 First Electric Aeroplane

After several years, several attempts were made for solar-powered aircraft. In 1979, Larry Mauro finished the original solar-powered plane. It was the ultra-light solar Riser. These solar cells on parts of "Solair I" give not sufficient energy for constant flight. Within 1981, the Solar-powered aviation that was created by "Gossamer Penguin" resulted to gained its most excellent international solar-powered trip through the English Channel (Boucher, 1984).

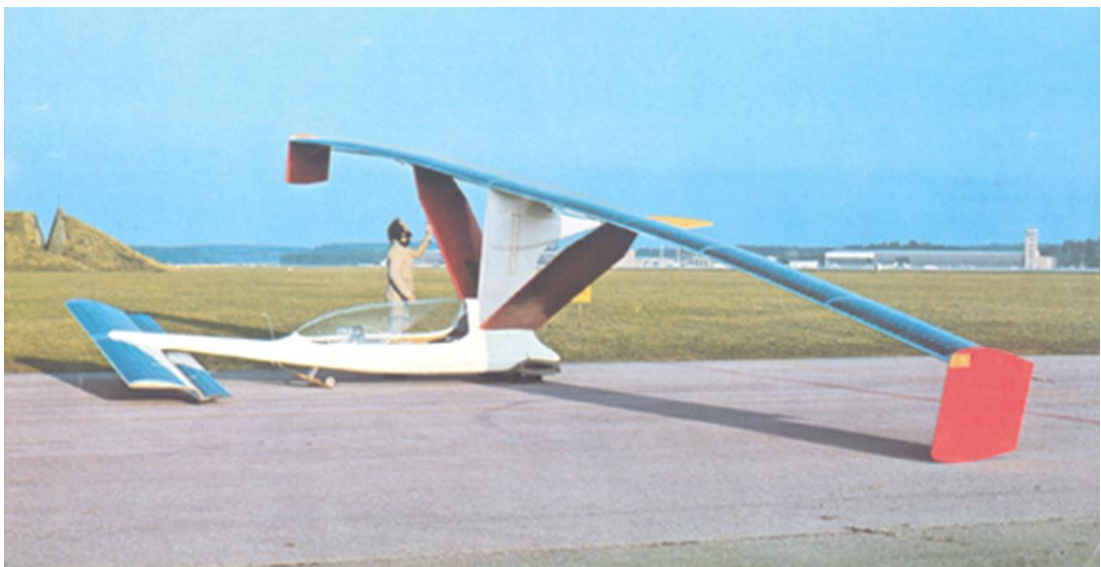


Figure 4: Solair I

At that time, all planes operated by battery or solar energy were very limited. With progress in the field of battery performance, the execution of electric drive operations improved. As a consequence, in 1997, the individual first commercial, Alisport Silent Club "ultra-light commercial," sails plan flew with electricity is used. In the year 2003, the German manufacturer succeeded to manufacture "Antares 20e", which is an electric plane equipped with a 42 kW brushless Motor that can fly up to 3000 meters (Marzinzik, october 2003).



Figure 5: Antares 20e

Following the initial popular from an electrical sailplane, besides the first commercial, the ultra-light aeroplane was prepared during 2007. The single "Electraflyer" provide an electric motor with a 13-kW, and a 35kg Li-ion polymer battery capable of taking a person during a flight up to 90 minutes (Electric Aircraft Corporation, n.d.).



Figure 6: The "Electraflyer."

After the significant progress in electric power, many experimental and commercial electric aircraft projects appeared in the following years. The CAFÉ Foundation launched a challenge called the Green Challenge. In the competition, the plane must fly for a distance of up to 320 km in a period no more than two hours and consume no more than 3.8 litres of Kerosene (a liquid which is obtained from petroleum. It is popularly used as a fuel in flying and to power jet engine of aircraft). Four aircraft took part in the race. The Slovenian team wins the competition. They produce the "Taurus 4" that consume one litre in each 171.8 km. It can carry four-people with entire consumption energy of 65.4 kWh. The "e-Genius," took the second place. The "e-Genius" was developed through the University of Stuttgart in Germany. This plane has two seats, and its consumption has reached 34.7 kWh only. Despite its lower consumption rate, it won second place, because it has lost two seats, while that which came in the first place is four seats. (Tomazic, et al., 2011) (Schumann , Geinitz, & Nitschmann, 2012).



Figure 7: "Taurus" (1st)



Figure 8: “E-Genius” (2nd)

Table 1: The Taurus” with “e-Genius”

| | Taurus | e-Genius |
|---------------------------------|---------------|-----------------|
| Span [m] | 21.4 | 16.9 |
| Length [m] | 7.4 | 8.1 |
| Empty weight [kg] | 632 | 384 |
| Battery weight [kg] | 500 | 336 |
| Power installed [kW] | 150 | 65 |
| System voltage [V] | 325 | 450 |
| Max. cruise speed [km/h] | 201 | 235 |

B. Design Methods Of Electric Propulsion Aircraft

During the past few years, there is significant and vital progress in many areas, including power electronics and electric motors. This development was due to the increasing demand and massive push from the entertainment market and the car market. However, in terms of greenhouse emission, there are many global discussions about climate change and the availability of fuel. For these discussions, weight, performance, and safety in the medium and long-time frame in electrical propulsion systems must improve. As a result, aircraft designers began to develop aircraft and move from small aircraft manufacturers to large commercial aircraft with concepts of hybrid and electric aircraft. Three basic approaches are being considered for future aircraft:

Electrical generating with fuel-based propulsion power:

Under this approach, the powertrain is applied to share energy. The powertrain takes energy from the combustion of the engines and then distributes them to the electric motors. The power train includes some generators that are powered via combustion generators and transmit electrical energy toward a power management and distribution (PMAD) operation. It includes electrical wires, switches, and sensors and assures protection with reliability to power the electric machines. This operation is commonly described as a hybrid mainly. The essential purpose of this method is to improve the working of the system within an enhanced range in drive system combination. When using the combustion of the fuel, there is none need to use a massive battery on the aircraft. There is more research about this field in (Felder, Kim, & Brown, 2009) (A. R. Gibson, et al., 2010) (E. M. Greitzer, Hollman, & Lord, 2010).

Hybrid Drive:

In interest to the storage of electrical power, like battery and fuel cells, they must combine with the generator. The hybrid powertrain is used, the engine and the electrical motor, both of them, are coupled to a standard fan shaft. The main goal in the design of the hybrid-electric drive method in aircraft is to decrease the burning of fuel and use electrical power. However, using them together leads to a higher weight on the plane, taking into consideration that the batteries are more massive than the importance of the fuel. A full analysis of hybrid powertrain

designs, including features, has been prepared in (L. Lorenz, H. Kuhn , & A. Sizmann, 2013). Determine the size, and calculate the performance methodologies for hybrid electrical plane drive systems have been explained in (C. Pornet, et al., 2013) (Pornet, et al., 2015). These papers focus on giving a generalised energy-based and sizing methodology and connect many sources of energy in an aircraft. Particular importance provides interaction of the generator and the electrical machine components. Moreover, the plane companies issued researchers for the future hybrid passenger plane: Boeing's Sugar Volt (Droney & Bradley, 2011) and Airbus thrust theory (Kluge, September 2013).

Complete Electrical Drive:

The best Propulsion on planes is, without a doubt, only electric. In the first step, it should remove the combustion engines and replace them with the electrical storage devices, like batteries or fuel cells. Using fuel cells require such pure hydrogen fuels. According to that, the batteries become the most suitable for electrical power storage. Using the batteries leads to reduce of Kerosene, which results in the most constant and efficient outcomes.

Nevertheless, as shown in the next chapters, designing some batteries that are equivalent to specific required power in order to operate the aircraft raises the weight on the plane. As a result, battery-powered aircraft may be restricted to the range of short and medium flights. In the recent past, aircraft manufactures and research institutes issued new investigations of electric aircraft. For example, in 2011, the Airbus Group designed an idea for a unique aircraft called "VoltAir."

the "VoltAir" operating system and the results and design of this aircraft can be found in (Stuckl, Vantoor, & Lobentanzer, 2012).



Figure 9: "Voltair" Electric Aircraft

III. ELECTRIC DESIGN OF MEA

After the notable and significant development in the field of aircraft, "more electric aircraft" has become the most reliable in the field of civil aviation intended for a large number of passengers who fly long distances. It is designed to reduce dependence on the use of hydraulic or high-pressure bleeder and replace it with an electric. The general parts of the plane's electrical system are shown in **Figure 10**, which included:

- Energy production
- Primary energy delivery and stability
- Power converter and store the energy
- Secondary energy delivery and stability

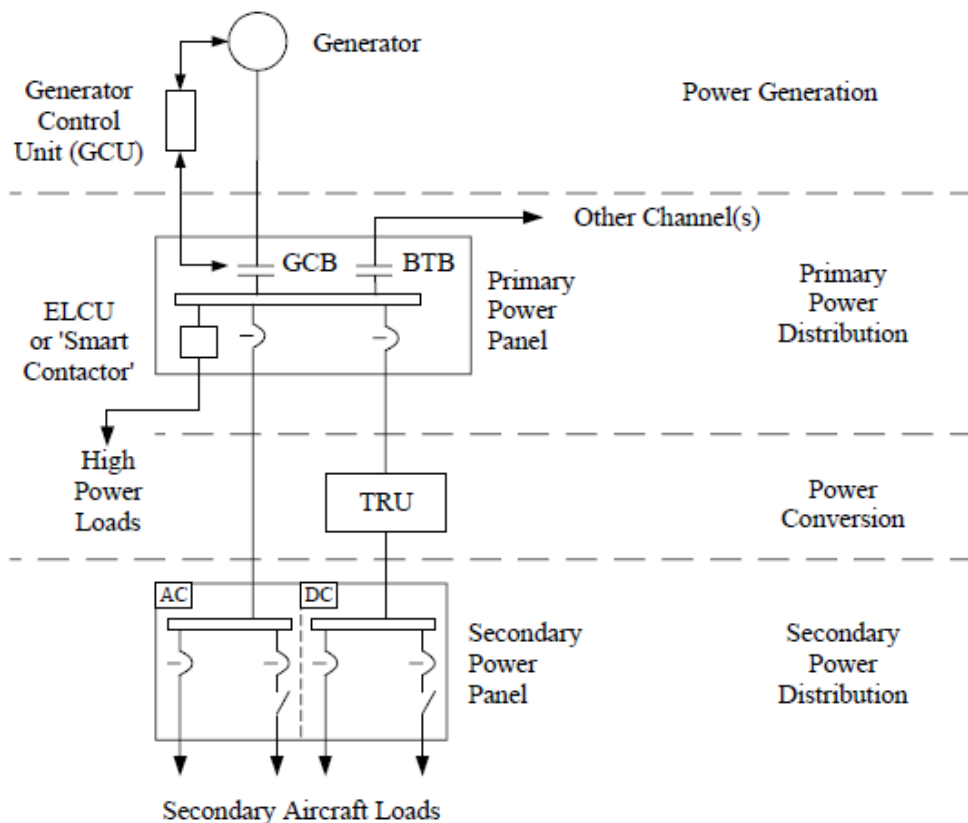


Figure 10: Ac Electrical System In The Aircraft

A. Power Generation

1. DC Power Generation

Generators are used to generate DC systems to feed the 28 volts DC loads on the aircraft. However, many systems need 270 volts. The Control system is used to maintain 28 volts DC which must remain constant at all times during the flight. DC generators are very exciting, as there are rotating electromagnets inside them that will generate electrical energy. The energy is converted by utilising a commutator that produces a single sine wave output voltage. The wave is effectively corrected to provide the required voltage with no ripples. Usually, the generators are shunt-wound by connecting in parallel the armature with high-resistance field coils, as presented in Figure 11.

With different, the engine on the aircraft, speed, and generator loads, the producing voltage can be lower than required. To overcome this problem, a regulator that adjusts the field current is used to ensure that the terminal voltage is maintained. Figure 12 illustrates the DC voltage regulator.

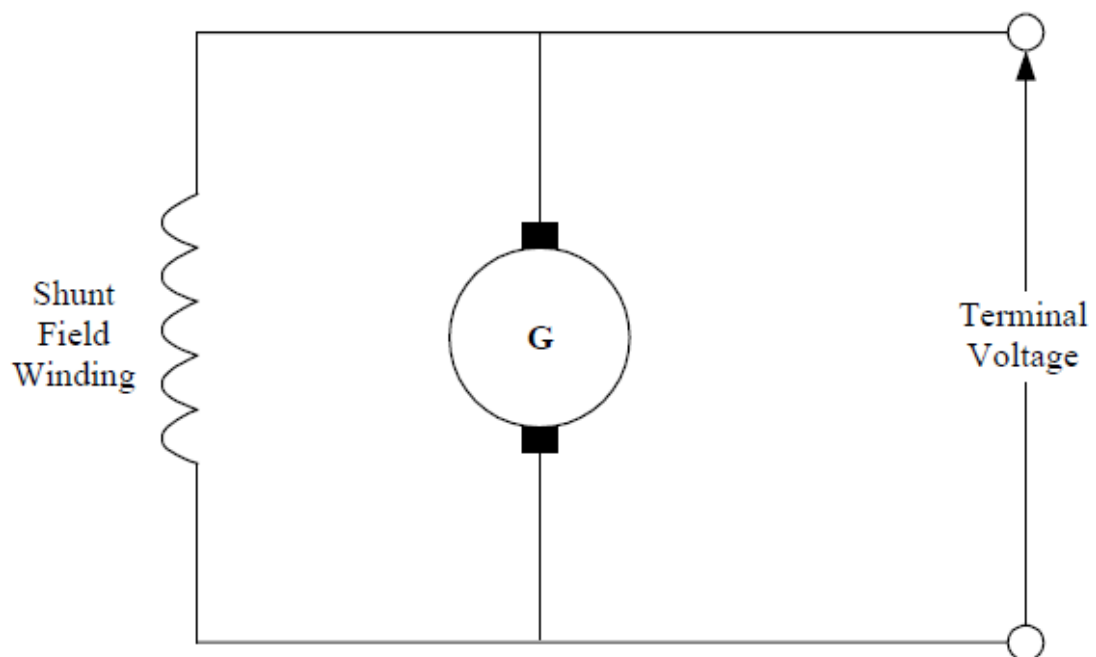


Figure 11: Shunt-Wound DC Generator

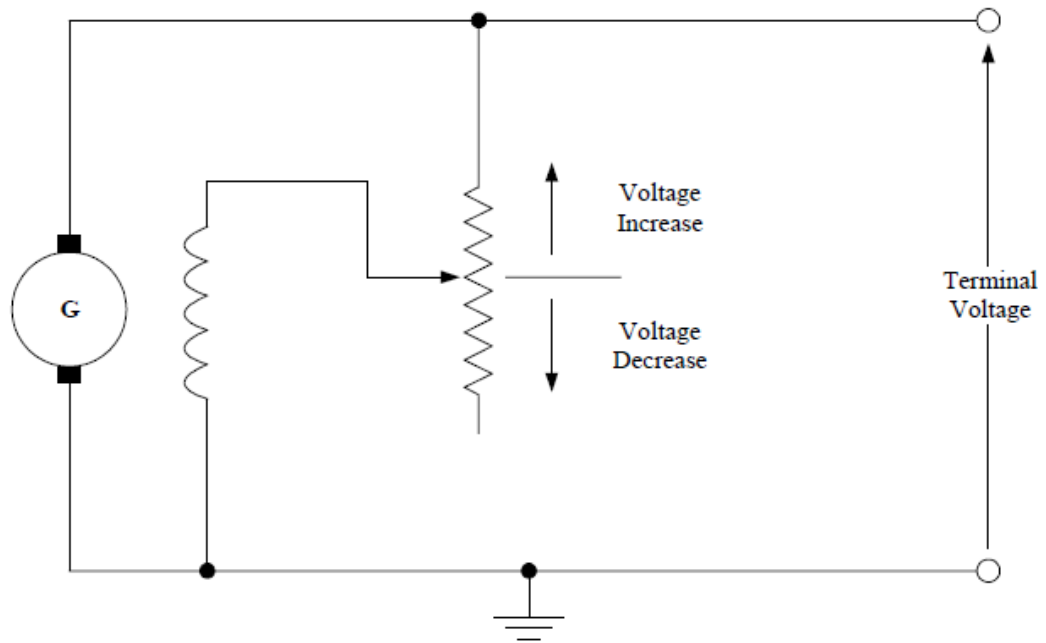


Figure 12: DC Voltage Regulator

2. AC Power Generation

Alternating current generators are utilised to make a sine wave of known specific voltage with a fixed frequency. The design of the alternator is more straightforward than DC, as there is no need to use a commutator. Traditional generators utilised slip rings to pass low current to/from turning windings, and their difficulty when carrying a significant current hurt from corrosion and damage. Modern alternating current generators are presented in Figure 13 that passing a high current suffered from corrosion and damage.

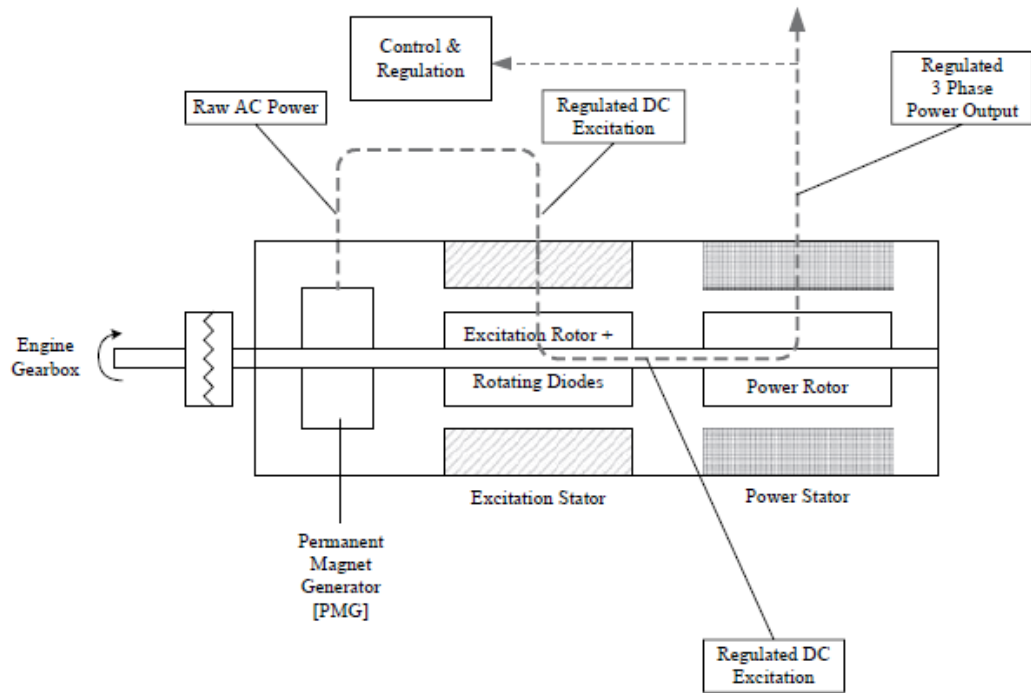


Figure 13: The Improved AC Generator

The alternating current generator consists of several parts on the shaft, the most important of which are:

- The Permanent Magnet Generator (PMG)
- An excitation stator and rotor holding rotating diodes
- A power rotor with power stator

In Figure 13, The dashed line presents the energy coming from generators. The PMG produces “raw” energy with variable frequency and voltage. The output of generators is therefore sensed and regulated by the generator controller. The benefit of this part is to adjust the DC flow in the excitation stator. Therefore, the voltage resulting from the excitation roles can be controlled. Within the rotor, there is a need to use diodes. The diodes used to regulate and control the DC voltage. During the rotation of the rotor, the rotor generates a rotating magnetic field and therefore produces AC voltage to the stator. The AC systems on aircraft are usually 400 Hz, three phases 115 VAC combined in stare configuration, as presented in Figure 14.

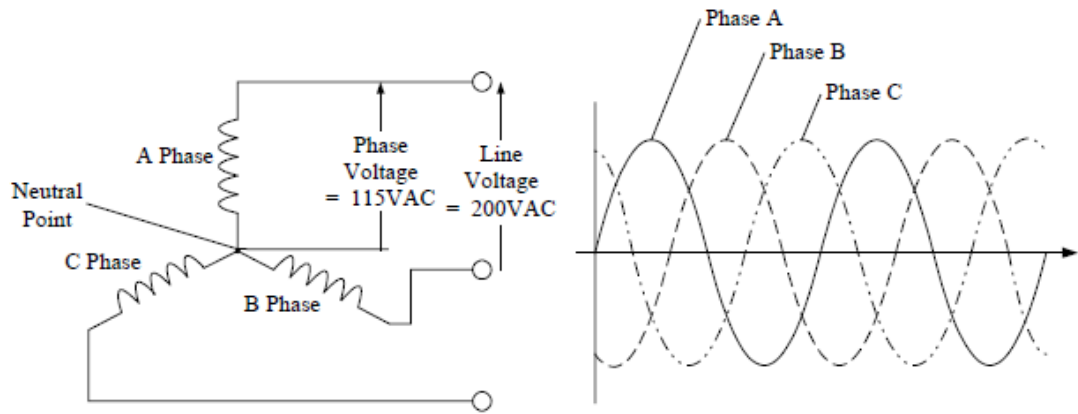


Figure 14: Three-Phase Generator Connected In Star Configuration

Through what has been explained, the advantage of AC systems is that it works at 115 VAC, while the DC systems work in 28 VDC. The advantage of using a higher voltage is the electrical current decreases with the increase in voltage. Consequently, the losses decrease, and it becomes possible to use connections and cables of less thickness and weight, which is a critical consideration for aircraft systems. However, with the use of high voltage, it accompanies many challenges. When using a higher current requires better standards of insulation.

3. Producing Power In case of Emergency

During accident conditions, the generators may not produce enough power. The aircraft battery may provide a short-term power storage capability that can work for 30 minutes. However, for more extended periods of running, there are needs of employed alternative generators. There are three methods to generate backup power:

1. RAT
2. Backup Power Converters
3. PMG

a. Ram Air Turbine (RAT)

During the flight, and for an unknown reason the engine has stopped working, there is a need for using an emergency generator that can provide enough power to maintain the flight. One of the proposed solutions is by using the Ram Air Turbine(RAT). RAT is utilised to generate alternative power. The RAT is a small turbine that generates

power with the flowing of air—usually stored in the aircraft ventral. It is a small emergency generator. Usually, the emergency generators feed the essential power of aircraft, such as the crew’s necessary flight instruments and some vital services, as illustrated in figure 15. Standard RAT generators can produce power among five and fifteen kVA depending upon the size of the RAT. Once the RAT is used, it continues working for the duration of the flight. The RAT is intended to supply sufficient power to maintain the aircraft steady while attempting to recover the principal generators.

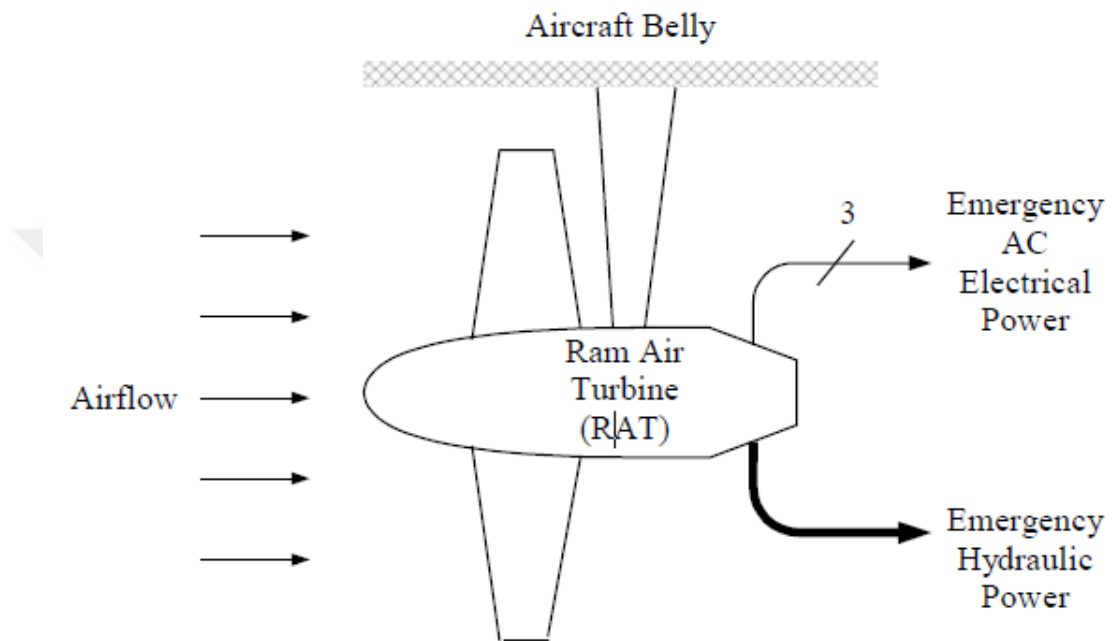


Figure 15: RAT



Figure 16: RAT Employed On MEA

b. Backup Power Converters

The conditions for the Extended Twin Operation System (ETOS) have directed to the requirement for an additional method of backup power supply. Short of using the RAT that should happen in only the most urgent emergency. The use of backup converters meets this requirement and is applied to the B777. The design of B777 is explained in (Andrade & Tenning, July 1992). Backup generators are operated by the same engine accessory gearbox but are entirely independent of the main IDG. The backup generators are VF (Variable Frequency). The VF generator is supplied into a backup converter, which, applying the DC link technique, first converts the AC power to DC using rectification. It converts to three-phase 115 VAC 400 Hz power using advanced solid-state power switching techniques. The result is an alternative power of AC power production, which can power some of the aircraft AC busbars. In this way, many essential loads of the aircraft electrical system can continue working; some of the non-critical load is switched off, such as the galleys by the Electrical Load Management System (ELMS).

c. Permanent Magnet Generators (PMG)

The advantage of PMG's has developed noticeably across the new decade. PMGs can be single-phase or multi-phase devices. Figure 17 shows three-phase PMG, including a converter. As can be seen, the backup converter operates with PMG for producing enough energy to the flight controller, which is 28 VDC. Also, PMG is used to provide double independent supplies to every bar of the Full Authority Digital Engine Control

(FADEC). Consequently, it can be seen that on aircraft like the B777, 13 PMG has operated across the aircraft control.

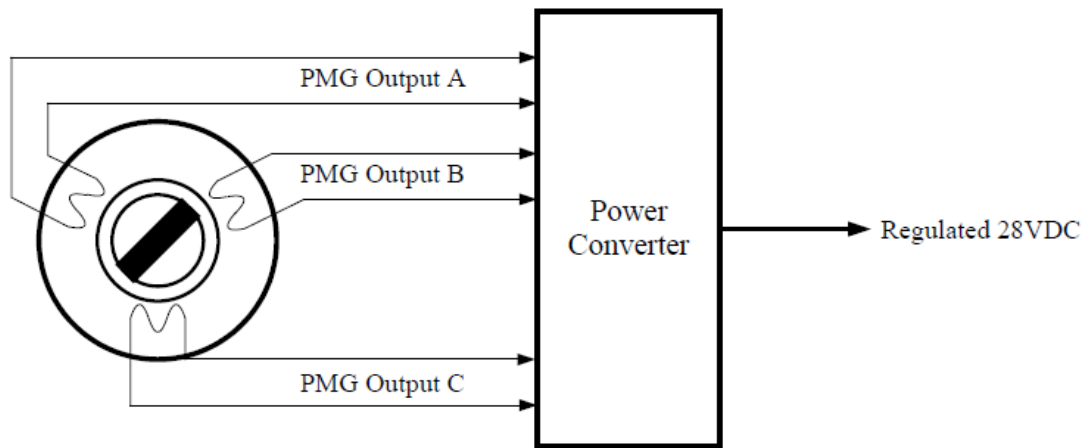


Figure 17: Three-Phase PMG With Converter

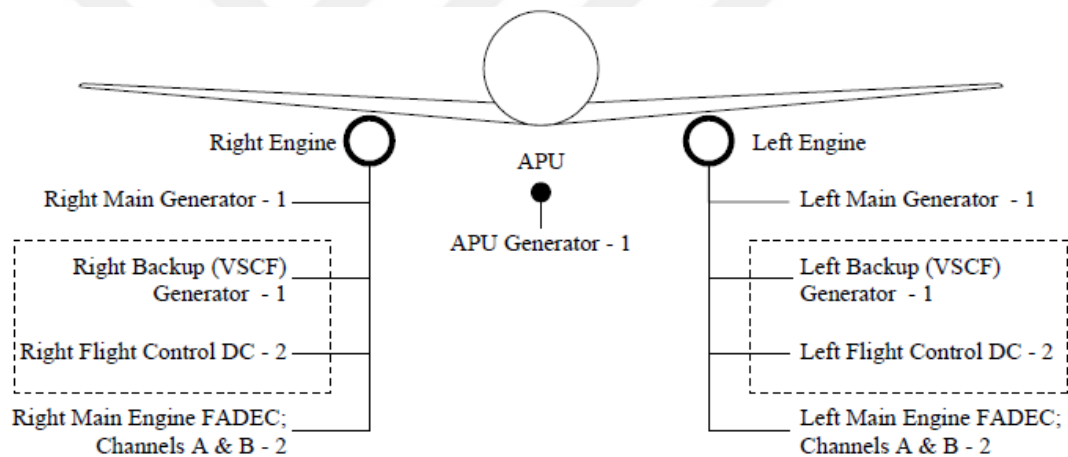


Figure 18: Boeing 777 PMG/PMA Complement

4. Power Generation Control

The main components of the power generation control are:

- DC systems
 1. Voltage regulation
 2. Parallel operation
 3. Protection function
- AC systems

1. Voltage regulation
2. Parallel operation
3. Protection functions

a. DC Systems Generation Control

Voltage regulation

DC production is operated using shunt-wound self-exciting devices as shortly explained earlier. The method of voltage regulation is represented in Figure 12 shows a changeable resistor in series with the field winding. Variable resistor adjusts the resistance of the field winding; consequently, the field current and producing voltage can be regulated. Moreover, it must be taken into attention that this regulation must be an automatic function and must keep constant. Therefore it does not change with the change in the speed of the engine or the load in aircraft. Systems are limited to nearby 400 amps or 12 kW per channel for two causes:

- The size of the connectors and switches to support the appropriate current becomes very expensive
- Brushing on generators becomes more exposed to damage due to high costs of maintenance if these levels are surpassed.

Parallel Connection:

Aeroplanes are consist of several generators. The energy must provide throughout the flight without interruption, and in the event of any damage, defect, or discontinuation of one of these generators, there must be a backup generator. Also, many sensitive flying devices and navigation devices should not be interrupted by energy. Some of these machines require restarting or re-applying them if they are disconnected from power. To satisfy these conditions, the generators must be in parallel to share the same energy for the electrical load.

Moreover, each generator is working in the presence of a controller. The controller controlled voltage regulators that automatically compensate for the differences. When operating the generators in a parallel way, the voltage regulators must be connected so that corresponding adjustments in the field current can adjust any additional load of the generators. This parallel feature is known as an equalising circuit, so energy can be obtained throughout the flight without interruption even if a problem of failure

happens. A clear diagram illustrates the principal elements of DC parallel operation in Figure 19.

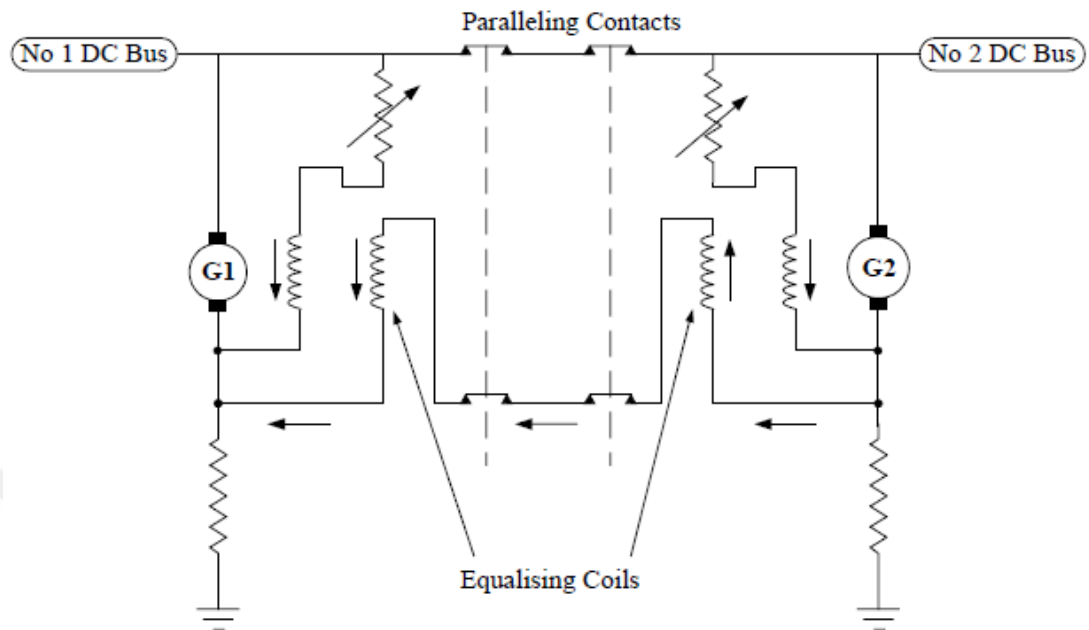


Figure 19: DC Generator Parallel Operation

Protection functions

The primary requirements to analyse the DC systems in follows:

- Overvoltage protection: During the field excitation, some problems in producing high voltage can happen. This overvoltage could then damage some electric loads. The solution is to use an overvoltage protection. The overvoltage senses the voltage, and in case of a high voltage, the controller opens the line contactor and protect the circuit.
- Low voltage protection: In the generator system, some voltage drop may occur, and therefore some devices may not operate with the required efficiency. Therefore it is necessary to use tools that protect or adjust the voltage output of the generators.

b. AC Systems Generation Control

Voltage regulation

As mentioned before, DC generators need a separate source to excite field coils. AC generator excitation is a complex subject for which the technical explications change

according to whether the generator is constant-frequency. Some of these solutions comprise high-level control circuits with error indicators.

Parallel operation

In DC generators, generators are combined in parallel to produce continuous power. Identically, AC generators can also be connected in the same way. This method utilises only to generators identical frequency. It is useless to implement variable frequency (VF) alternators. Some of the loads on a plane, such as the anti-defrosting / defrosting parts are almost insensitive to frequencies. To parallel AC machines, the control task is more complicated as both real, and reactive (imaginary) load vectors have to be synchronised for effective load distribution.

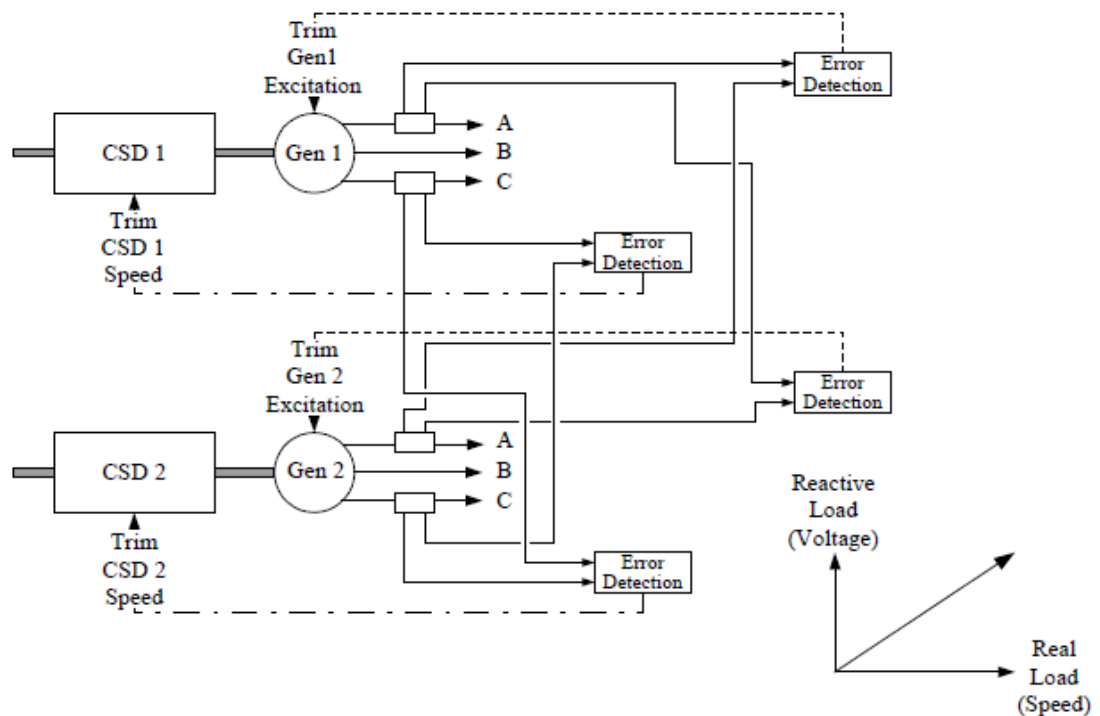


Figure 20: AC Generator Parallel Operation

Protection functions

Regular supervisory or protection functions offered by a standard AC generator controller unit or GCU are prepared under:

- Superior voltage
- Lower voltage
- Lower/higher excitation

- Lower/higher frequency
- Differential current protection
- Adjust phase rotation

5. Advanced AC Electrical Power Generation Types

In the previous sections, basic power generation systems are defined. While for DC generators, they are limited to currents over 400 amps. Moreover, for alternating current generators, they are fixed frequency, such as an integrated motor-generator (IDG). Indeed, with developments in the field of aircraft, there are many types of power generation applied today. Several new papers have recognised the problems and supposed the aircraft's electrical energy requirements to progress in the civil aviation environment. Nevertheless, not only electric planes develop the system energy levels, but the variety of original power generation types is increasing.

The various kinds of electrical energy production modernly being examined are displayed in Figure 21. The Constant Frequency (CF) 115 VAC, three phases, 400Hz generation models are symbolised by the Integrated Drive Generator (IDG), Variable Speed Constant Frequency (VSCF) Cycloconverter and DC Link options.

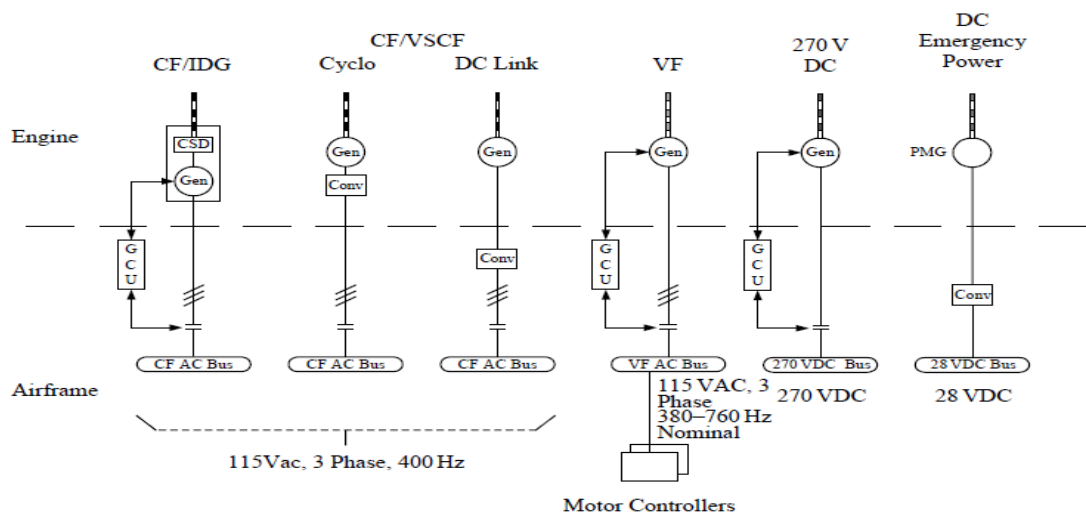


Figure 21: Electrical Power Generation Types

Constant Frequency / IDG Generation

In this sort concerning generator, a Constant Speed Drive (CSD) is used. CSD convert from variable speed and make it fixed speed. It is used to keep the generator shaft

speed at a constant number of revolutions per minute, appearing in a fixed frequency product of 400Hz. Consequently, the product voltage produced by the generator will not change with varying engine speed. However, when CSD is using it must be taken into account:

- Always must maintain and pay attention to the level of oil charging and cleanliness of the oil.
- The system is costly to obtain & repair; mainly due to the difficulty of Constant Speed Drive (CSD)

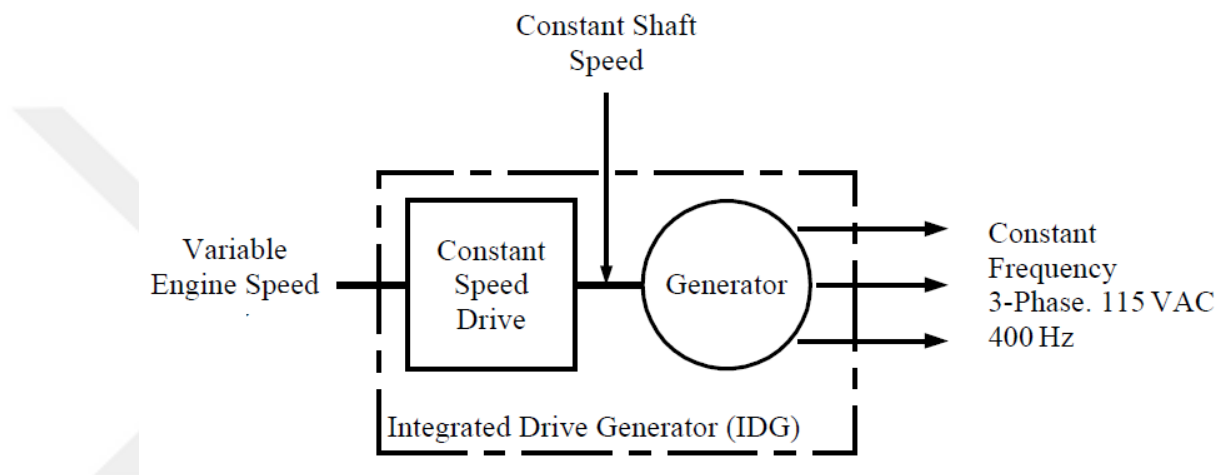


Figure 22: Constant Frequency / IDG Generation

Constant frequency / IDG Generation

The Variable Frequency (VF) power generation is shown in Figure 23, is the most convenient and most durable form of power production. In this way, the generator output is regulated to 115 VAC, and the frequency change from 380 to 720 Hz. There can consequently be an issue that has to overcome in the production of different aircraft operations, such as fuel, ECS, and hydraulics. During some cases, changes in

motor/pump performance may be included. However, in the worst cases, there is a need for the motor controller to replace a more comfortable control condition.

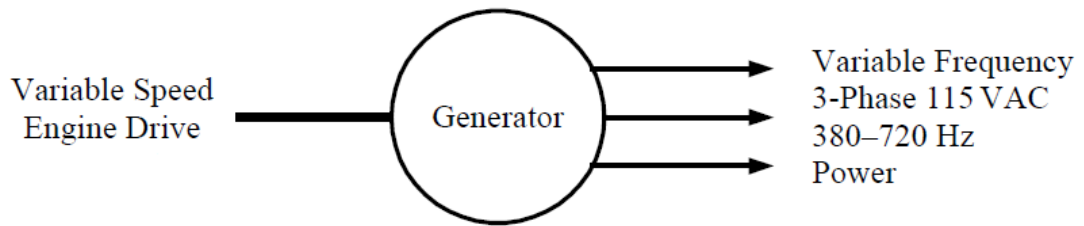


Figure 23: Variable Frequency Power Generation

VSCF power generation

Variable Speed Constant Frequency (VSCF) power generation is presented in Figure 24. In this way, the variable-frequency power is electronically converted using solid-state power switching devices to a constant frequency of about 400 Hz, 115 VAC power. There are two methods:

- DC link: In the DC link, the power is transformed to DC power before being electronically regenerated into three-phase AC power. DC link technology has been used at the B737, MD-90 and B777 still must to examine the safety of constant or variable frequency power production.

Cyclo converter: The cyclo converter makes many sources. Six phases are provided at approximately high frequencies above 3000 Hz—also the solid-state methods rearrange in a programmed and accurately controlled manner. The result is to electronically restore the input and provide three phases of the constant frequency of about 400 Hz power. The cyclo converter methods have been famously applied on fighting aircraft in the US: F-18, U-2, and the F-117 stealth fighter. Table 2 presents the standards of power generation concerning civilian and army (fighter) aircraft platforms during the 1990s. In that year, the levels of electric energy began to increase, and the diversity of methods of electricity generation increased.

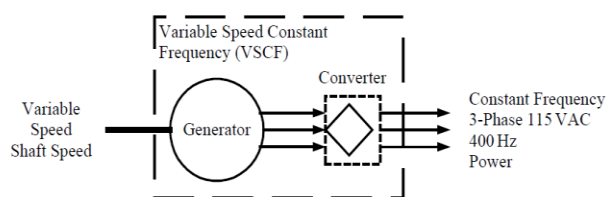


Figure 24: VSCF Power Generation

Table 2: Recent civil & military aircraft power system developments

| Generation type | Civil application | Military application | |
|---|--------------------------|---|-----------------------|
| IDG/CF | B777 | 2 × 120K VA | |
| | A340 | 4 × 90K VA | |
| | B737NG | 2 × 90K VA | |
| | MD-12 | 4 × 120K VA | |
| | B747-X | 4 × 120K VA | |
| | B717 | 2 × 40K VA | |
| | B767-400 | 2 × 120K VA | |
| VSCF (Cyclo converter) [115 VAC /400 Hz] | | F-18C/D 2 × 40/45K VA F-18E/FS 2 × 60/65K VA | |
| VSCF (DC Link) [115 VAC /400 Hz] | B777 | 2 × 20K VA | |
| | MD-90 | 2 × 75K VA | |
| VF [115 VAC / 380-760 Hz] | Global Ex | 4 × 40K VA | Boing JSF 2 × 50 VA |
| | Horizon | 2 × 20/25K VA | |
| | A380 | 4 × 150K VA | |
| VF [230 VAC] | B787 | 4 × 250K VA | |
| VF [270 VDC] | | | F-22 Raptor 2 × 70KVA |

B. Primary Power Distribution

The power distribution method is based on the organisation of all aircraft electrical generating powers. In a civil aircraft, the power sources are from:

- Main aircraft generator: The main generator supplies all the elements on board. It is attached to Generator Control Breaker (GCB) controlling by GCU.
- Emergency generator: The Emergency generator is applied during accident or loss to main generators. It is joined to BusTie Breaker controlling through Bus Power Control Unit (BPCU).
- APU generator: The APU generator feeds aircraft operations (air-conditioning, electrical, hydraulic, pneumatic, fuel, instruments, etc.). APUs are regularly run on the ground to start working of main generators. APU reduce fuel burning, and it is connected to APUiGCB controlling by the BPCU.
- Ground Power Unit: The Ground Power Unit is one of the essential aircraft Ground Support Equipment(GSE), which is applied for aircraft maintenance purposes on the ground to support the flight power. It is connected to External Power Contactor (EPC) under the control of the BPCU.

The power applied between different generators is changed by the power contactor or breaker. Powerful loads are switched from the primary aircraft bus bars by using Electronic Load Control Units (ELCUs) or ‘smart contactors’ for load protection.

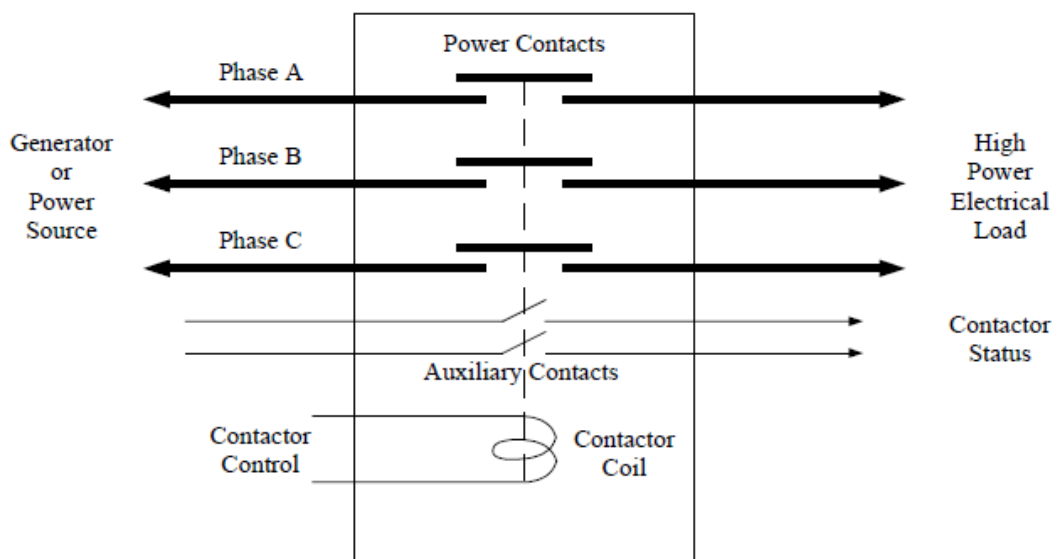


Figure 25: Power Contactor

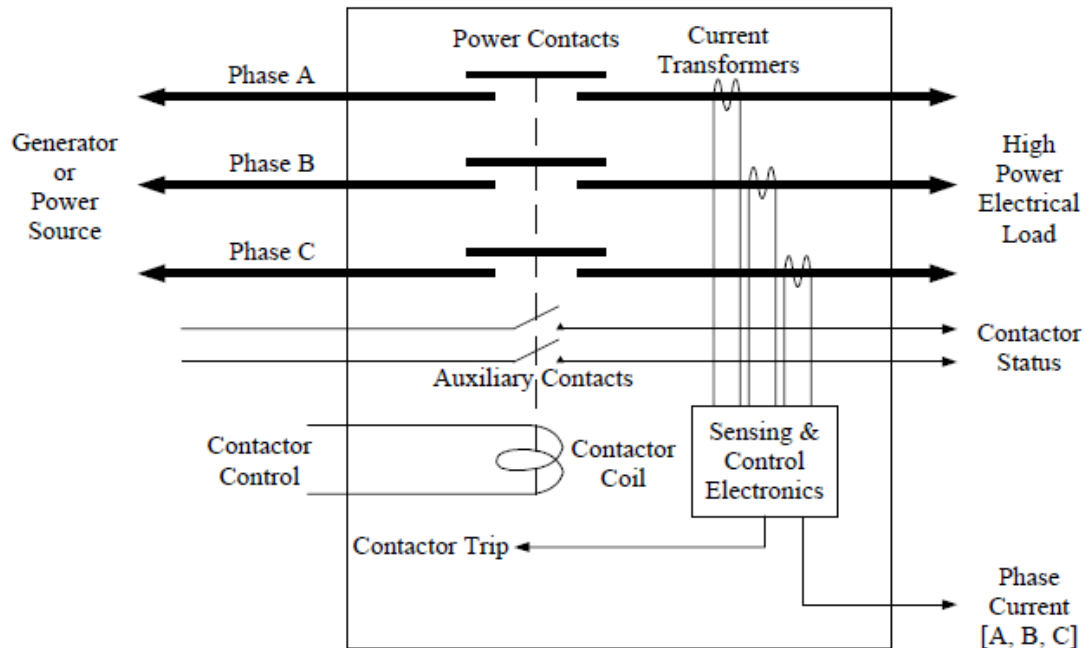


Figure 26: ‘Smart Contactor

1. Different Components

As a consequence, the elements of onboard electrical loads are defined. The electrical storage, electrical transmission, power switches circuit, breakers, electric motors, equipment cooling, motor inverters, controllers, propeller are explained in detail.

a. Power Conversion

There are many types of electric loads on the plane. Some loads require a specific voltage that differs from the others. There is a load that requires DC, and there is a load that requires AC voltage. Usually, there is a primary generator feeding all members of the plane. Still, sometimes depending on the type of load, some load cannot be connected directly to the generator due to the different operation of the load. To do this, it must use a power converter to transfer the energy from the generator and purify it to fit all types of loads on the plane. Famous examples of power transformation are:

- Conversion DC to AC power: That conversion uses inverters to convert 28 VDC to 115 VAC single-phase or three-phase power.
- Conversion AC to DC: That conversion uses Transformer Rectifier Units (TRU). Usually, converts from 115 VAC to 28 VDC power.
- Conversion AC to AC; a regular conversation would be from 115 VAC to 26 VAC.

b. Inverter

The principle of the inverter's work is by converting DC to AC. It is used to control the speed of the motors by using a suitable control. The inverter transmits different frequencies to obtain the desired speed and keep this speed constant despite the change of the load on it. Figure 27 shows the circuit needed to perform this conversion. They are typically established utilising solid-state MOSFET, IGBT, or thyristor switches and filters to exclude disturbance in the power signal. The switches $s_1 - s_3$ switch in a specific frequency to produce AC power. They produce electric current to the armature winding in the motor. During the inverting process, losses happen due to voltage drop in semiconductor elements and due to switching losses. Average efficiencies of the motor controller achieve an efficiency of 95%, (Masson & Luongo., 2007).

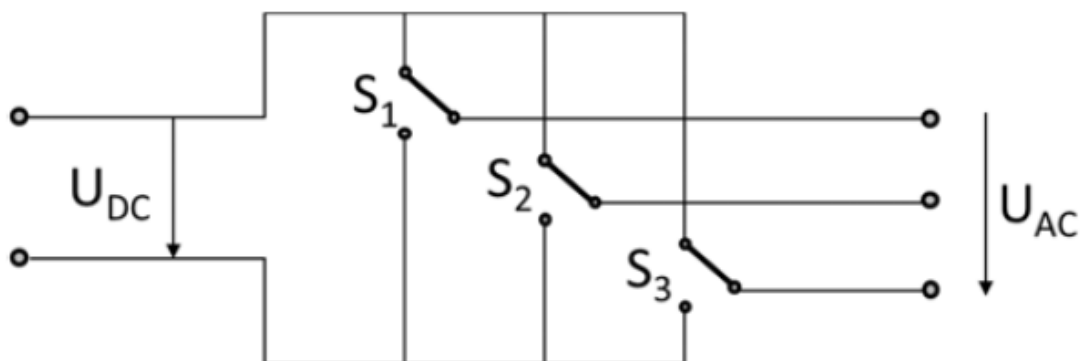


Figure 27: Basic Motor Inverter

Prospective possibilities for the controllers cover new elements such as the Si-C semiconductors. One advantage of Si-C is its more powerful working temperature compared to traditional semiconductors. Therefore, the losses in switching, forward resistance, and the filters can be decreased while the semiconductors are

cooled (Haldar, et al., June 2005). The efficiency using these controllers is 99.8%; they are described in (Brown, 2011).

c. Transformer Rectifier Unit [TRU]

The Transformer Rectifier Unit (TRU) combines the roles of the transformer and rectifier toward a unique system. In aircraft, TRU converts the 115VAC power to 28V DC power. It uses for supplies many electrical loads. Moreover, TRU consumes heat; therefore, it needs an air-cooled.

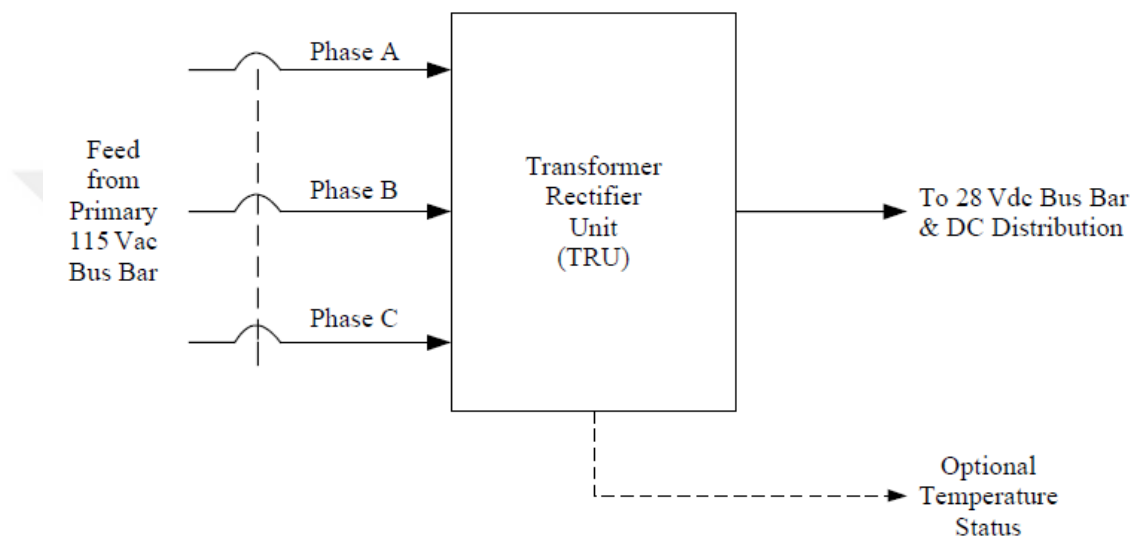


Figure 28: Transformer Rectifier Unit (TRU)

d. Auto Transformers

In some electrical systems, auto-transformers are used to provide step-up or step-down voltage. They transform from 115 V to 26 V AC to light the aircraft equipment.

e. Electrical Storage

In electric aircraft planes, electrical storage of high efficiency and lightweight must be used to obtain the longest flight possible. There is much electrical storage; they vary depending on storage capacity, weight, and performance. The most common are batteries, fuel cell systems, and capacitors. Capacitors are better than batteries in terms of power capacity per weight unit. Capacitors work great for a few seconds, but after that, they are considered useless because they do not have much storage space. Therefore, capacitors are applied for a short time, including high-power applications. For the fuel cell, a fuel cell transforms

chemical energy into electrical energy. The fuel cell system better than batteries in low-power applications over the long term, especially in terms of weight. For higher power demands, the batteries are better because it is not able to produce enough power to feed the loads (Balakrishnan, 2007). As a consequence, batteries are considered between fuel cells and capacitors. The batteries are mostly employed aircraft.

f. Battery Cells

In principle, inside the battery, there are chemical reactions; these reactions convert to an electrical current. In the batteries that can be charged, they can be used multiple times. Inside the battery, it contains positive electrodes (the cathode) and negative electrodes (the anode). Between the electrodes, there is an electrolyte that separates the electrodes. It allows only the transit of ions and does not allow the transportation of electronics. A description of a battery is shown in Figure 29 (H. J. Bergveld, 2002). Densities and the electrochemical potentials of the suitable metallic electrode elements versus a conventional hydrogen electrode are displayed in Figure 30.

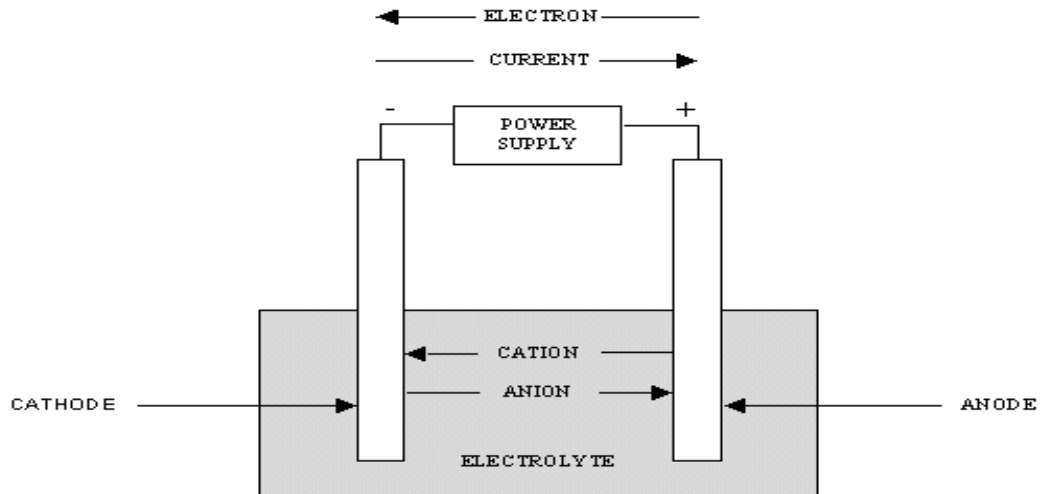


Figure 29: Basic Battery Cell Schematic

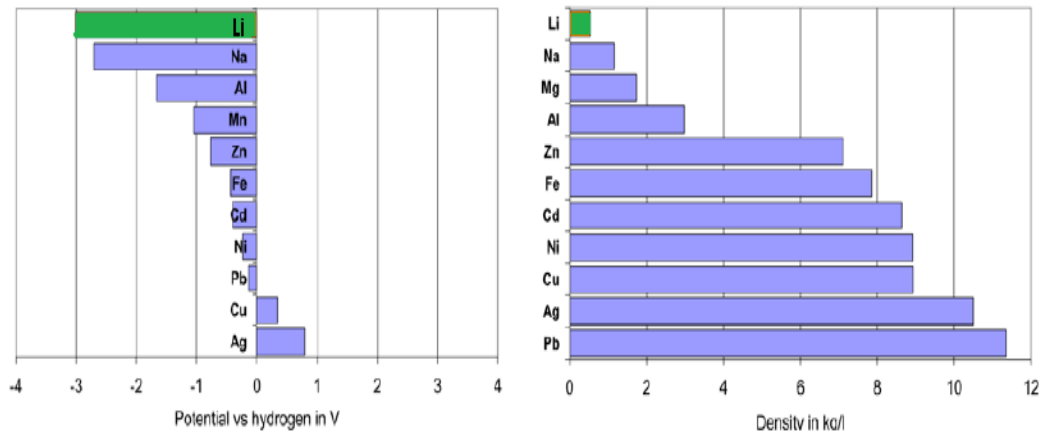


Figure 30: Standard potential And Density Of Electrodes Elements (Wohlfahrt-Mehrens, 2007)

The Li-Ion cell is the most applied today, especially in all types of portable electrical applications, because the battery is small-sized and lightweight. The performance of the battery cell depends mostly on the environmental circumstances and the discharge coil. Commonly, the capacity of a battery is defined by the discharge current, and the cell voltage principally given in equation (1)

$$E = \int V(t).I(t)dt \quad (1)$$

Rate of discharge(C-rate):

The discharge of the battery cell is at a specific discharge rate, or the so-called "C rate," signifies the amount of discharge current in one hour. For example, a battery of C rate 10 Ah, and a load consume one amper per hour can handle for 10 hours. During the discharging process, there is a voltage drop. The voltage drop occurs due to internal losses R_i of the cell. The voltage drop of Li-ion batteries is 4.2 during charge and vary between 2.7 and 3.0 V during discharge. (Jossen & Weydanz, 2019).

State of charge (Soc):

The "state of charge "determines the valuation of the remaining charge. Through the discharge, the cell voltage gives a little drop created by the impacts of

chemical cell effects. It requirement be taken into attention; the cell should not be discharged under the smallest cell voltage, which called cut-off voltage because the results produce loss to the electrode elements. A full specification can be taken from (Jossen & Weydanz, 2019). Standard cell discharge curves are presented in Figure 31.

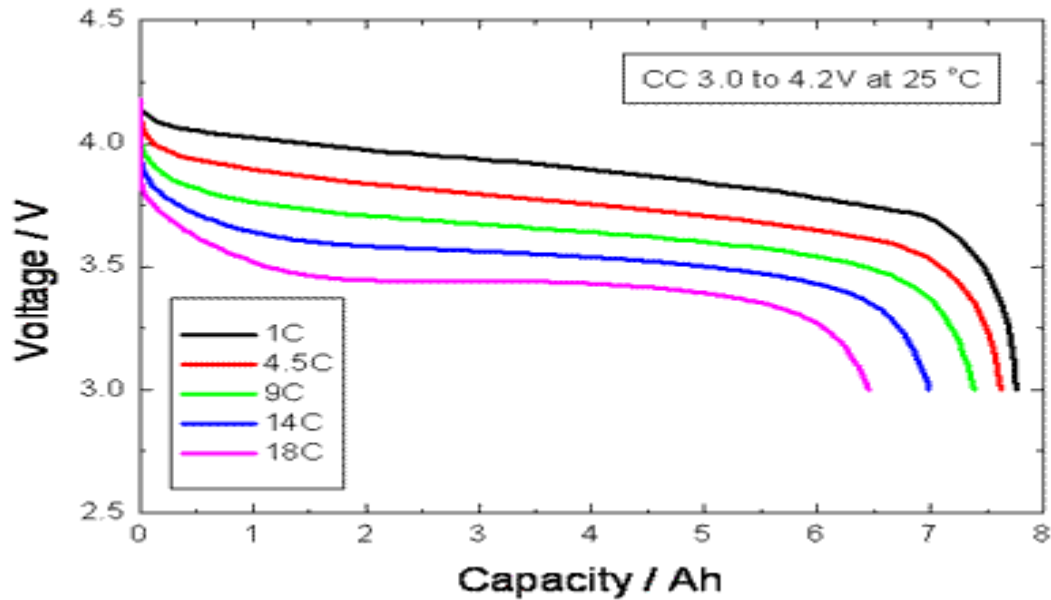


Figure 31: C-Rate Effect On Discharge Characteristics (Jossen & Weydanz, 2019)

Temperature:

The temperature has a significant and sensitive factor that affects the performance of the cell in three ways. First, the reaction of the chemical cell is affected by the temperature, because through the Arrhenius equation.

$$K = k_0 e^{\frac{-e}{RT}} \quad (2)$$

Where e is the activation energy, k_0 is a constant, and the other parameters are the gas constant. Secondly, the spread of reaction species and the mechanism of transfer of the primary ions affect the temperature. The higher the spreading rate increases the heat, according to Fick's law. Thirdly, increasing temperatures lead to an increase in the ohmic resistance of metallic components. Moreover, lower the resistance of the electrolytes because the electrolytes are regularly the dominating supporter of ohmic losses. In standard Li-ion cells, they deteriorate

in heat more than 50 ° C and create cell loss and failure (Jossen & Weydanz, 2019). The discharge properties of a Li-ion cell for several temperatures are shown in Figure 32.

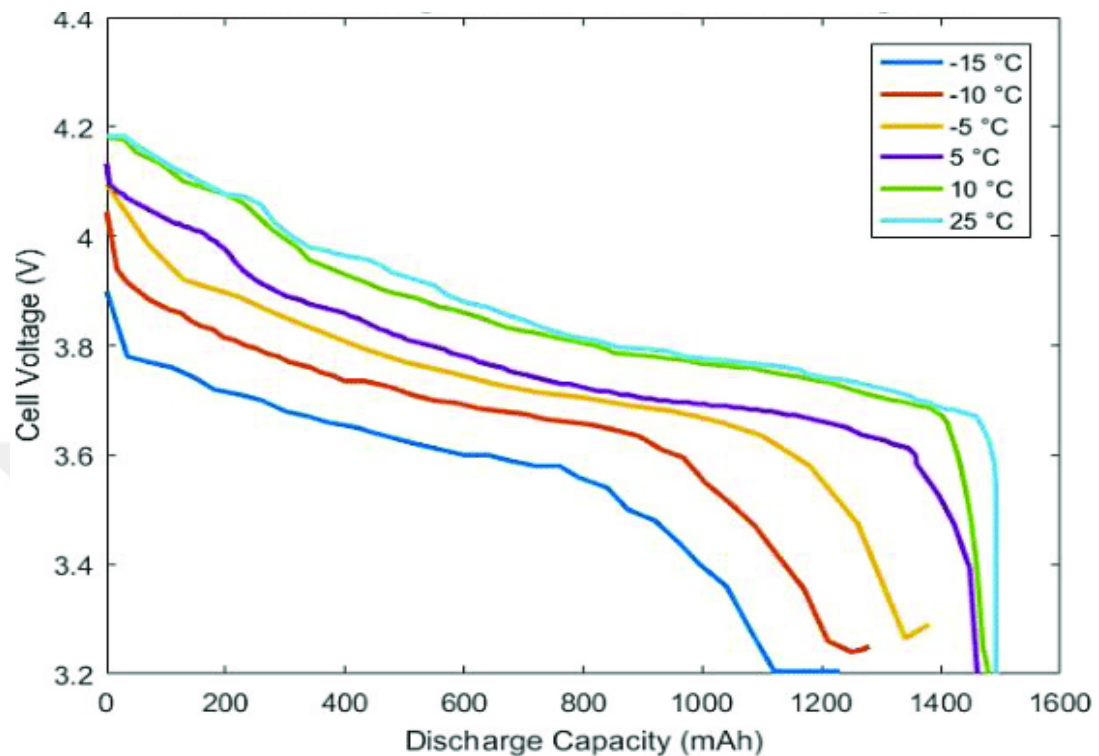


Figure 32: Temperature effect On Discharge Characteristics (Jossen & Weydanz, 2019)

Cycle durability

When storing the battery for a certain period, a slight leak occurs that drives to a slow continuous self-discharge. The rate of battery discharge depends on the type of cell, concentration losses, and ohmic losses. In fact, with repeated use of the battery, the storage capacity of the rechargeable battery cell decreases with the number of charges and discharge cycles, and this is due to reactions and corrosion effects. Cycle durability of a Li-ion cell. Figure 33 displays the cycle display of a lithium-ion cell with a capacity of 720 mAh at a discharge rate of 1 C.

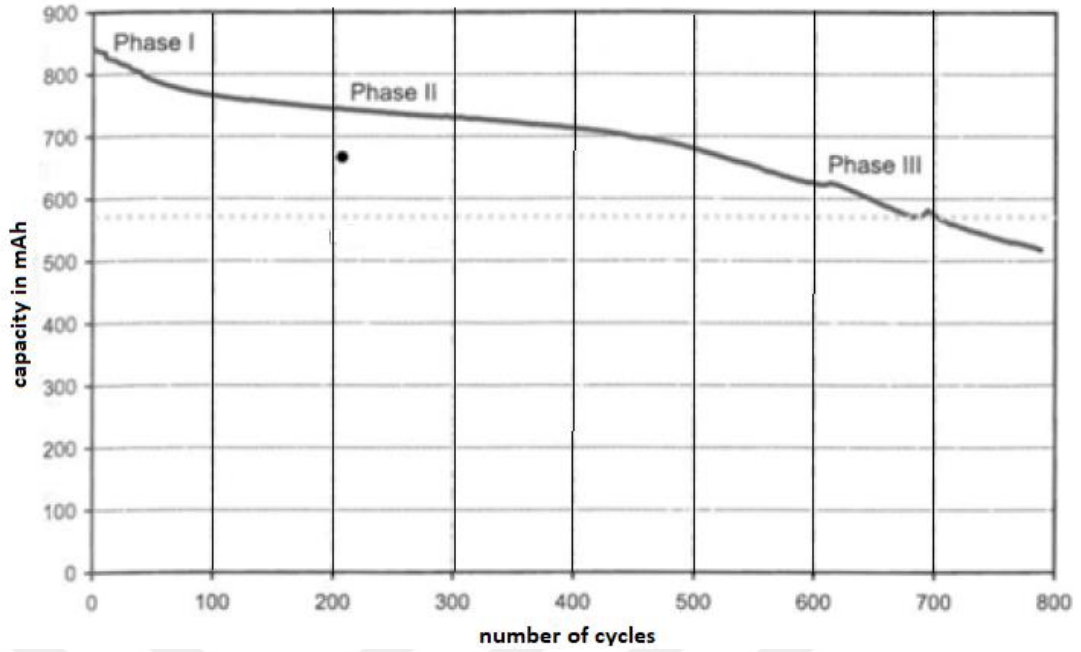


Figure 33: Cycle Durability Of A Li-Ion Cell (Jossen & Weydanz, 2019)

Heat output

During discharge, the loss of the battery capacity occurs through heat. Two main factors vary due to the change in temperature: the resistance and polarisation losses. A clear circuit diagram of these heat causes is presented in Figure 34. A representation of the losses by resistance and polarisation consequences is presented in equations (3) and (4).

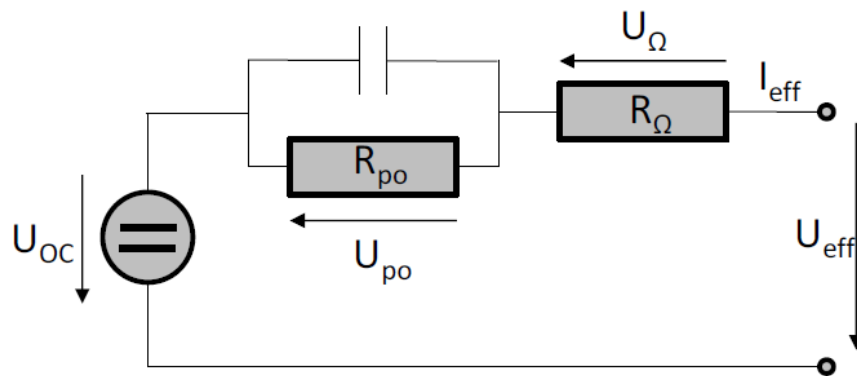


Figure 34: Main heat sources of a battery cell, based on (Jossen & Weydanz, 2019)

$$P_{heat,\Omega} = R_{\Omega} \cdot I_{eff}^2 \quad (3)$$

$$P_{heat,p} = U_p \cdot I_{eff} \quad (4)$$

g. Battery Cells Modelling

Designing a battery on the aeroplanes should be studied through thermal properties, weight, and energy. An easy way is to know values for the particular energy e_{cell} , the specific power p_{cell} and the required energy E_{req} . After recognising, it can be defined. The cell weight w_{cell} for a provided application case as follows:

$$w_{cell} = \frac{E_{req}}{e_{cell}} \quad (5)$$

And therefore the maximal discharge power P_{cell} is

$$P_{cell} = p_{cell} w_{cell} \quad (6)$$

The requirement volume and heat rise can be defined using the energy density v_{cell} and discharge efficiency η_{dis} . Therefore, the cell volume implies:

$$V_{cell} = \frac{E_{req}}{v_{cell}} \quad (7)$$

Moreover, the heat losses produced by the cell is defined by:

$$P_{heat,cell} = P_{cell} * (1 - \eta_{dis}) \quad (8)$$

2. Electrical Power Transmission

The conductors are the connecting link between the supplied energy and the loads. They are the main element of the transmission system, as they provide electricity to loads such as actuators, avionics, and the air conditioning system. On "More Electric Aircraft," the electrical distribution transfers high power (in megawatts), which represents a new challenge on the aircraft. Therefore, a model for high power conductors is explained hereafter.

a. Traditional Elements For Power Transmission

In general, among the conductor's materials, copper and aluminium are more prevalent in design on today's aircraft, where these materials are used onboard

the plane in electrical networks. To choose a better material, it should take into consideration the resistivity, density, and resistance. In terms of density, the copper is a denser metal than aluminium. Similarly, in terms of resistivities, copper is better than aluminium. For example, the resistivity of pure copper and aluminium is 1.7 and 3.2, while the densities are 3.2 and 2.7, respectively. The dependence of these substances is only on the material itself, not through the size or shape of the material. On the other hand, the resistance depends on the size and shape of the material. To calculate the resistance, it should take into consideration three things:

- Length " l ," The longer the distance of the wire, the higher its resistance
- Cross-sectional area " A ," the more significant the area, the smaller its resistance
- the resistivity of the material " ρ ," the higher the resistivity, the bigger its resistance.

$$R = \frac{\rho l}{A} \quad (9)$$

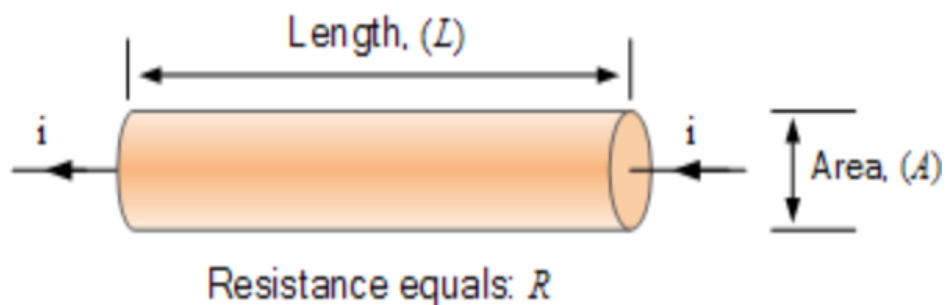


Figure 35: Single Line Conductor

Copper is more used on aircraft compared to aluminium since flexibility and corrosion features are better in using, and conductor cross-sections are smaller (Hufnagel, 1988). The batteries supply the DC loads, and for getting AC loads, the inverter unit changes DC to AC for feeding to AC loads systems. The electric power given in a DC conductor can be represented by

$$P = U.I \quad (10)$$

In the conducting cables, there is a resistance that differs from material to another. This resistance leads to a loss of energy that is in the form of heat. With different resistance value, the amount of loss varies. It can be designed with temperature coefficient α for aluminium and copper, according to the equation (11).

$$R = R_{20}(1 + \alpha.\Delta t) \quad (11)$$

The resistivity of the aluminium and the copper at various temperatures are presented in Table 3

Table 3: Conductor Temperature Characteristics

| Specific Resistivity | | |
|-----------------------------|------------------|---------------|
| Temperature | Aluminium | Copper |
| 20 | 0.0286 | 0.0178 |
| 60 | 0.0332 | 0.0205 |
| 90 | 0.0366 | 0.0255 |

As temperatures rise to above 90, the loss begins to affect negatively, and as the energy in the cable increases, temperatures rise with it. Figure 36 and Figure 37 illustrate the specific losses of related cables for a single cable with an aluminium and copper conductor, respectively.

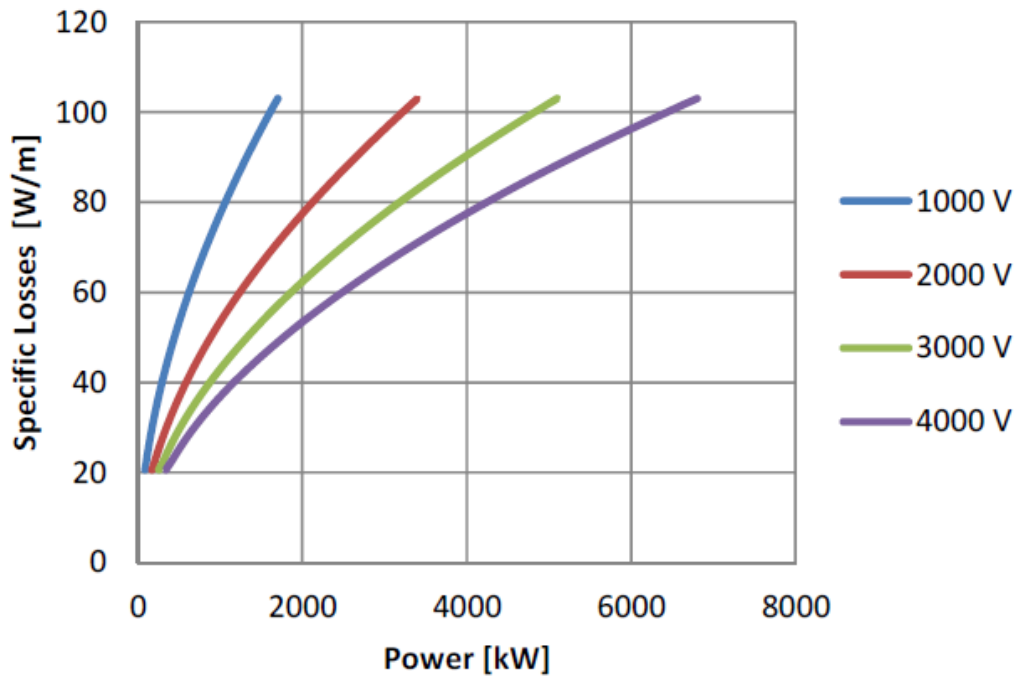


Figure 36: Aluminium Cable Losses

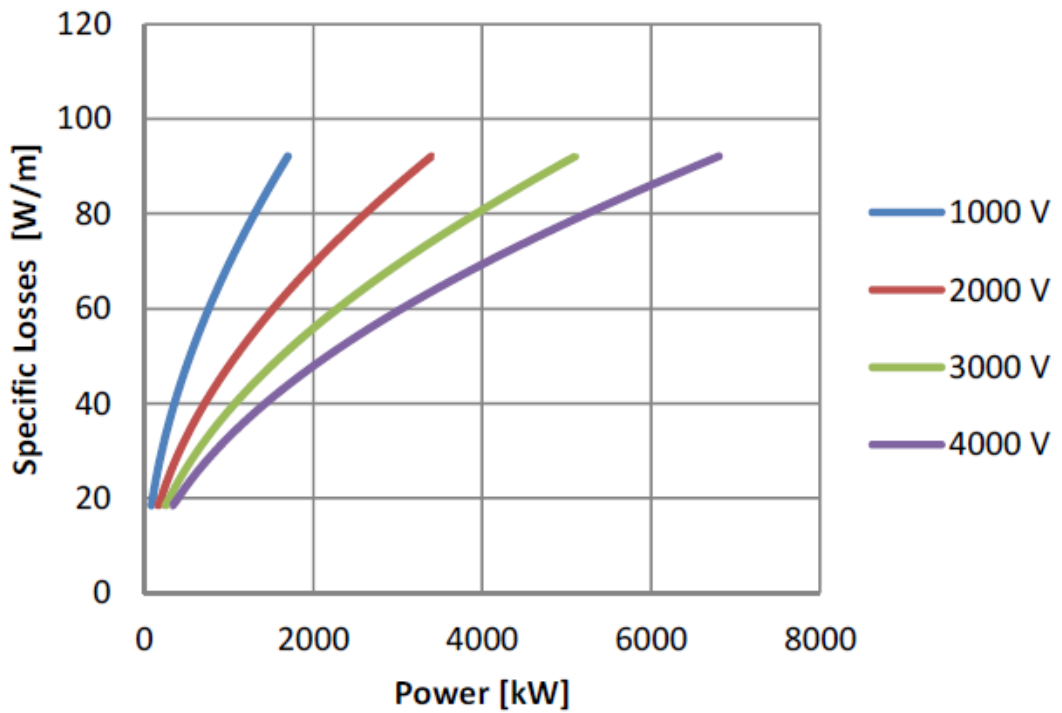


Figure 37: Copper Cable Losses

b. Superconducting Materials For Power Transmission

At a low level of power, standard cables using metallic conductors give suitable energy transmission. However, in a high level of power, standard cables are not useful due to heat losses. To solve this problem, using superconducting wires is the most suitable solution due to high temperature superconducting (HTS). When the superconducting wires are cooled below the transition temperature, they become nearly zero resistance. So, in this case, the conductor HTS will be capable of enduring massive current density compared to the traditional conductor materials. HTS use saves the cable weight and reduces waste. However, the drawback of this technology is that a cooling system employed onboard. Using a cooling system for the cable, in turn, adds weight and demand to the transportation system. HTS use saves the cable weight and reduces waste. However, the drawback of this technology is that a cooling system employed onboard. Using a cooling system for the cable, in turn, adds weight and demand to the transportation system. Superconducting DC cables are the new technology in medical screening applications (Magnetic Resonance Imaging, MRI) and also using for ground-based high-power transmission systems (Weber & Farrell, 2009, DOE Cooperative Agreement Number DE-FC36-03GO013301). Although the resistivity is almost zero in the HTS conductor, it results in heat flow in the cryogenic system which must be removed by the cooling system to preserve the temperature, and the principal sources of induction of heat are:

- Defects of vacuum tube insulation (spacers, defective vacuum, heat transmission).
- Termination: thermal conductivity and ohmic losses in the resistor that connects the HTS wires to the conventional network.

Cable Construction

- Conductor Stabilizer
 - HTS Phase Conductor
 - Conductor Screen
 - Electrical Insulation
 - Insulation Screen
 - HTS Shield
 - Core Binder
 - Inner Cryostat
 - Thermal Insulation
 - Vacuum Spacer
 - Outer Cryostat
 - Outer Sheath
- 

Figure 38: HTS Cable Construction

C. Secondary Power Distribution

To operate and turn off any electrical load, it should use a suitable switch or circuit breaker. When the load is small, choosing a switch or breaker is not tricky or complicated. However, with the use of a high load, it is more challenging. The use of switches in large loads causes sparks, which prevent the electric disconnection and raise the temperature of the switches. It must adopt a switch or circuit breaker that can withstand this high power and can switch on and off any payload safely and securely. To do this, it should use a proper switch that can handle the high loads. There are two types of switches, mechanical and solid-state devices. Most loads are electrically controlled, and the solid-state switches can manage the controlling because there are easy to use and maintain. Therefore, Solid-state switches are used today in a wide range from low power products up to high voltage, significant current employment in power grid modes. In Figure 40, the popular switch models and their working ranges are displayed. On aircraft,

IGBT's are more proper and therefore examined for additional studies. Solid-state switches are more reliable than mechanical switch systems for several reasons:

- Solid-state switches are not dependent on the moving parts, while the mechanicals has moving parts that can be disrupted with frequent use.
- Solid-state switches are small and lightweight, and this reduces the weight on the plane.
- Controlling the solid-state switches is more comfortable than the mechanical, because it controls electrically, while the mechanical switches are controlled manually.

An ideal state of IGBT's weight is presented in Figure 39. According to this data, a weight is obtained in equation (12).

$$w_{IGBT}[kg] = 1.6 \times 10^{-4} \cdot P_{IGBT}[KW] + 0.6 \quad (12)$$

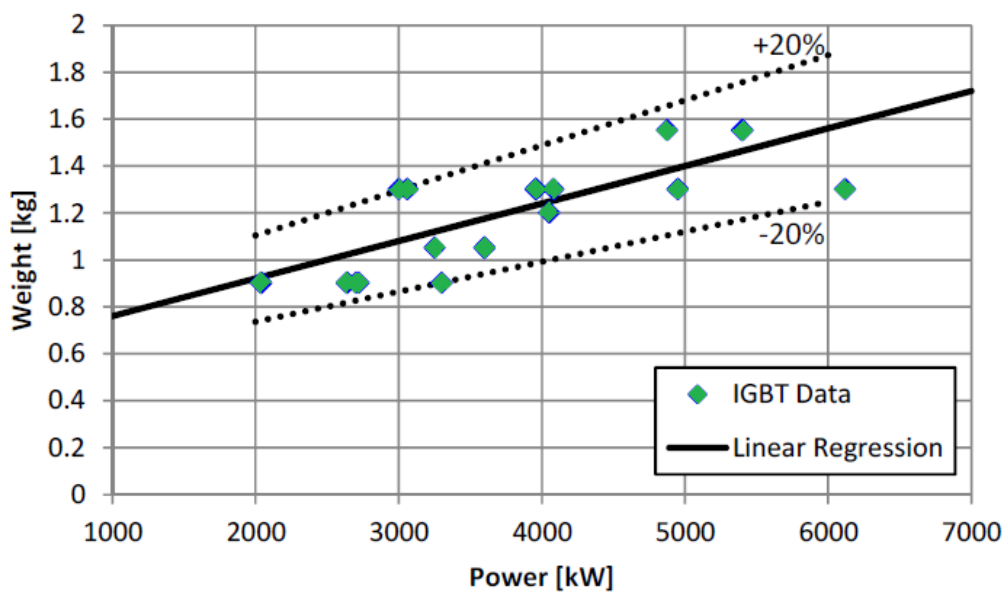


Figure 39: IGBT Weight VS Power

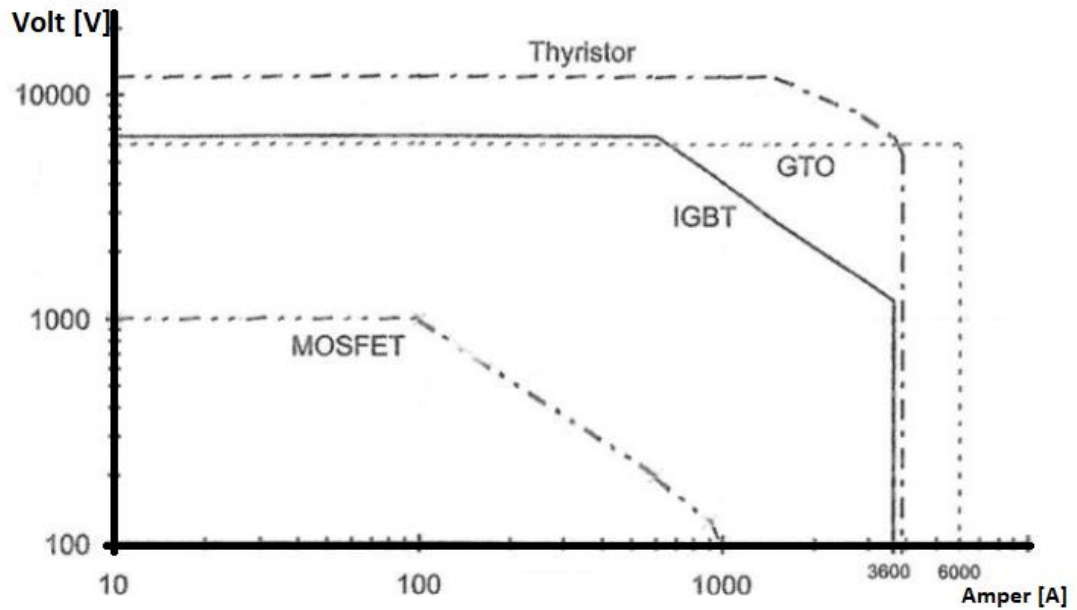


Figure 40: Solid-State Switch Models (Hofmann, 2010)

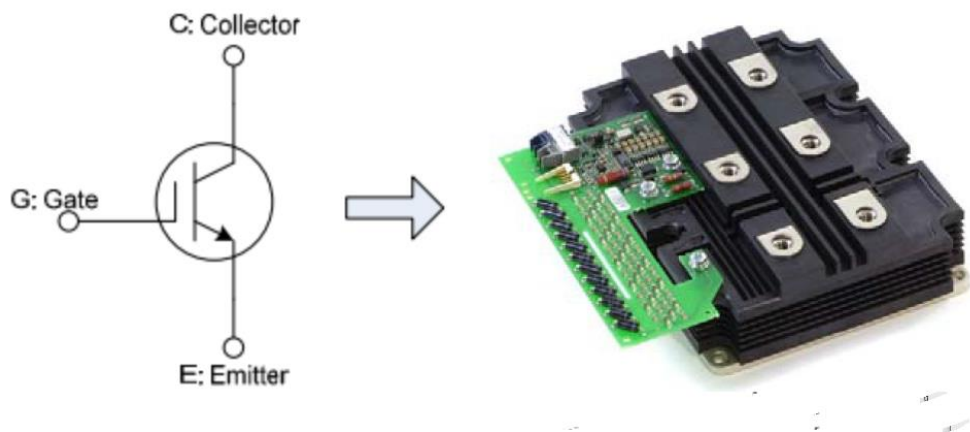


Figure 41: IGBT Module

During the forward connection state, the voltage drops U_{drop} due to the intrinsic semiconductor properties. And through equation (13), the power transmission losses P_{Loss} can be determined. This voltage drop creates heat, which must be eliminated through suitable coolers. Through Figure 42, typical voltage drop values for the most recent IGBT are shown. Based on Figure 42, a linear regression equation was established, as presented in equation (14).

$$P_{Loss} = U_{drop} \cdot I \quad (13)$$

$$U_{drop}[V] = 4.3 \times 10^{-4} \cdot U_{block}[V] + 1.4 \quad (14)$$

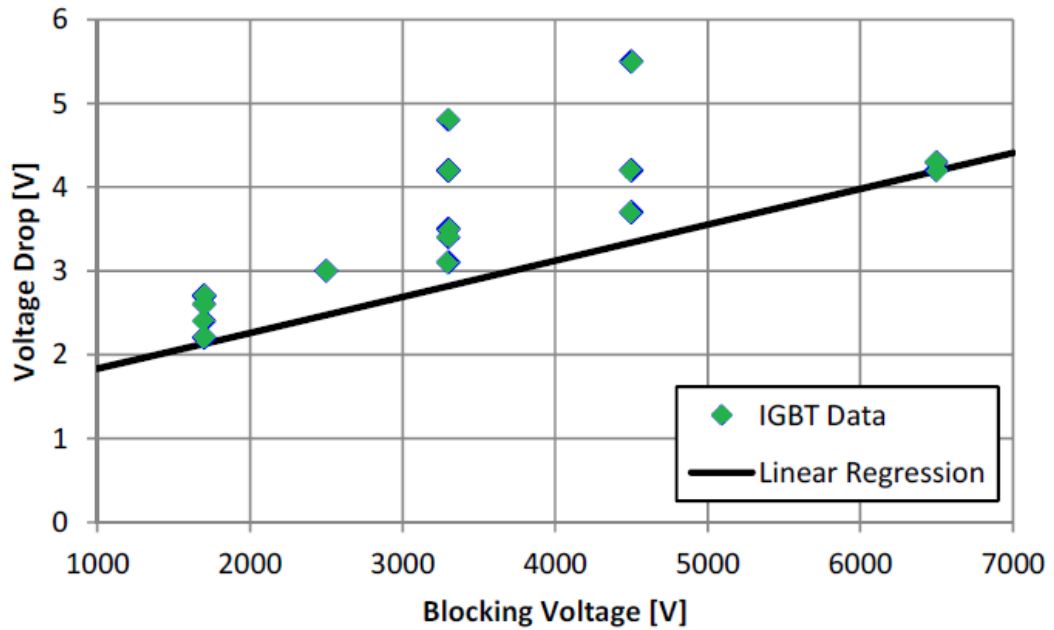


Figure 42: IGBT Voltage Drop U_{drop} VS Blocking Voltage U_{block}

Vacuum conductors

One of the disadvantages using semiconductor is during a shutdown; there is no galvanic separation. (Galvanic isolation is a system of separating working parts of electrical operations to block current flow). If the galvanic separation is applied, the mechanical switch of the solid-state switch must be examined. It should take into consideration that this mechanical relay is only used for switching in the absence of a load. Therefore, no problems related to high-current DC switching occur. However, it is worth noting that at high altitudes, the electrical insulation strength decreases, and in this case, vacuum breakers should

be used. The use of vacuum switches leads to an increase in the weight on the plane.

1. Electric Motors

Electric motors are an essential component of a plane. Electric motors convert electrical energy toward mechanical force. The mechanical power is determined by the shaft speed rotation N_{shaft} and the torque M_{shaft} :

$$P_{shaft} = N_{shaft} \cdot M_{shaft} \cdot 2\pi \quad (15)$$

During the running of the motor, some loss occurs due to resistance, eddy currents, and mechanical losses. Thus, the motor efficiency η_{mot} is measured by dividing the mechanical power P_{shaft} with input power P_{in} as represented in the following equation:

$$\eta_{mot} = \frac{P_{shaft}}{P_{in}} \quad (16)$$

In Figure 43, there are properties of typical operating characteristics of electric motors. It can be observed that at the low speeds of the shaft, the torque is at its maximum rated motor power. Then the shaft speed increases more strongly with a constant force until the maximum allowable speed of the shaft is reached.

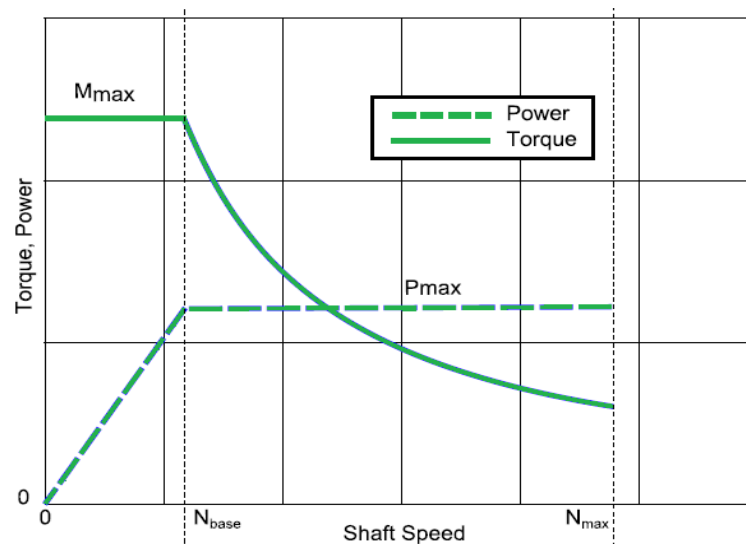


Figure 43: Ideal Electric Motor Characteristics (Hofmann, 2010)

With a lot of electric motors entering many areas, studies and research have been done to make small, and lightweight motors and they have been used in many fields, especially for bicycles, motorcycles, cars, and buses. The most standard motors used were the asynchronous motor, synchronous motor, and switched reluctance motor. The details explanation for each motor is described in (Hofmann, 2010). As for the generators currently used for aircraft and electric cars, its energy output is about 2-6 kW / kg, except for the weight that is intended for cooling. The efficiency of these motors is about 90 % (Dudley, 2010) (Schumann , Geinitz, & Nitschmann, 2012).

a. Induction AC Motors

AC induction motors are one of the most popular motors for aircraft applications. The induction motor rotor often is squirrel cage, that rotates with the turning of the magnetic field. The exciting thing in the induction motor is that there are no needs for using slip ring brush gear. The motor speed rotation depends on the speed of frequency and number of poles present in the rotor. Other advantages of this motor are that there is always an alternating and stable AC power source onboard and that it is also considered not quite expensive in terms of cost.

b. Three-Phase PMSM

In the development of technology in the last centuries, the Permanent Magnet Synchronous Motors (PMSMs) become one of the most used in high-performance application compared to other types of ac motor due to numerous advantageous features including high torque to current ratio, immense power to weight ratio, higher efficiency, and robustness (Maamoun, Alsayed, & Shaltout, 2013). The synchronous motors work at constant speed despite changing the load. The synchronous motors work in high performance and are applied mostly in a precision application. The rotor of the synchronous motor creates a constant magnetic field, and the stator creates a rotary magnetic field. The rotor is excited by a DC power supply, so it acts like a permanent magnet. Therefore, the rotor and rotating magnetic field pull each other and therefore lock magnetically. Synchronous speed can be determined according to:

$$N_s = \frac{120 f_{se}}{P} \quad (17)$$

Where N_s is the rotating speed in rpm, f_{se} is the frequency of the electricity, and P is the number of poles.

Mathematical Model of PMSM

The Permanent Magnet Synchronous Motor (PMSM) can be represented mathematically in the following equation (Kamel, Hasanien, & Ibrahim, 2009) :

$$v_d = R_s i_d + \frac{d\phi_d}{dt} - w\phi_q \quad (18)$$

$$v_q = R_s i_q + \frac{d\phi_q}{dt} + w\phi_d \quad (19)$$

Where R_s represents the stator resistance, i_d represents the current of the d-axis current, ϕ_d represents flux in the d-direction, ϕ_q represents flux in the q-direction, and i_q represents the q-axis current. Flux-linkage is represented in d-q coordinates:

$$\phi_d = L_d i_d + \phi_m \quad (20)$$

$$\phi_q = L_q i_q \quad (21)$$

Where L_d represents the inductance of d-axis, Ψ_m represents the flux-linkage, and L_q represents the inductance of q-axis. The mechanical motor energy is defined:

$$T = J \frac{dw}{dt} + BW + T_L \quad (22)$$

Where T is the motor torque, T_L the load torque, J moment of inertia, and B the friction coefficient. This equation reveals that when there is a difference within the motor torque T and the load torque T_L , the rotor speed will increase. Acceleration relies on the moment of inertia J , and the friction coefficient B . The motor torque representation with d-q magnitudes is:

$$T = 1.5P(\phi_d i_q - \phi_q i_d) \quad (23)$$

Where p is the number in pole pairs in the rotor, also, the motor torque can be reached from the magnet flux-linkage and the d-q axis currents in the following:

$$T = 1.5P(\Phi_m i_q - (L_q - L_d)i_q i_q) \quad (24)$$

Equation (24) explains that, if the d-axis inductance L_d is similar to the q-axis inductance L_q , the motor torque rely just on the q-axis current component i_q as in the following equation:

$$T = 1.5P\Phi_m i_q \quad (25)$$

Speed Control of PMSM

As shown in Figure 44, the controller receives the reference speed and the actual speed as input and i_q as output. Then, the current regulator takes the desired current i_q and actual current to give us the corresponding pulses. Furthermore, the power converter makes these pulses to converts the direct current (DC) into three-phase alternating current, which in turn feeds the motor.

Traditional PI Controller:

The PI controller has a long history in controlling the motors. It is widely used in industrial control systems. In a closed control loop, the pi controller keeps eliminating the error to achieve the desired parameters. The output of the PI controller in the time domain is defined (Kamel, Hasanien, & Ibrahim, 2009):

$$v_0(t) = k_p e(t) + k_i \int_0^t e(t) dt \quad (26)$$

Where v_0 is the output of the controller, k_p is the proportional gain, and $e(t)$ is the speed error signal. The error signal is formed by subtracting the desired value with the actual value. The main advantage is used to eliminate the small steady-state error.

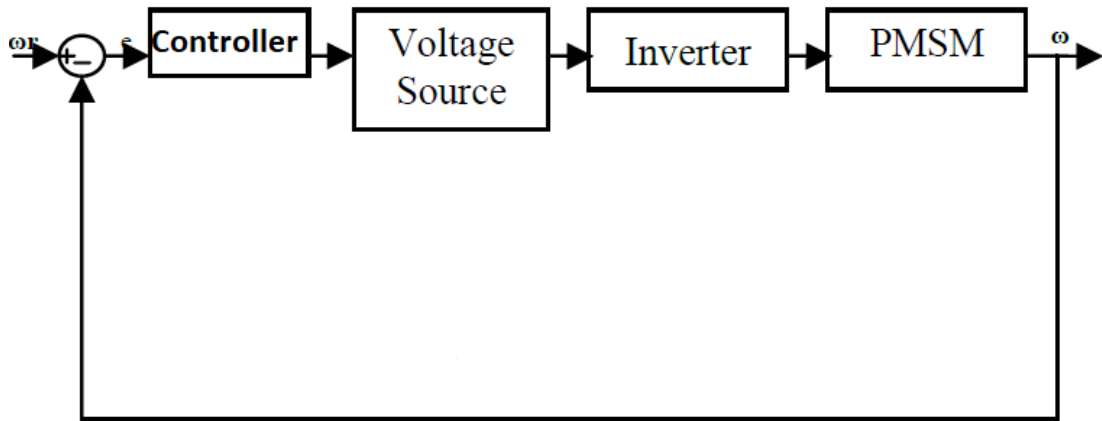


Figure 44: Speed Control Of The PMSM

Fuzzy Logic Controller:

The structure of the fuzzy controller is presented in Figure 45. It has two inputs and one output. The first input $e(t)$ is the speed error, and the second is the error speed change $ce(t)$. The output is changed in reference phase current $\Delta i_q^*(t)$

The variables $e(t)$ and $ce(t)$ are (Karakaya & Karakas, 2007):

$$e(t) = W^*(t) - w(t) \quad (27)$$

$$ce(t) = e(t) - e(t - 1) \quad (28)$$

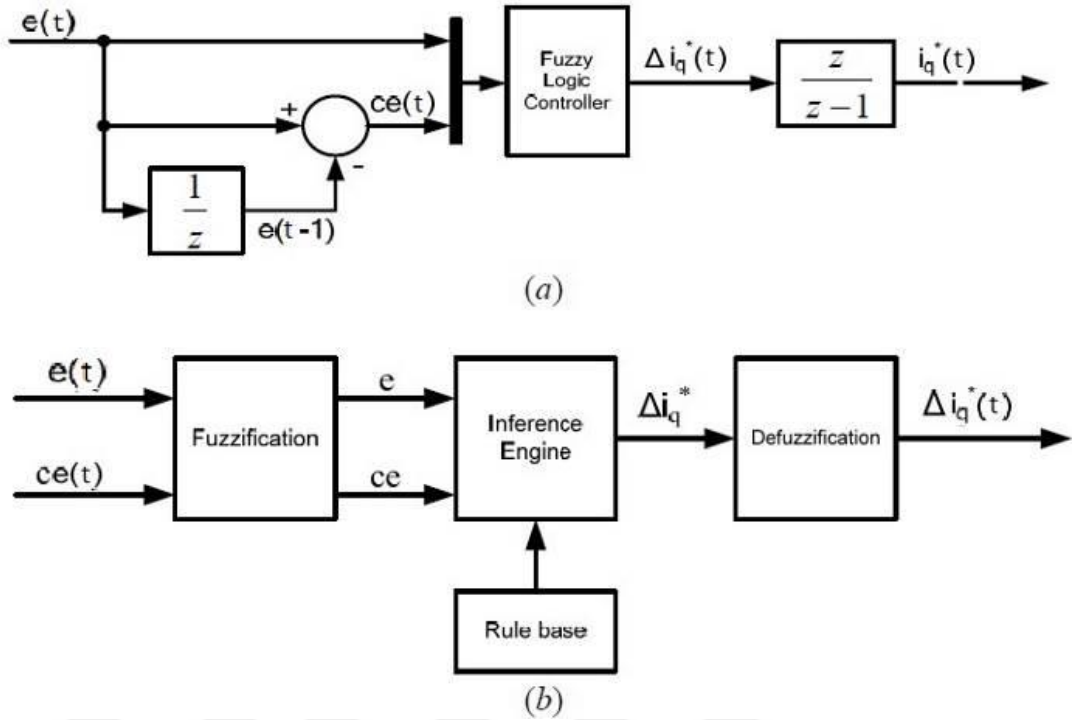


Figure 45: FLC Structure

Where $w^*(t)$ is the reference speed, and $w(t)$ is the actual speed value. The features of FLC are fuzzification, rule base, and defuzzification. In fuzzification, the crisp variables $e(k)$ and $ce(k)$ are outlined into the membership function and expressed by the fuzzy logic's linguistic variable. The mapping could be in a triangle, a trapezoid, a bell, or any other appropriate form. The universes of the discourse of the input variables (e , ce) vary from -1 to 1. The output varies from 0 to 1. Each universe of discourse is divided into seven fuzzy sets: Negative Big (NB), Negative Medium (NM), Negative Small (NS), Zero (Z), Positive Small (PS), Positive Medium (PM), and Positive Big (PB). After that, the FL controller executes the 49 control rules shown in Table 4. The rules are implemented using the knowledge and experience of control engineers. According to the rules, the FLC analyses the inputs and executes the corresponding. The membership function is shown in Figure 46, and the rules are shown in Table 4.

The reference current is

$$i_q^*(t) = i_q^*(t - 1) + \Delta i_q^*(t) \quad (29)$$

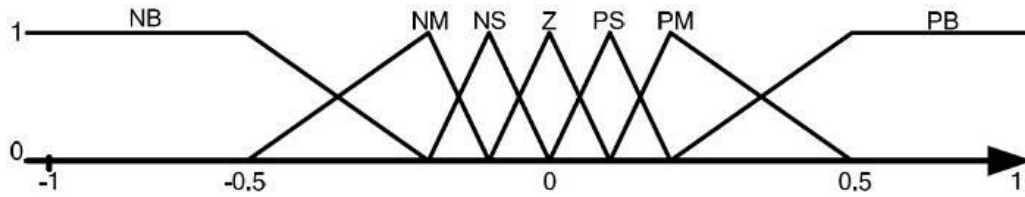


Figure 46: FLC Membership Function Of Fuzzy Logic Controller For E, CE, And ΔI_q

Table 4: FLC Rules

| | | Error "e" | | | | | | |
|-------------------------|----|-----------|----|----|----|----|----|--|
| | | NB | NS | Z | PS | PM | PB | |
| Change of error "ce" | NB | NB | NB | NB | NM | NS | Z | |
| | NM | NB | NB | NM | NS | Z | PS | |
| | NS | NB | NM | NS | Z | PS | PM | |
| | Z | NB | NM | Z | PS | PM | PB | |
| | PS | NM | NS | Z | PM | PB | PB | |
| | PM | NS | Z | PS | PB | PB | PB | |
| | PB | Z | PS | PM | PB | PB | PB | |

c. Five-Phase PMSM

Recently, multiphase drives have obtained developing attention. Indeed, multiphase drives present numerous benefits over three-phase drives in high power applications such as decreasing the current per phase without raising the voltage per phase, lower DC link current harmonics, and higher reliability. Multiphase motors can continue working under the failure of one or more phases (Kamel, Abdelkader, & Said) (Xue & Wen, 2005) (Chen, Hsu, & Chang, 2014). Also, for the three-phase motors, the windings are combined either in Y-connection or Δ -connection, but for the five-phase motors, there are three connections for the windings, which can expand the speedrunning range (Chen, Hsu, & Chang, 2014). Multiphase machines constitute either induction or synchronous multiphase machines. The five-phase permanent magnet synchronous motor has become more and more considered in different applications. (Chen, Hsu, & Chang, 2014).

Mathematical Model of Five-Phase PMSM

The equivalent model of the five-phase PMSM is presented in a rotating reference (d_p q_p d_s q_s) frame (Hosseyni, Trabelsi, & Mimouni, 2018)

$$v_{dp} = R_s I_{dp} + L_p \frac{dI_{dp}}{dt} - W_e L_p I_{qp} \quad (30)$$

$$v_{qp} = R_s I_{qp} + L_p \frac{dI_{qp}}{dt} + W_e L_p I_{dp} + \sqrt{\frac{5}{2}} \Phi_m W_e \quad (31)$$

$$v_{ds} = R_s I_{ds} + L_s \frac{dI_{ds}}{dt} - 3W_e L_s I_{qs} \quad (32)$$

$$v_{qs} = R_s I_{qs} + L_s \frac{dI_{qs}}{dt} + 3W_e L_s I_{ds} \quad (33)$$

$$J \frac{d\Omega}{dt} = T_{em} - T_L - f\Omega \quad (34)$$

The electromagnetic torque is given by

$$T_{em} = \sqrt{\frac{5}{2}} \Phi_m I_{qp} \quad (35)$$

$$\frac{dI_{dp}}{dt} = b_1 I_{dp} + W_e I_{qp} + \frac{1}{L_p} v_{dp} \quad (36)$$

$$\frac{dI_{qp}}{dt} = b_1 I_{qp} - W_e I_{dp} + b_2 W_e + \frac{1}{L_p} v_{qp} \quad (37)$$

$$\frac{dI_{ds}}{dt} = b_3 I_{ds} + 3W_e I_{qs} + \frac{1}{L_p} v_{ds} \quad (38)$$

$$\frac{dI_{qs}}{dt} = b_3 I_{qs} - 3W_e I_{ds} + \frac{1}{L_p} v_{qs} \quad (39)$$

$$\frac{d\Omega}{dt} = T_{em} + b_5 T_L + b_6 \Omega \quad (40)$$

$$b_1 = -\frac{R_s}{L_p}; b_2 = -\frac{\sqrt{\frac{5}{2}}\phi_f}{L_p}; b_3 = -\frac{R_s}{L_s}; b_4 = \frac{\sqrt{\frac{5}{2}}P\phi_f}{J}; \quad (41)$$

$$b_5 = -\frac{1}{J}; b_6 = -\frac{f}{J}$$

Five-Phase Inverter

The five-phase power circuit inverter is shown in Figure 47. It contains ten switches. Each switch consists of two power—semiconductor devices, the bipolar transistor or IGBT and a diode. The switches are connecting in anti-parallel. The relation between the input inverter's switches and the outputs voltage is (Kesraoui, Echeikh, Iqbal, & Mimouni, 2019)

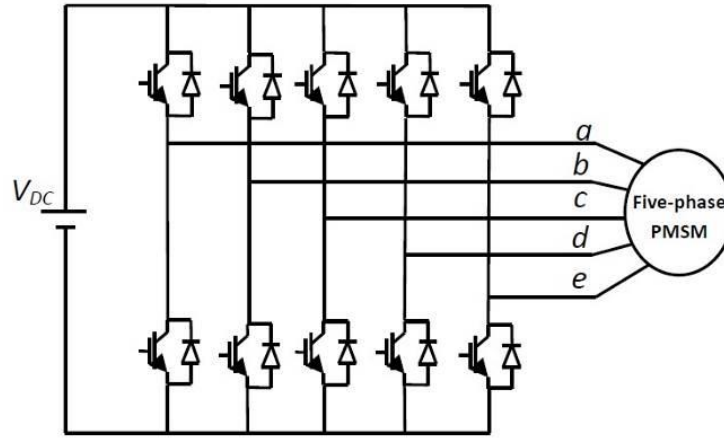


Figure 47: Schematic Diagram Of A Five-Phase Voltage Source Inverter

There is thirty-two space voltage vector in the five-phase inverter; thirty nonzero voltage vectors and two zero voltage vectors. These space vectors are projected ($\alpha_p\beta_p$) subspace and ($\alpha_s\beta_s$) subspace. These space vectors are projected in Figure 48 and Figure 49 (Parsa & Toliyat, 2007):

$$v_\alpha = Re \left\{ \frac{2}{5} v_{dc} \left[S_1 + S_2 e^{j\frac{2\pi}{5}} + S_3 e^{j\frac{4\pi}{5}} + S_4 e^{-j\frac{4\pi}{5}} + S_5 e^{-j\frac{2\pi}{5}} \right] \right\} \quad (42)$$

$$v_{\beta} = \text{Re} \left\{ \frac{2}{5} v_{dc} \left[S_1 + S_2 e^{j\frac{2\pi}{5}} + S_3 e^{j\frac{4\pi}{5}} + S_4 e^{-j\frac{4\pi}{5}} + S_5 e^{-j\frac{2\pi}{5}} \right] \right\} \quad (43)$$

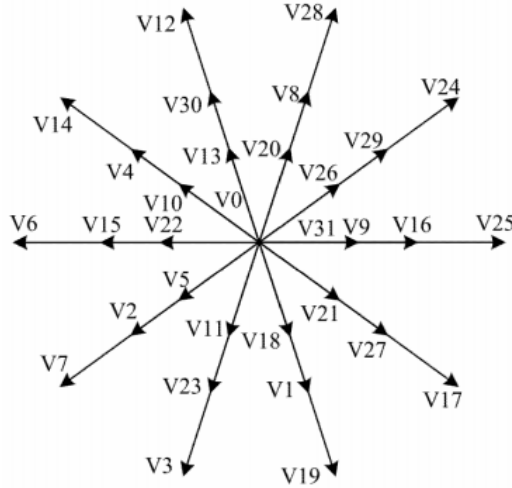


Figure 48: Fundamental Switching Voltage Vectors

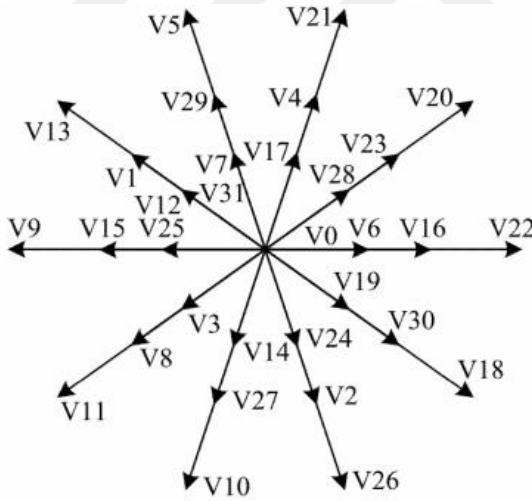


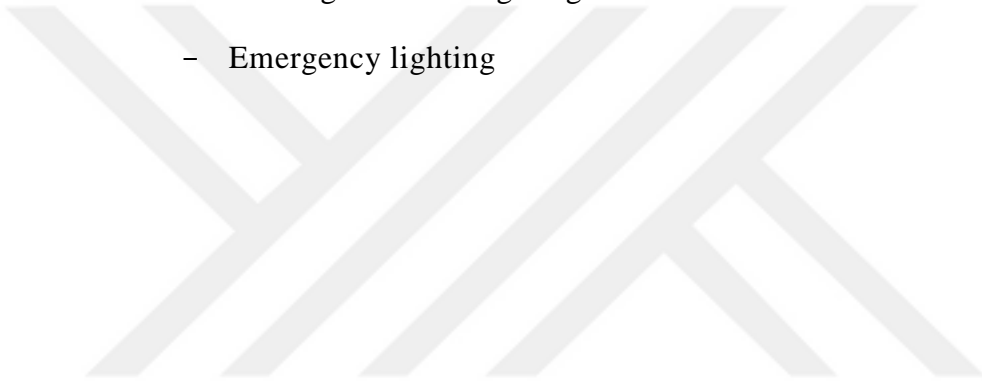
Figure 49: Harmonic Switching Voltage Vectors

2. Lighting

Lighting systems describe an essential element of the aircraft's electrical services. A large number of new aviation operating time happens during night or low-visibility situations. The availability of sufficient lighting is required for the safe operation of the aircraft. Lighting systems may be classified as follows:

- Outside Lighting Systems
 - Flying lights

- Working lights
- Strobe lights and High-Intensity Strobe Lights (HISL)
- Landing lights
- examination lights (wing/engine anti-ice)
- Emergency departure lights
- Searchlights (for exploration and rescue or police aircraft)
- Inside Lighting Systems
 - Cockpit lighting
 - Passenger service lighting
 - Emergency lighting



IV. PROPOSED MEA DESIGN

The schematic of the system is presented in **Hata! Başvuru kaynağı bulunamadı.. Hata! Başvuru kaynağı bulunamadı.** describes a half-aircraft model on MEA. A full-aircraft includes other components such as APU, and alternative generators are not included. The electricals systems include a generator, an AC bus, and loads.

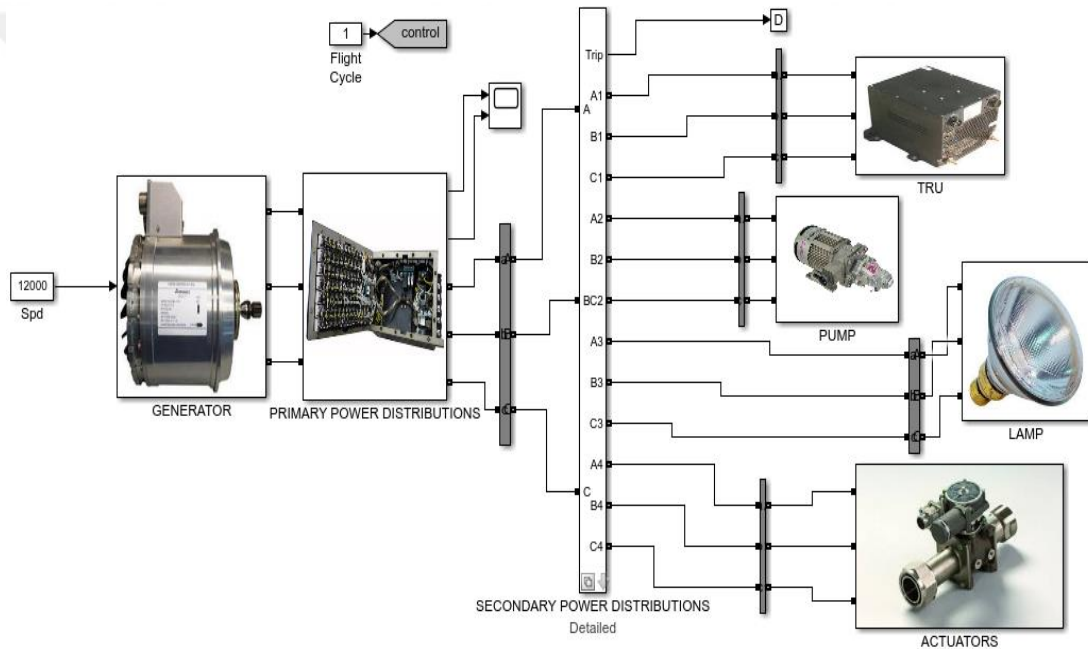


Figure 50: Typical MEA Design

A. Generators

There is a range of options for generating power on aircraft. The generators on aircraft are typically driven by a connection from the gas turbine to the turbines at different speeds. As described before, three types of generators can be applied:

- Integrated Drives
- VSCF Cyclo-Converter
- VSCF DC Link

1. Integrated Drives

As described before, the gas turbine rotates the generator' shaft to generate power. The output of generators is controlled bu using a generator control unit. The GCU takes the output voltage and current and produce a suitable magnetic field to remain the output voltage constant. The output voltage and currents are switched on/off by using a generator control breaker GCU.

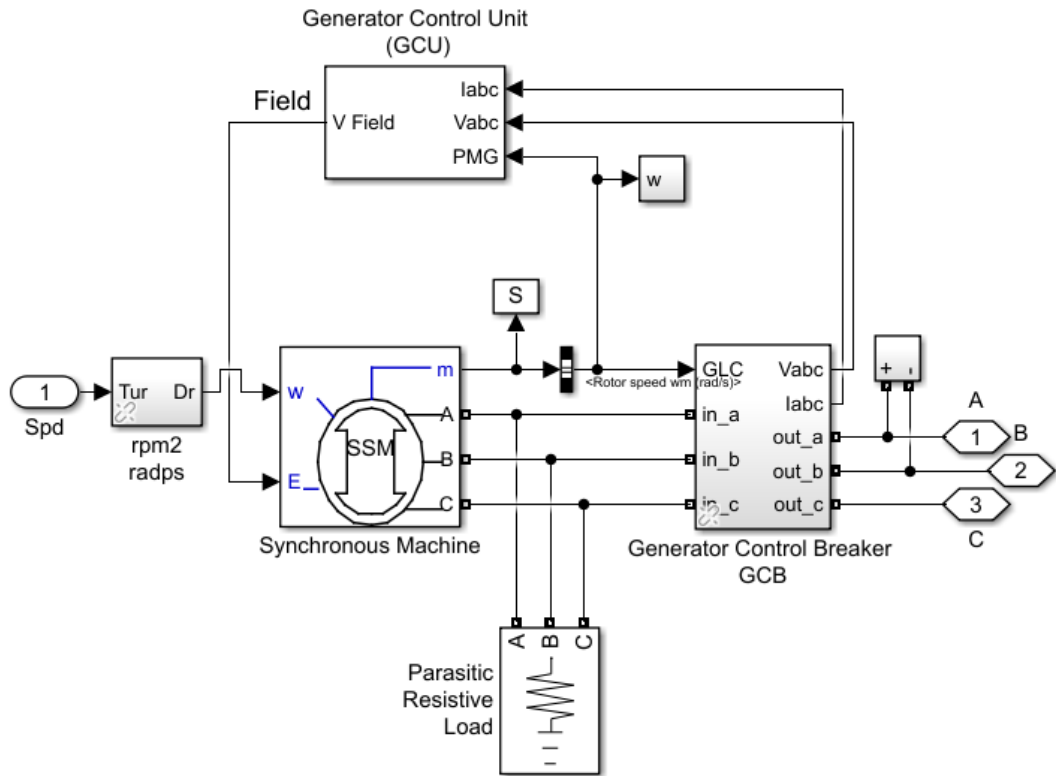


Figure 51: Integrated Drive Generator

2. VSCF Cyclo-Converter

The VSCF consists of three main parts: power source, transformer, and cyclo-converter. The generators include three transformer and three cyclo-converters. The cyclo-converter converts the frequency and voltage without using any standard DC link. The producing voltage and frequency of a cyclo-converter can be changed continuously and individually using a control circuit. It consists of back to back combined controlled rectifiers whose producing voltage and frequency can be

controlled by tuning firing angles of rectifiers. The output power of cyclo-converter is, therefore, connected to GCB.

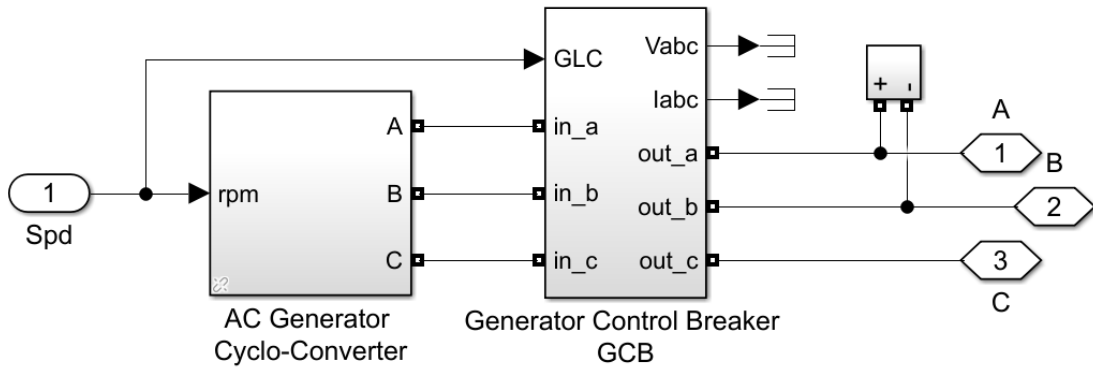


Figure 52: VSCF Cyclo-Converter System

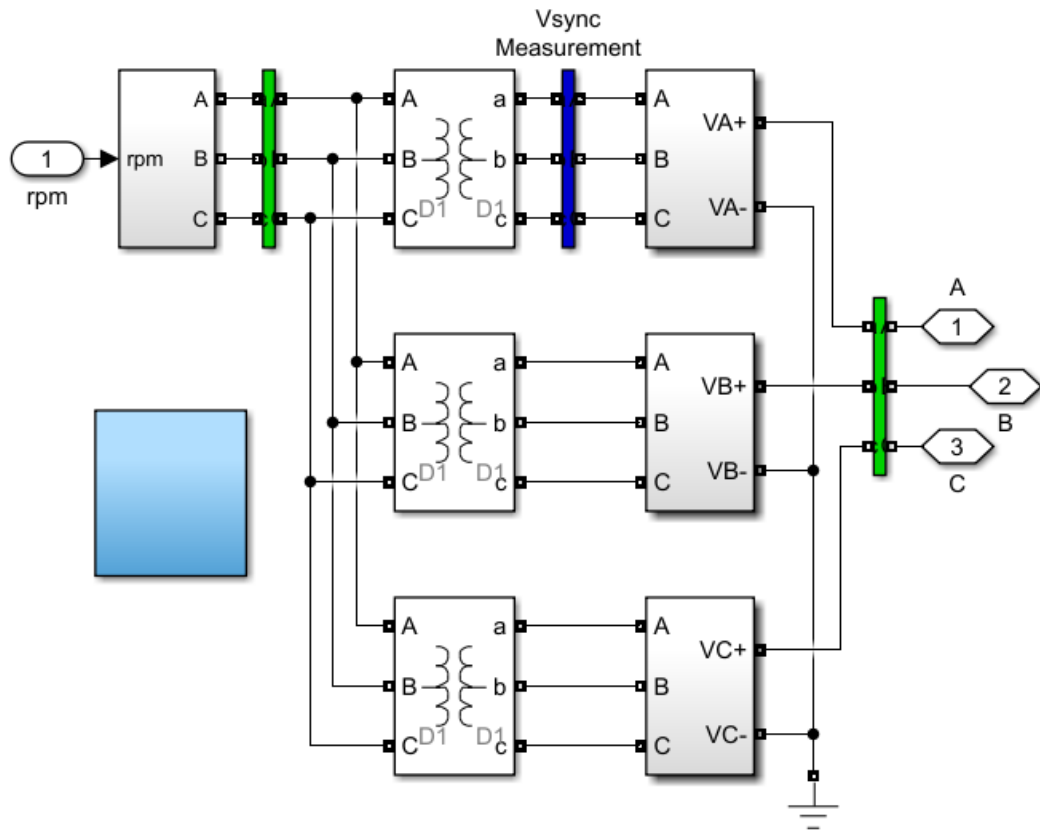


Figure 53: VSCF Cyclo-Converter Generator

3. VSCF DC Link

As In VSCF DC-Link, the essential part is the ac ac inverter. It converts the AC voltage to dc-link then AC voltage with different frequencies. The output is connected to an LC filter. The voltage regulator measures the output voltage and generates suitable gates to remain the output at the desired value.

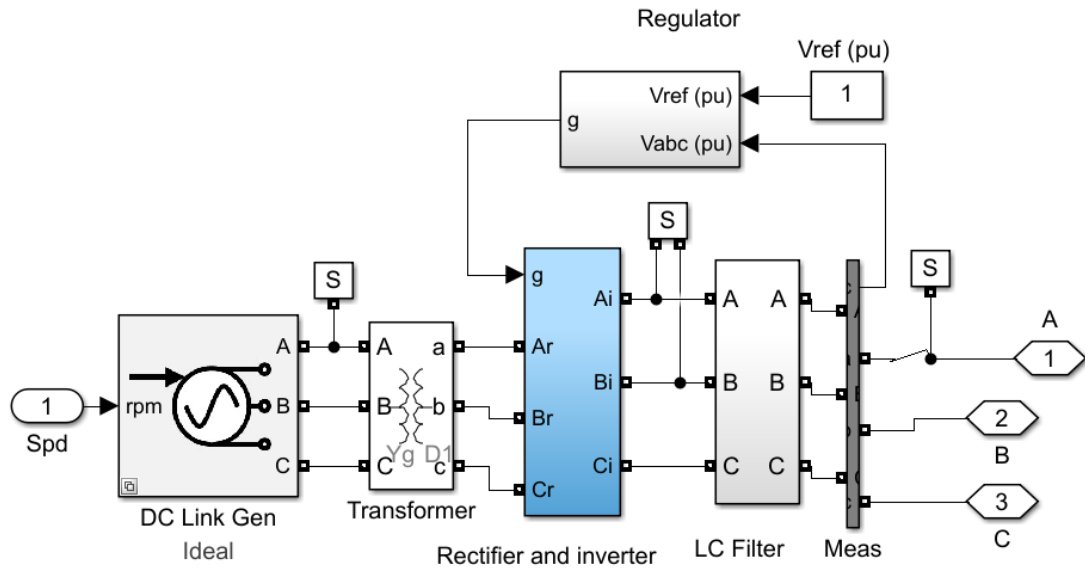


Figure 54: VSCF DC Link

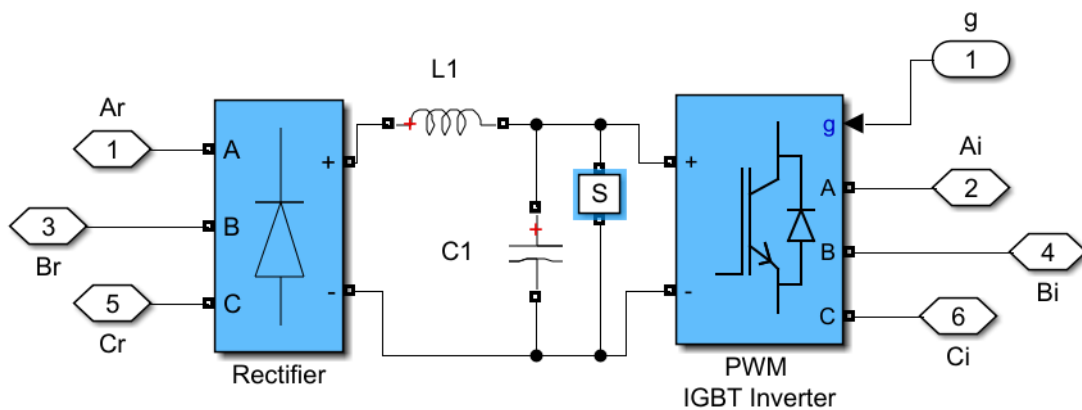


Figure 55: AC/AC Inverter

B. Primary Power Distribution

The first power generation includes three-phase measurement, GCU, and GCB. The Three-Phase V-I Measurement block is utilized to calculate instantaneous three-phase voltages and currents in a circuit. The instantaneous three-phase voltages and currents are sent to GCU to produce a suitable field for the generator. The GCU, as presented

in Figure 56, it converts the three-phase time-domain signals from a stationary phase system (ABC) to a rotating system (dq0). Therefore the rotating coordinate system (dq0) is transformed into the corresponding magnetic field using the excitation system block.

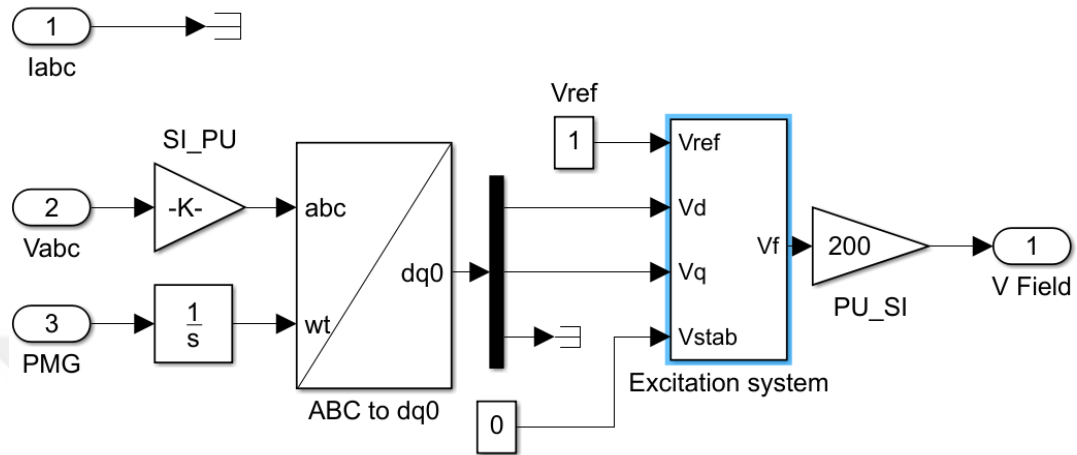


Figure 56: GCU

C. Secondary Power Distribution

The secondary power distribution consists of multiple contactors and breakers. Each load is connected to a corresponding breaker to protect the loads from over high current. The loads are switch on/off according to the flight cycle.

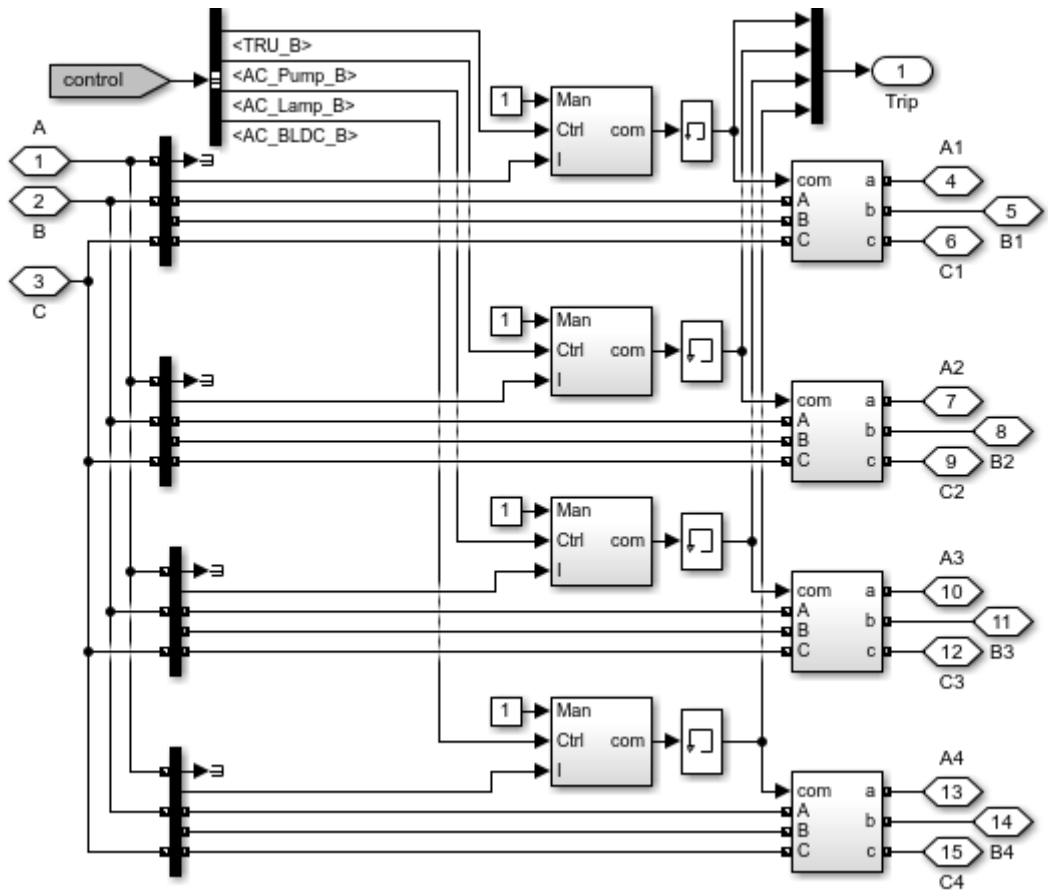


Figure 57: Secondary Power Distribution

D. Transformer Rectifier Unit

The TRU transforms the AC voltage to 28 DC voltage. The transformers are using to transforms the generator AC voltage to 28V AC. Then, 28 AC voltage is converted to DC by using two universal bridge. The output of TRU is connected to DC power distribution that includes switches and breakers to each DC loads. DC loads include lamps, a heater, a fuel pump, and a battery.

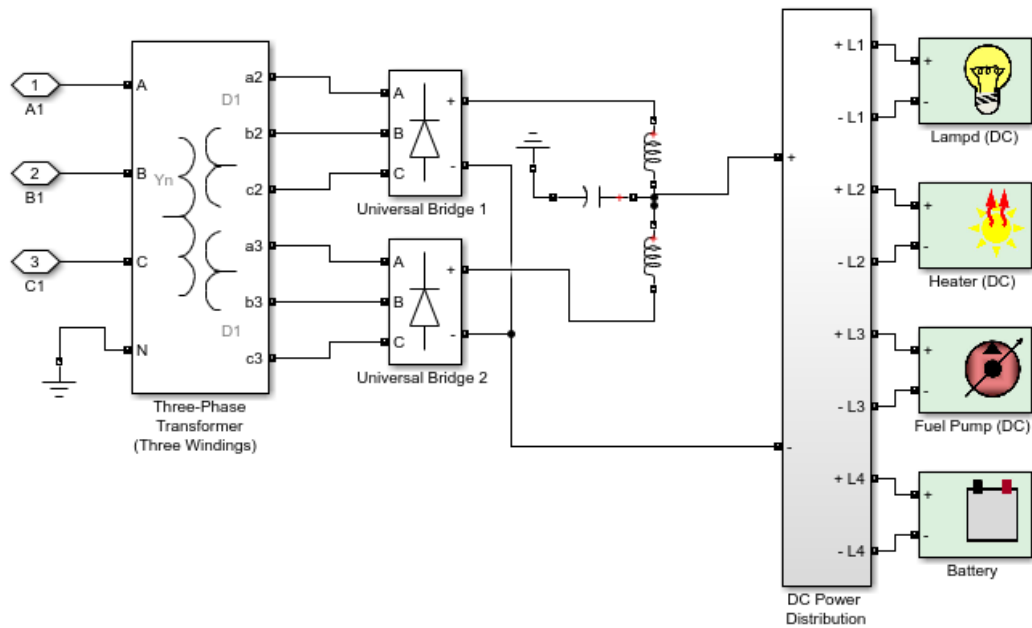


Figure 58: TRU System

E. AC Pump

Five phases PMSM is used as an AC pump for MEA, as represented in Figure 59. A converter is used to transform the power-producing from generator to five-phase. A self-tuning fuzzy logic controller controls the speed of the motor. Permanent magnet synchronous motors have been popularly applied due to their high power density, efficiency, high torque-to-inertia ratio, and reliable operation. In usual, many PMSM control systems apply the conventional PI regulator as non-linear, time-varying and significant lag. However, the traditional PI for this non-linear system is challenging to obtain the desired reference control. Also, the PI regulator parameters require to make the corresponding correction when the characteristic of controlled object changes (Si & Wang, 2010).

Many strategies have been proposed to control the PMSM. The controller's role is not only to achieve the reference parameter but also to get the fast response, the lowest overshoot, and the most reasonable starting current in the transient part. With changing the load effect and desired parameter, the controller should always track the reference parameters. At present, most of the ac motors are using the proportional plus integral (PI) controller. However, conventional PI controllers need accurate mathematical models describing the dynamics of the system under control (El-Sharkawi, El-Samahy,

& El-Sayed, Jun 1994). In addition to that, the high nonlinearity between speed and torque, high starting overshoot, and slow response lead us to replace the traditional PI controller with an intelligent controller based on the fuzzy logic controller (Saad, Salim, & Khodja, 2018).

In general, the scaling factor of the FLC cannot adjust. In that case, some problems such as dynamic and static state performances cannot solve in the FLC. To improve the performance, an advanced controller is used, namely, the Self-tuned Fuzzy PI Controller. It accomplishes better results in terms of percentage peak overshoot in speed and settling time. This controller comprises both Fuzzy and PI Controllers in which the Fuzzy Controller is used to tune the proportional gain constant (K_p) and integral gain constant (K_i) values of the PI Controller.

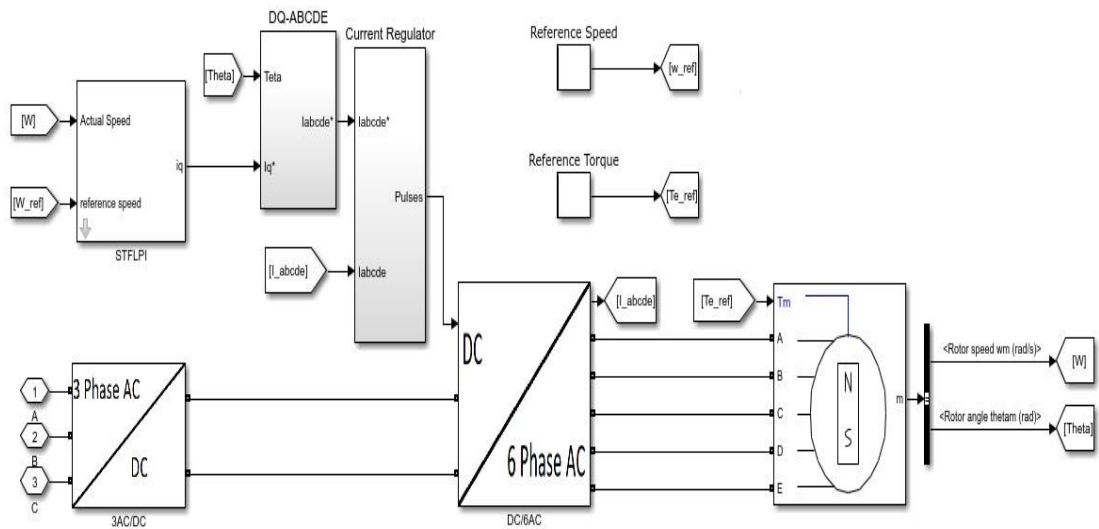


Figure 59: Five-Phase PMSM System

1. Structure For PIFLC

The regular transfer function of the conventional continuous-time PI control law is defined by

$$u(t) = k_p[e(t) + \frac{1}{T_i} \int_0^t e(t) dt] \quad (44)$$

Where:

$e(t)$: Input Signal

$u(t)$: Output Command

k_p : Proportional Controller Gain

T_i : Integral Time Constant

Let T_s be the sampling period of the continuous-time signals in the digital control system. Employing the standard mapping, ‘s’ is substituted by $\frac{z-1}{T_s z}$. Thus, it transforms the continuous-time system into its discrete-time equivalent in the z-frequency domain. Under the mapping. Therefore, it can be represented by

$$\frac{1}{T_i s} = \frac{T_s z}{T_i (z-1)} \quad (45)$$

that relationship between the Laplace transforms of $u(t)$ and $e(t)$ is

$$U(s) = k_p \left(1 + \frac{1}{T_i s}\right) E(s) \quad (46)$$

Where $k_i = \frac{T_s}{T_i} k_p$. As a result, equation (50) can be described as follows:

$$(1 - z^{-1})U(z) = k_p \left[(1 - z^{-1}) + \frac{T_s}{T_i} \right] E(z) \quad (47)$$

2. Design For PIFLC

The block diagram of the STFLPI controller is presented in Fig. 4. A self-tuning mechanism enhances the production of the FL controller. The essential background for this mechanism is shown in the following.

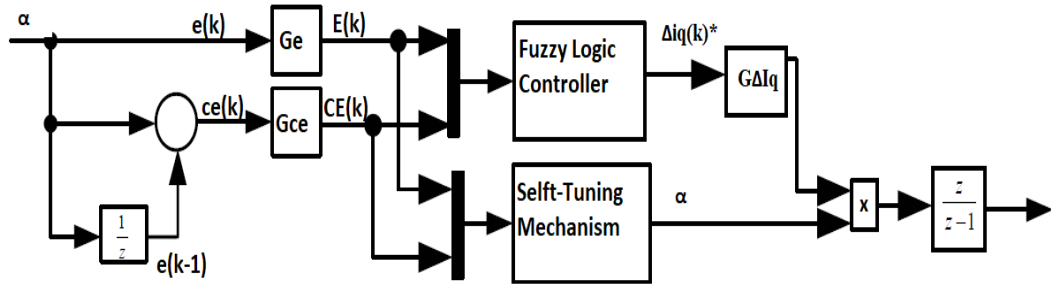


Figure 60: Block Diagram Of STFLPI Controller

3. Membership Functions

The inputs of the fuzzy logic control are $e(k)$ and $ce(k)$, which have values between -1 and 1. On the other hand, the output membership function is $\Delta Iq^*(k)$, which varies between -1 and 1. In addition to that, the self-tuning mechanism has the same inputs and has the scaling factor α as an output. The output changes between 0 and 1. The membership functions are shown in Figure 61, and the rules are shown in Table 5. The essential characteristic of the self-tuning mechanism is that α is not dependent on any process parameters. The value of α only depends on the instantaneous process states. For measurement of gain updating factor α (7x7), control rules are as presented in Table 5 which are

Z: Zero

VS: Very Small

S: Small

SB: Small Big

MB: Medium Big

B: Big

VB: Very Big

4. Scaling Factors

The relation between the scaling factor ($G_e, G_{ce}, G_{\Delta Iq}$), and the controller are:

$$E(k) = e(k) \times G_e(k) \quad (48)$$

$$CE(k) = ce(k) \times G_{ce}(k) \quad (49)$$

$$\Delta i_q^*(k) = \alpha \Delta I_q(k) \times G_{\Delta I_q}(k) \quad (50)$$

5. The Rule Base

The Rules of the FLPI controller are presented in Table 4. The gain updating factor (α) is determined using fuzzy rules. The rule base in Table 5 is utilized for the calculation of α .

Table 5: Scaling Factor α

| | | Error "e" | | | | | | |
|-------------------------|----|-----------|----|----|----|----|----|----|
| | | VB | B | MB | SB | S | VS | Z |
| Change of error "ce" | VB | VB | VB | VB | B | SB | S | Z |
| | B | VB | VB | B | B | MB | S | VS |
| | MB | VB | MB | B | VB | VS | S | VS |
| | SB | S | SB | MB | Z | MB | SB | S |
| | S | VS | S | VS | VB | B | MB | VB |
| | VS | VS | S | MB | B | B | VB | VB |
| | Z | Z | S | SB | B | VB | VB | VB |

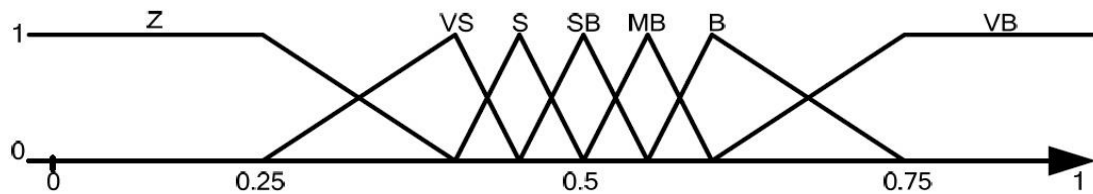


Figure 61: Membership Functions Of STFLPI Controller For α

F. AC Lamps

The lamps in MEA are represented as a three-phase resistance. The assumed power that the dc lights consume is 1kw.

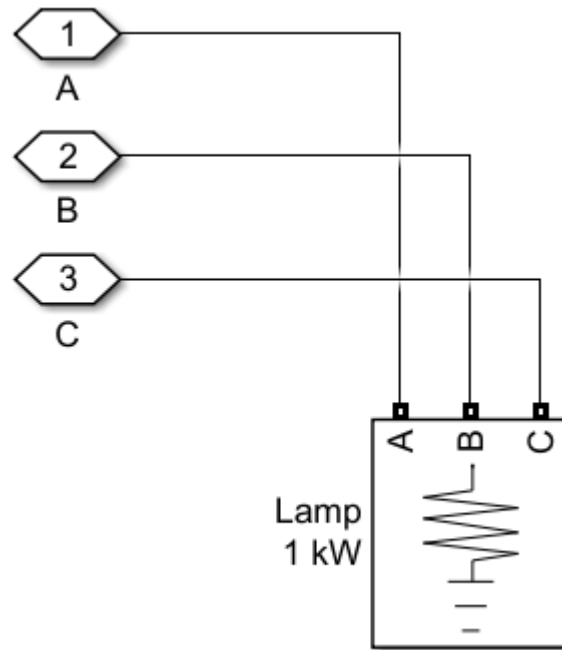


Figure 62: AC Lamps

G. Actuators

The actuators used to control the flight direction and landing. It controls the primary flight control, such as aileron, spoiler, flap, elevator, rudder, slat, and pitch. The primary flight control is described in Figure 63. The Matlab representation is presented in Figure 64. The actuators use three-phase PMSM that is also controlled by a self-tuning FLC.

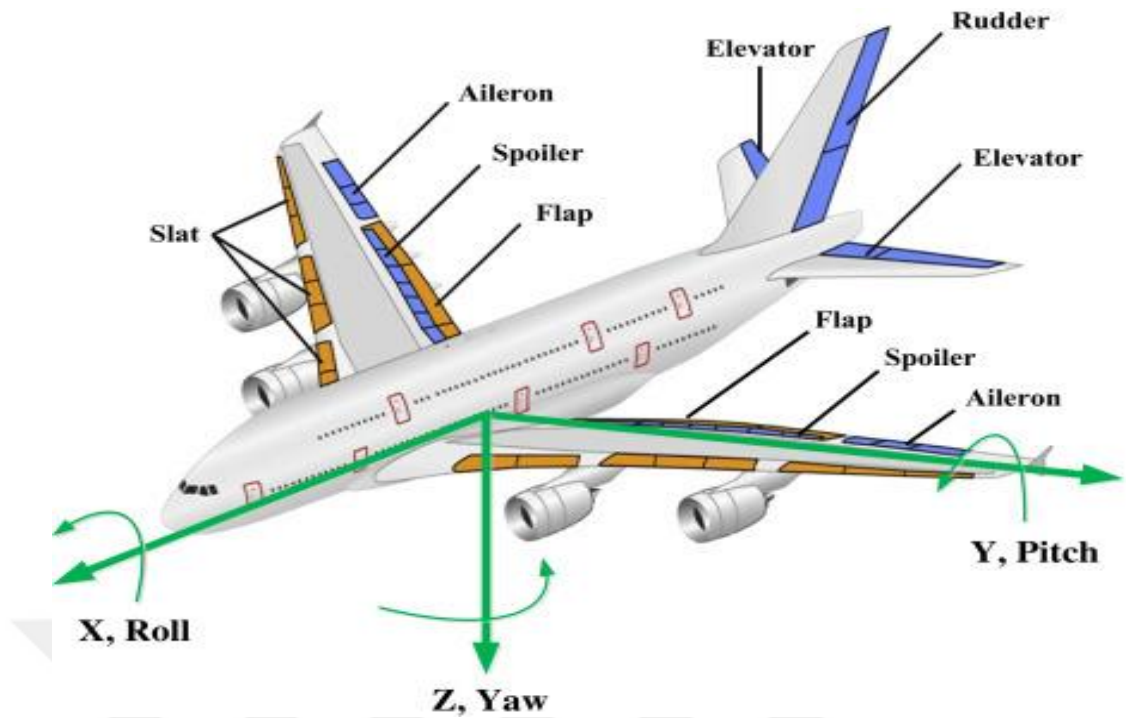


Figure 63: Primary Flight Control

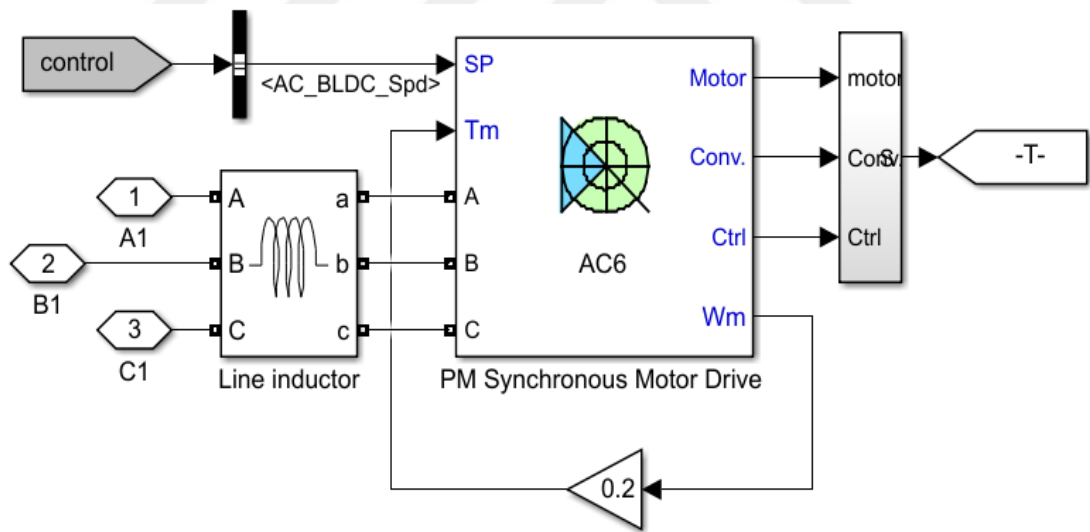


Figure 64: Actuators

V. SIMULATION RESULTS

A. AC Pump

The performances of motors are comparing between the induction motors that are employed on MEA and the five-phase PMSM with PI and STFLPI Controller.

Table 6: Induction Motor Parameters

| Parameters | Symbols | Value |
|----------------------------|------------------------------|--------------|
| Nominal power | $P_n(\text{VA})$ | 12000 |
| voltage (line-line) | $V_n(\text{V}_{\text{rms}})$ | 200 |
| frequency | $f_n(\text{Hz})$ | 400 |
| Stator resistance | $R_s(\text{ohm})$ | 0.2761 |
| Stator inductance | $L_{ls}(\text{H})$ | 0.0002191 |
| Rotor resistance | $R_r'(\text{ohm})$ | 0.16 |
| Rotor inductance | $L_{lr}'(\text{H})$ | 0.0002191 |
| Mutual inductance | $L_m (\text{H})$ | 0.07614 |
| Inertia | $J(\text{kg.m}^2)$ | 0.01 |
| friction factor | $F(\text{N.m.s})$ | 0 |
| pole pairs | $p()$ | 8 |

Table 7: Five-Phase PMSM Parameters

| Parameters | Symbols | Value |
|--|--------------------|--------------|
| Stator Resistance (ohm) | $R_s(\text{ohm})$ | 0.12 |
| Stator Inductance (H) | $L_s(\text{H})$ | 1350e-6 |
| Flux Constant | Φ | 0.03 |
| Inertia | $J(\text{kg.m}^2)$ | 0.002 |
| Friction factor | $N.m.s$ | 0.02 |
| Pole pairs | $P ()$ | 8 |
| Proportional gain | k_p | 0.5 |
| Integral gain | k_i | 40 |
| Speed cutoff frequency | $F_c (\text{Hz})$ | 400 |
| Current controller hysteresis bandwidth | $HCC (A)$ | 0.1 |
| Maximum switching frequency | $F_s (\text{Hz})$ | 50e3 |
| Controller sampling time | T_s | 2e-5 |
| Base sample time | T_{s_base} | 1e-05 |

1. PI Controller

a. Speed Test

The simulation, as performed in the figures below, was set up utilizing MATLAB Software to verify the proposed MEA. Figure 65 represents the different speeds on MEA. The black colour defines the speed of the induction motor, while the blue colour is for five-phase PMSM and the orange colour to determine the reference speed. The speed controller for the five-phase PMSM is the PI controller. The PMSM is faster than the induction motor. In this module, the performance of the motors was tested by changing the speed five times. The estimates reference speeds are 307, 376, 330, 365, and 342 rpm, respectively. They are represented in Figure 66, Figure 67, Figure 68, and Figure 69, respectively. Table 8 illustrates the speed comparison between Induction Motor and Three-Phase PMSM controlled by PI Controller. Where T is the time required to achieve the reference speed, and Δh is the overshoot value ($W^* - W$). The Induction Motor Parameters are recorded in

Table 6.

According to Table 8, it can be seen that the PMSM is better than the Induction motor in terms of achieving the reference value and low starting overshoot.

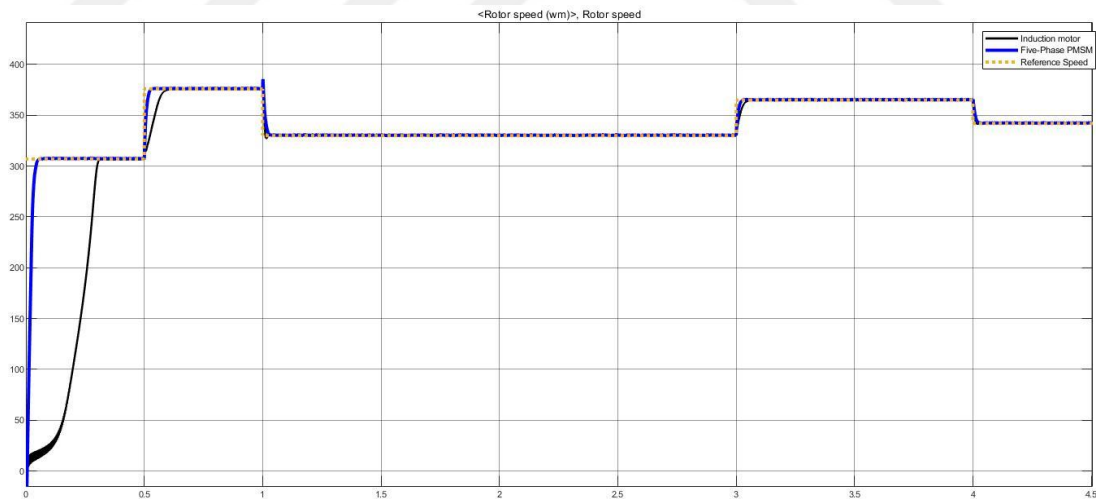


Figure 65: Speed Comparison Between Induction Motor And Five-phase PMSM

Figure 65 is shown in the flight cycle on MEA. The Five-Phase PMSM seems faster in tracking the reference speed, but it has overshoot speed during the operation. The following figures represent the speed comparison at each stage.

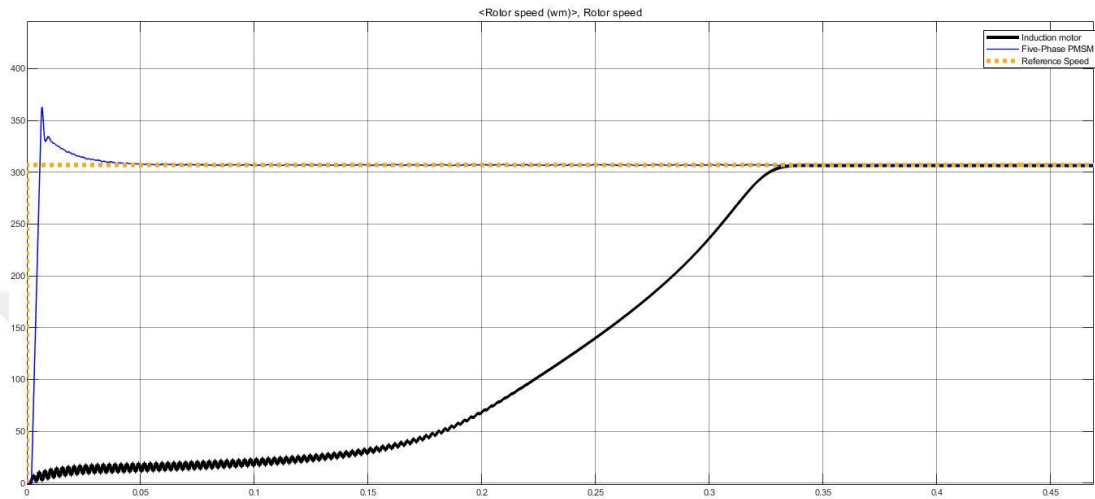


Figure 66: First Stage Reference Speed $\omega^*=307$

In the first stage in Figure 66, the PMSM motor reached the required speed in a period not exceeding 50 ms while the induction motor reached the speed required for 300 ms. This means that the PMSM motor is six times faster than the induction

motor. On the other hand, the PMSM exceeded the reference speed with an overshoot exceed 50 rpm.

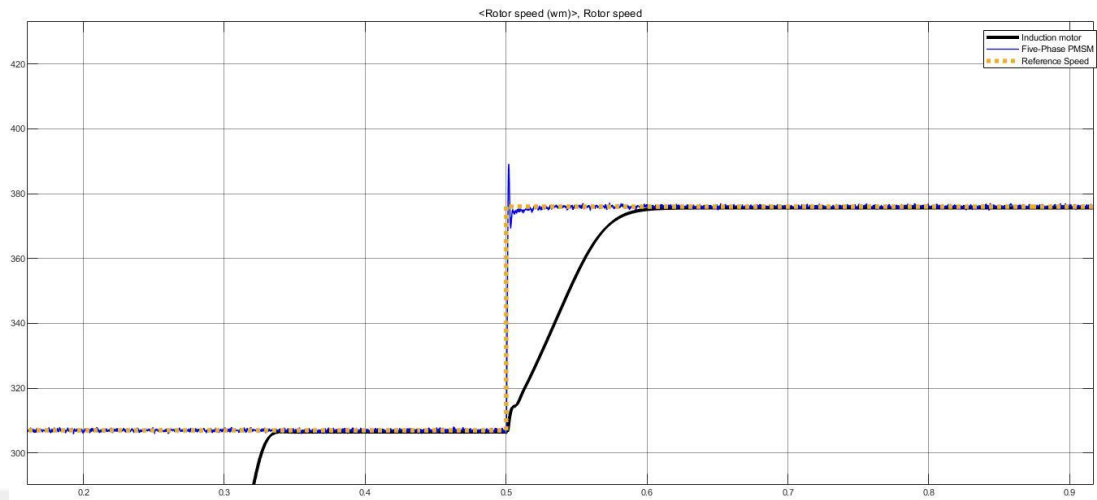


Figure 67: Second Stage Reference Speed $W^*=376$

In the second stage described in Figure 67, the PMSM motor arrived at the required speed in a period not exceeding 10 ms while the induction motor arrived at the required speed for 100 ms. In this case, the PMSM motor is ten times faster than the induction motor. Moreover, the PMSM exceeded the reference speed with an overshoot exceed 15 rpm.

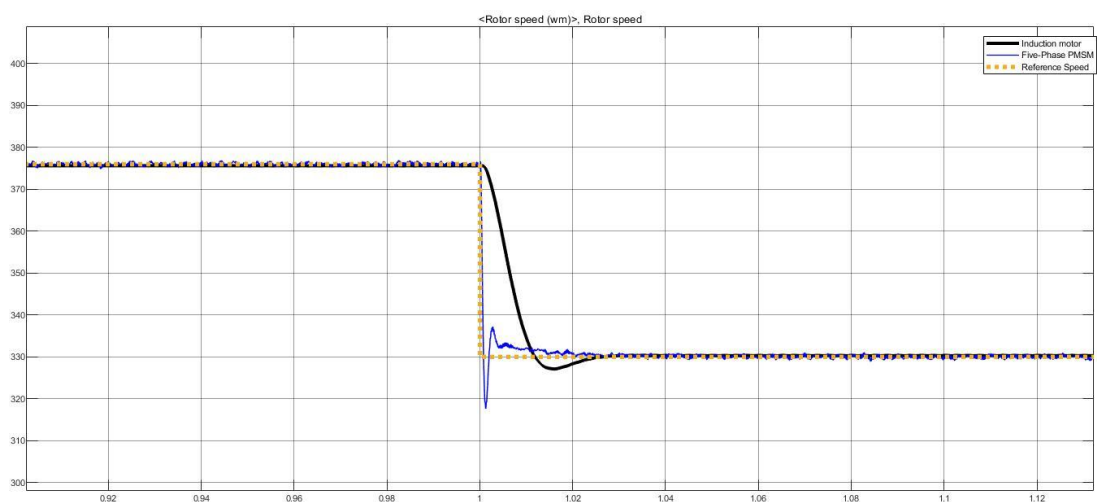


Figure 68: Third Stage Reference Speed $W^*=330$

In the third stage Figure 68, while going from the top (376 rpm) to the bottom speed (330 rpm), it can be observed that the two motors have reached the desired speed at the same time during 30 ms, but the PMSM motor has started to change the speed with overshoot exceeded 10 rpm.

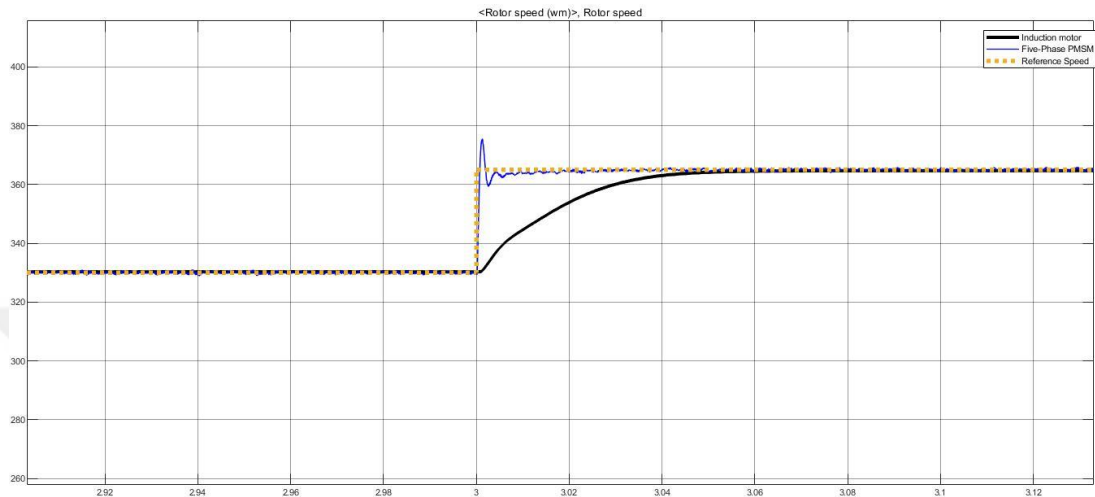


Figure 69: Fourth Stage Reference Speed $W^*=365$

The fourth stage is represented in Figure 69, and the PMSM motor reached the required speed in a period not passing 10 ms, while the induction motor reached the speed required for 60 ms. This means that the PMSM motor is six times faster

than the induction motor. The PMSM exceeded the reference speed with an overshoot exceed 10 rpm.

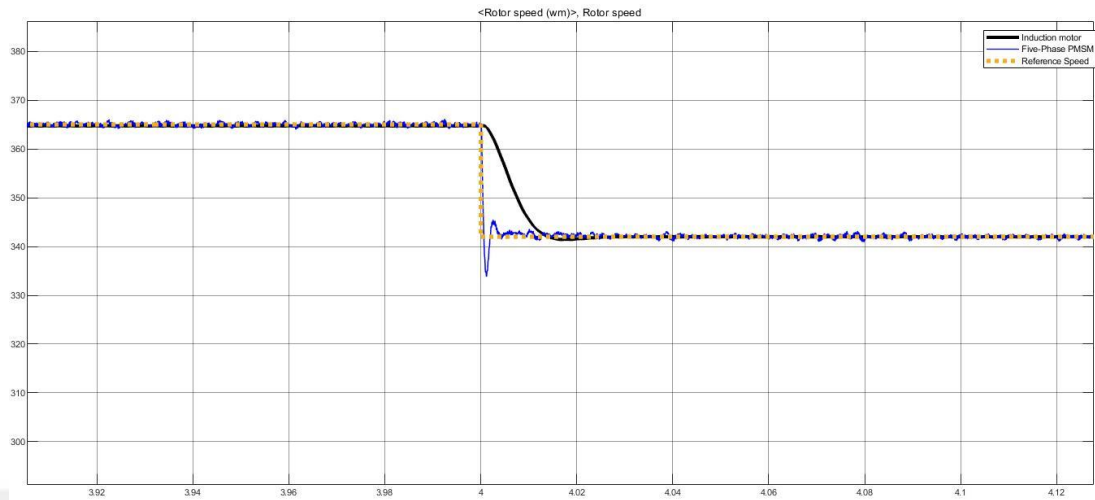


Figure 70: Fifth Stage Reference Speed $W^*=342$

In the fifth stage that is described in Figure 70, while going from the top (365 rpm) to the bottom speed (342 rpm), The PMSM motor reached the required speed within 10 ms, while the Induction motor reached in 20 ms. The PMSM exceeded the reference speed with an overshoot exceed 10 rpm.

Table 8: Speed Comparison Between Induction Motor And Five-Phase PMSM (PI Controller)

| Motor Type | First Stage | Second Stage | Third Stage | Fourth Stage | Fifth Stage |
|--|--------------------------------|--------------------------------|-------------------------------|-------------------------------|-------------------------------|
| Induction Motor | T= 300 ms ($\Delta h= 0$) | T= 100 ms ($\Delta h= 3$) | T= 30 ms ($\Delta h=3$) | T= 60 ms ($\Delta h= 0$) | T= 20 ms ($\Delta h=0$) |
| Five-Phase PMSM (PI Controller) | T= 50 ms ($\Delta h=53$) | T= 10 ms ($\Delta h=15$) | T= 30 ms ($\Delta h=10$) | T= 10 ms ($\Delta h=10$) | T= 10 ms ($\Delta h=10$) |

b. Torque Test

The torque during the flight varies, the motor must always reach the torque of the load. It was assumed by MATLAB that the torque change in five stages. In the first stage, the torque of the load will be 17, then 21, then 18, then 20, and 19 Nm. Figure 71 represents the torque comparison between the induction motor and five-phase PMSM. It can be seen that in all stages, the induction has high torque overshoot while the PMSM has very low torque overshoot. According to Table 9, it can be seen that the STFLPI is better than the PI controller in terms of achieving the reference value and low starting overshoot.

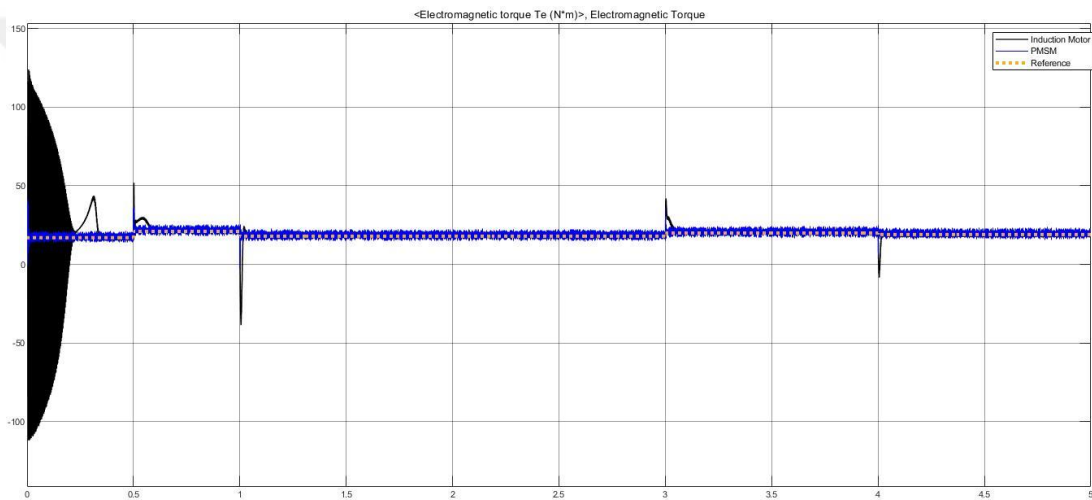


Figure 71: Torque Comparison Between Induction Motor And Five-Phase PMSM

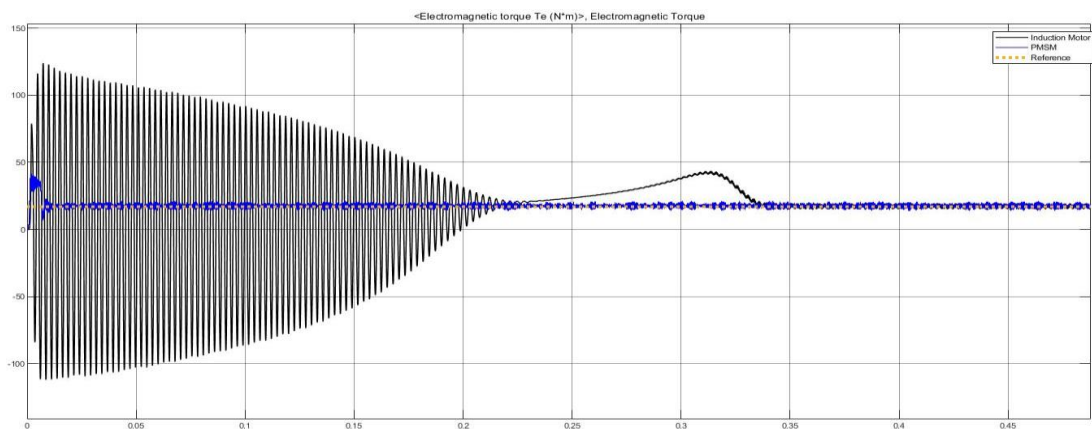


Figure 72: First Stage Reference Torque $T_{e^*} = 17 \text{ nm}$

In Figure 72, the first stage is represented. The PMSM motor was able to meet the torque of the load within 5 ms and in an overshoot that reached 40 Nm. While the induction motor was able to meet the load within 300 ms and the torque overshoot motor had reached more than 110 nm. The first motor is 60 times faster at satisfying the torque.

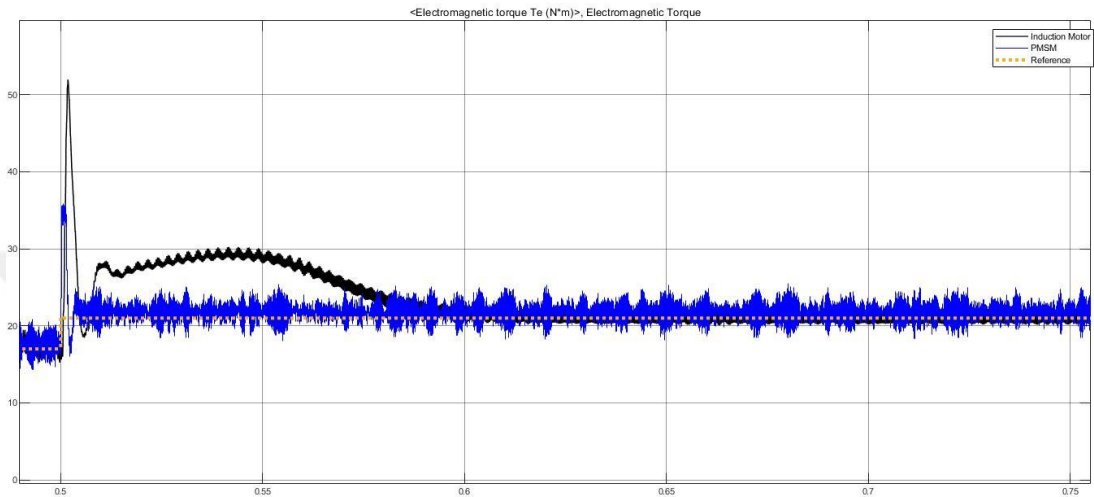


Figure 73: Second Stage Torque Reference $T_{e^*} = 21 \text{ nm}$

The second stage is represented through Figure 73; the PMSM motor was able to meet the torque of the load in 10 ms, and overshoot arrived at 35 Nm. While the induction motor was able to meet the load within 60 ms and the torque

overshoot motor had reached more than 50 Nm. The first motor is 60 times faster at satisfying the torque.

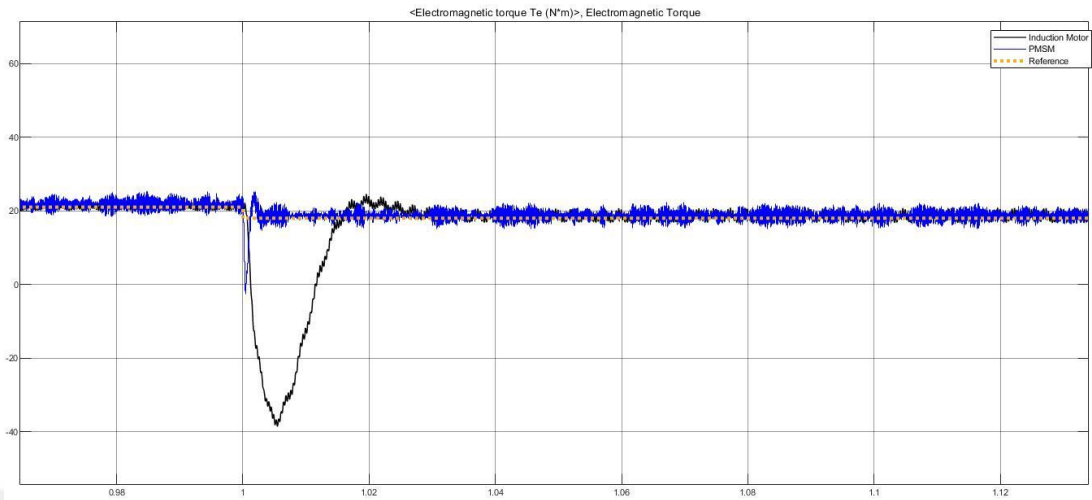


Figure 74: Third Stage Torque Reference $T_e^*=18$ Nm

Through Figure 74, the third stage is represented, the PMSM motor was able to meet the torque of the load in 10ms and in overshoot that exceed 20 Nm from the reference torque. While the induction motor was able to meet the load within 30 ms and the torque overshoot motor had reached more than -30 Nm.

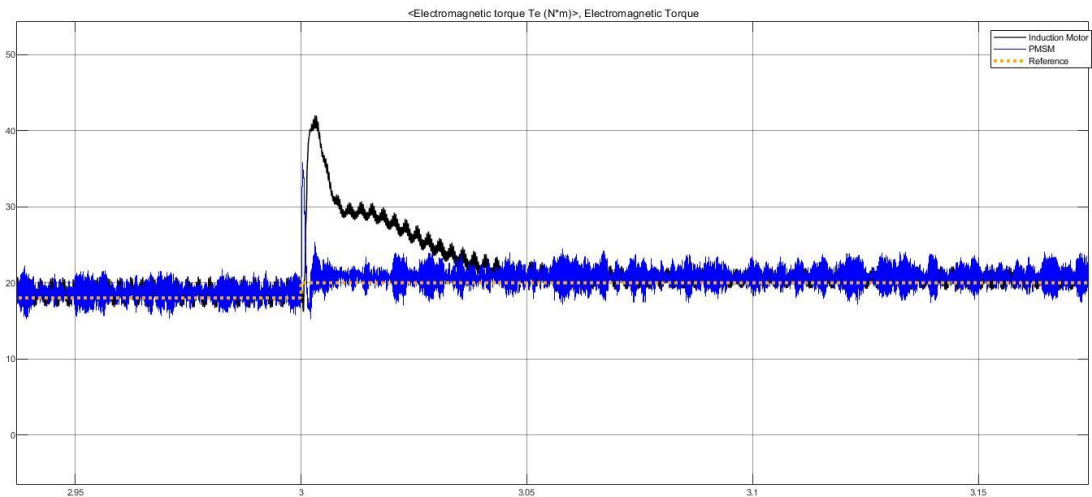


Figure 75: Fourth Stage Torque Reference 20 Nm

The fourth stage is defined through Figure 75; the PMSM motor was able to meet the torque of the in 10 ms and in overshoot that arrived at 35 Nm. While the

induction motor was able to meet the load within 50 ms and the torque overshoot motor had reached more than 40 Nm. The first motor is five times faster at satisfying the torque.

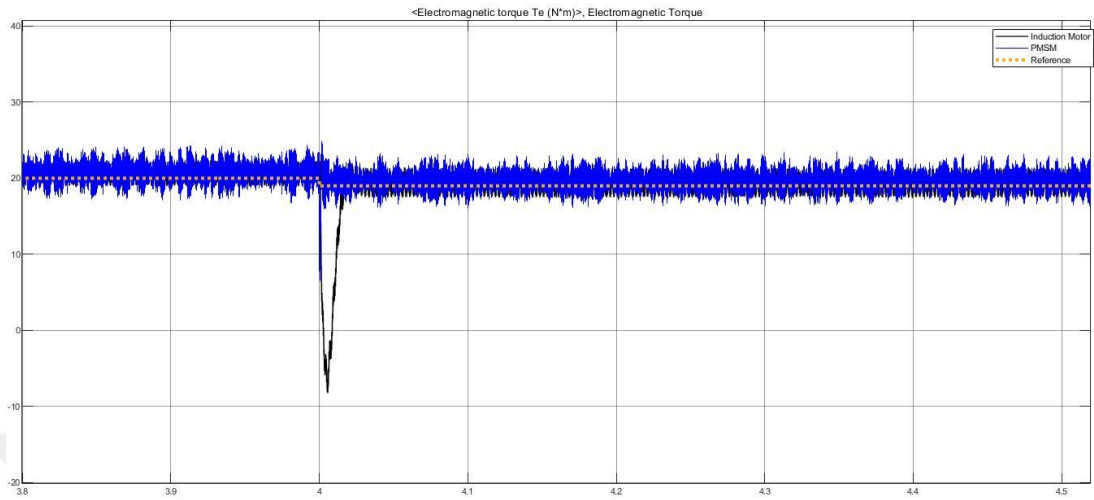


Figure 76: Fifth Stage Torque Reference 19 nm

Through Figure 76, the PMSM motor was able to meet the torque of the load in 10 ms and overshoot higher than the reference speed for 10 Nm. While the

induction motor was able to meet the load within 15 ms and the torque overshoot motor had reached more than -10 Nm.

Table 9: Torque Comparison Between Induction Motor And Five-Phase PMSM (PI Controller)

| Motor Type | First Stage | Second Stage | Third Stage | Fourth Stage | Fifth Stage |
|--|---------------------------------|--------------------------------|-------------------------------|--------------------------------|-------------------------------|
| Induction Motor | T= 300 ms ($\Delta h= 93$) | T= 60 ms ($\Delta h= 29$) | T= 30 ms ($\Delta h=22$) | T= 50 ms ($\Delta h= 20$) | T= 15 ms ($\Delta h=30$) |
| Five-Phase PMSM (PI Controller) | T= 10 ms ($\Delta h=23$) | T= 10 ms ($\Delta h=14$) | T= 10 ms ($\Delta h=20$) | T= 10 ms ($\Delta h=15$) | T= 10 ms ($\Delta h=20$) |

c. Current Test

When comparing motors, it must consider the amount of current consumed at each stage. Figure 77 shows the different current consumed for both motors at different stages. It is clearly can be seen that in all stages, the PMSM has lower overshoot

current than an induction motor. Moreover, in the steady-state, both motors barely have the same consumption current.

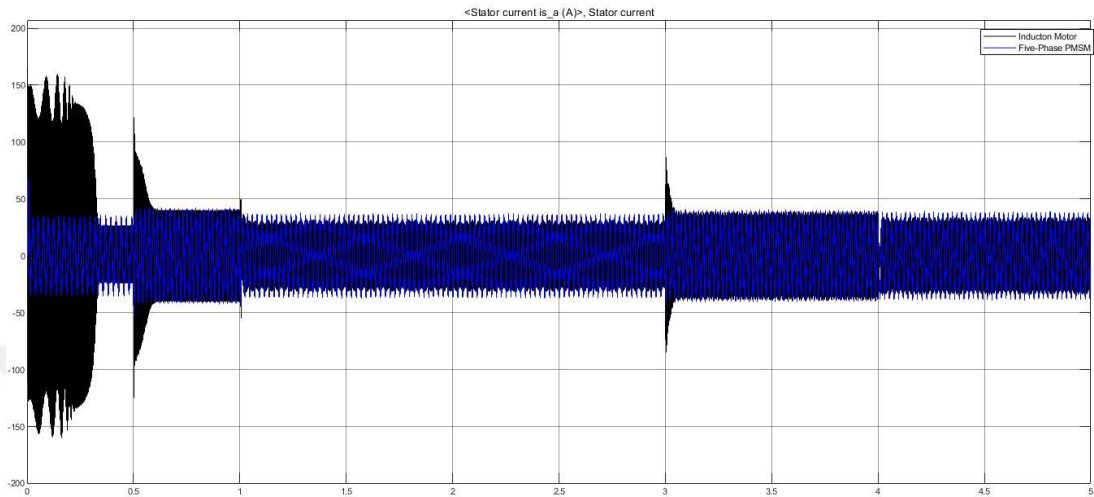


Figure 77: Stator Current Comparison Between Induction Motor And Five-Phase PMSM

2. STFLPI Controller

The five-phase PMSM achieved good results compared with an induction motor. To improve more, the STFLPI controller is examined. for five-phase PMSM

Table 10: STFLPI Controller Parameters

| Controller Parameters | Value |
|-----------------------|-------|
| Ge | 1 |
| Gce | 70 |
| Giq | 2 |

a. Speed Test

The flight cycle speed using the STFLPI controller can be seen in Figure 78. Due to high accuracy, it is hard to notice the difference between the reference speed

and actual speed. In the next figures, it can be seen the different speeds at each stage. In five-phase PMSM, the speed controller is replaced by an STFLPI. The STFLPI achieves perfect results in terms of tracking the reference speed. In Table 11 represents the speed comparison of five-phase PMSM using PI and STFLPI controller. According to Table 11, it can be seen that the STFLPI is better than the PI controller in terms of reaching the reference value and low starting overshoot.

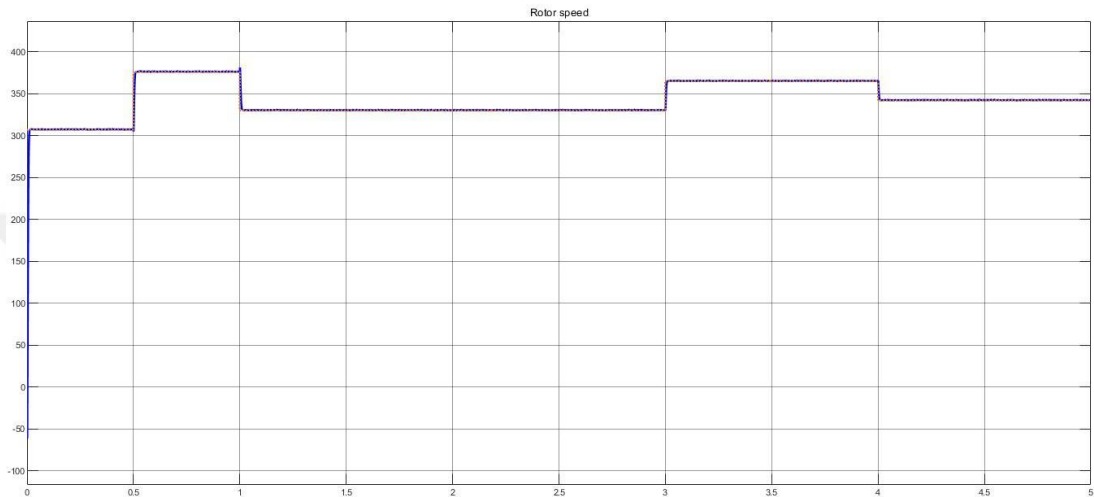


Figure 78: Flight Cycle On MEA Using STFLPI Controller

The STFLPI reaches the desired speed in a remarkably short time with overshoot nearly zero. Figure 79, Figure 80, Figure 81, Figure 82, and Figure 83 represents the actual speed using STFLPI for stage 1, 2, 3, 4, and 5, respectively. In Figure 79, the STFLPI controller reaches the desired speed in a duration not exceeding 12 ms without an overshoot. In Figure 80, represents the second stage, the STFLPI reaches the desired speed in only 10 ms and without overshoot speed. In Figure 81, the STFLPI controller reaches the desired speed also in 10 ms with a little overshoot that is arrived at 382 rpm in the beginning. In Figure 82 and

Figure 83, they represent the fourth and fifth stages, respectively. They also reach the desired speed in 10 ms and without overshoot speed.

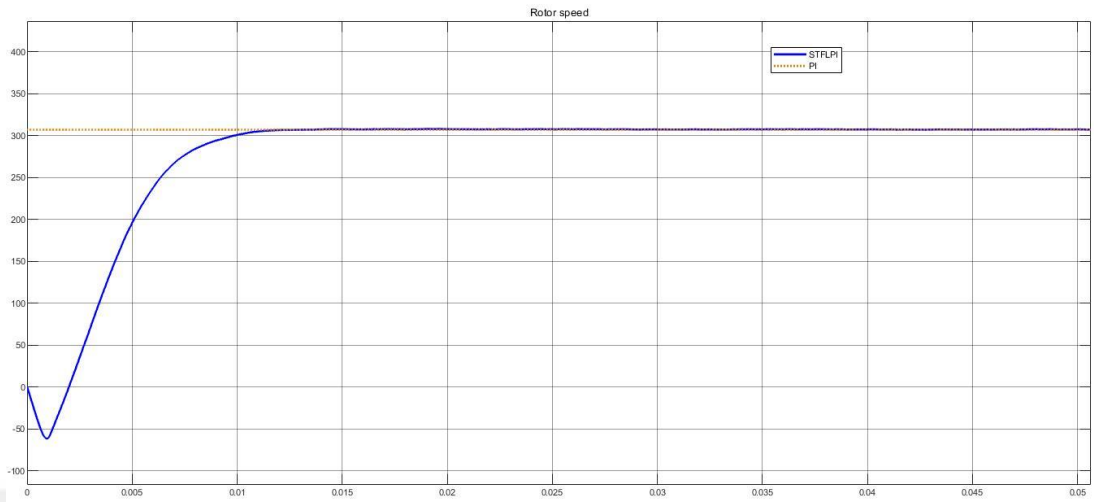


Figure 79: First Stage Reference Speed $W^*=307$

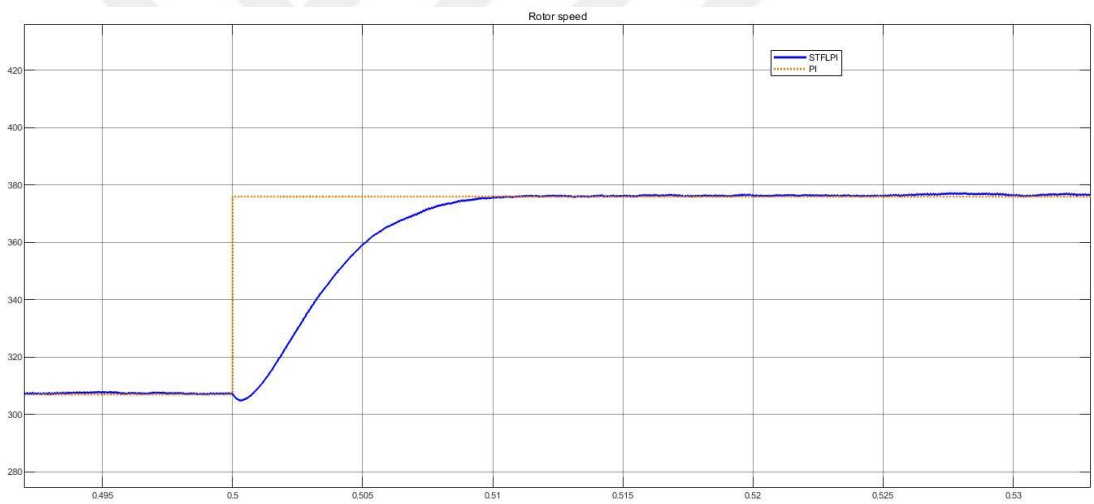


Figure 80: Second Stage Reference speed $W^*=376$

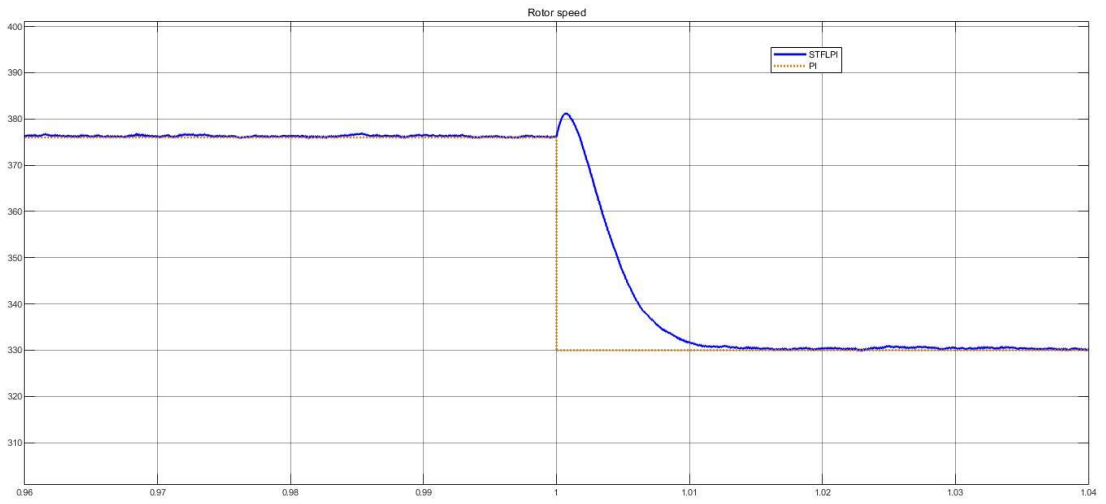


Figure 81: Third Stage Reference Speed $W^*=330$

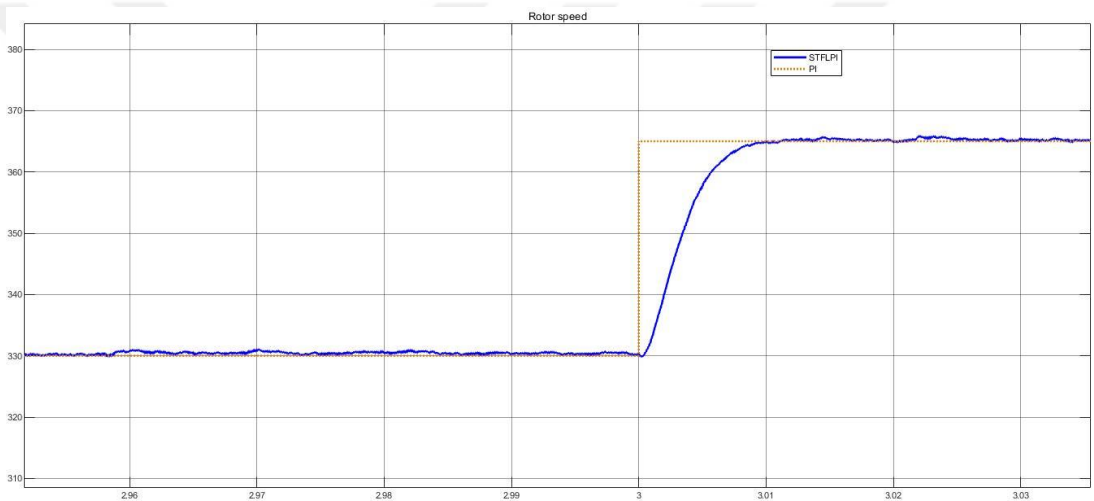


Figure 82: Fourth Stage Reference Speed $W^*=365$

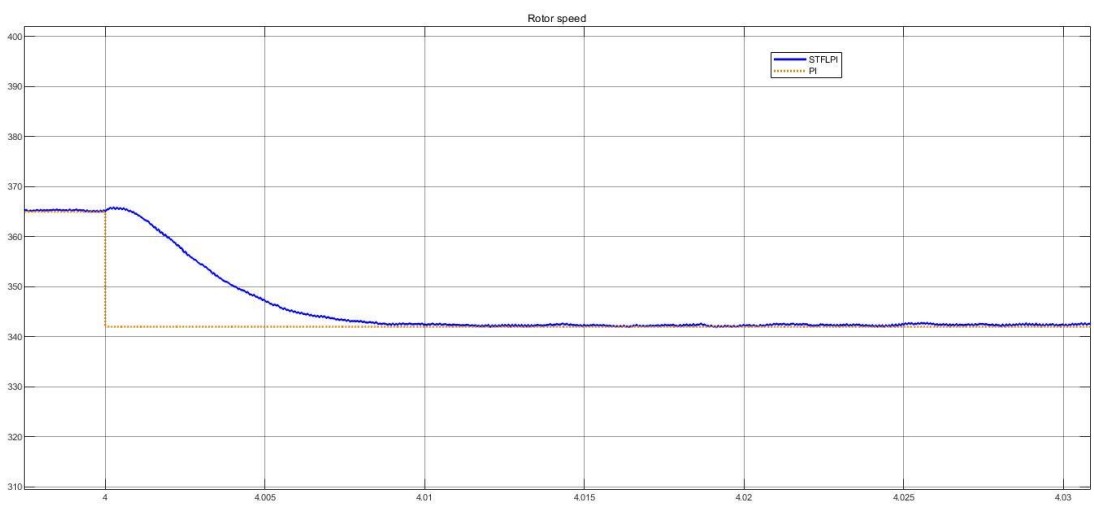


Figure 83: Fifth Stage Reference Speed $W^*=342$

Table 11: Speed Comparison Of Five-Phase PMSM between
(PI Controller) And (STFLPI)

| Motor Type | First Stage | Second Stage | Third Stage | Fourth Stage | Fifth Stage |
|--|-------------------------------|-------------------------------|-------------------------------|-------------------------------|-------------------------------|
| Five-Phase PMSM (STFLPI Controller) | T= 12 ms ($\Delta h= 0$) | T= 10 ms ($\Delta h= 0$) | T= 10 ms ($\Delta h=0$) | T= 10 ms ($\Delta h= 0$) | T= 10 ms ($\Delta h=0$) |
| Five-Phase PMSM (PI Controller) | T= 50 ms ($\Delta h=53$) | T= 10 ms ($\Delta h=15$) | T= 30 ms ($\Delta h=10$) | T= 10 ms ($\Delta h=10$) | T= 10 ms ($\Delta h=10$) |

b. Torque Test

The STFLPI controller reaches always reaches the desired torque directly with an overshoot nearly zero. It has a starting torque, only 35 Nm, while the reference speed is 17 Nm. In Table 12 represents the torque comparison of five-phase PMSM using PI and STFLPI controller. According to Table 12, it can be seen that the STFLPI is better than the PI controller in terms of achieving the reference value and low starting overshoot.

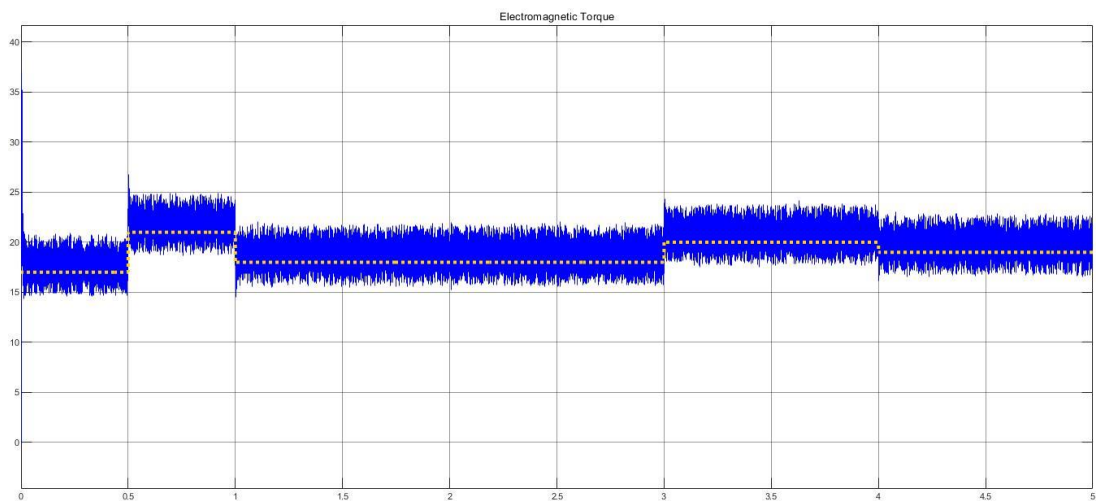


Figure 84: Torque Using STFLPI Controller

Table 12: Torque Comparison Of Five-Phase PMSM Between
(PI Controller) And (STFLPI)

| Motor Type | First Stage | Second Stage | Third Stage | Fourth Stage | Fifth Stage |
|--|-------------------------------|-------------------------------|--------------------------------|-------------------------------|-------------------------------|
| Five-Phase PMSM (STFLPI Controller) | T= 0 ms ($\Delta h= 0$) | T= 0 ms ($\Delta h= 0$) | T= 0 ms ($\Delta h=0$) | T= 0 ms ($\Delta h= 0$) | T= 0 ms ($\Delta h=0$) |
| Five-Phase PMSM (PI Controller) | T= 10 ms ($\Delta h=23$) | T= 10 ms ($\Delta h=14$) | T= 30 ms ($\Delta h=200$) | T= 10 ms ($\Delta h=15$) | T= 10 ms ($\Delta h=20$) |

c. Current Test

The STFLPI controller also has the advantage of not consuming a large amount of energy in the beginning and in steady-state. In the photo, it shows the different current at different stages. It has a starting current only 38 A.

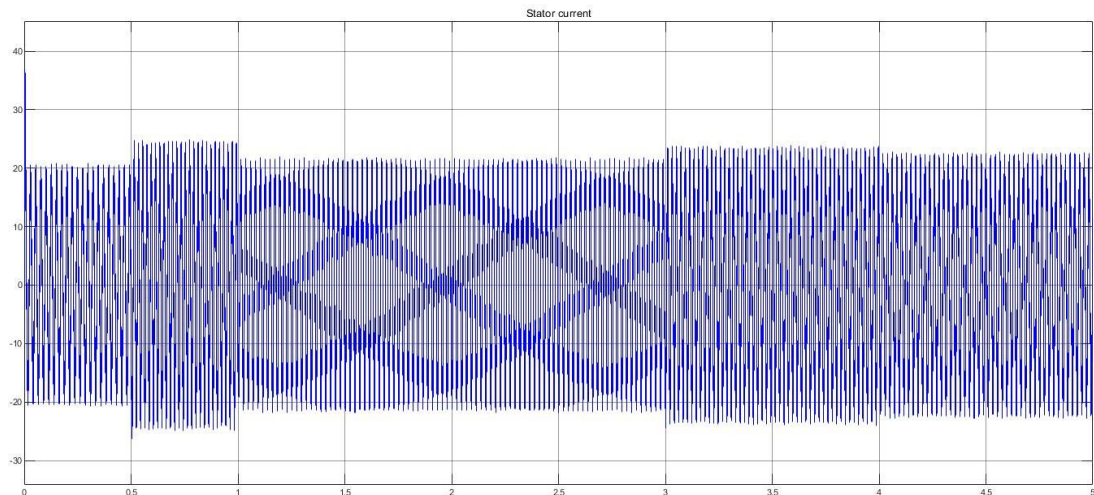


Figure 85: Consuming Current Using STFLPI Controller

B. Actuators

The actuators employed in MEA are three-phase PMSM. The actuator works differently from the pumps; the speed of the actuator should increase gradually while the pumps should increase directly. Figure 86 shows the work of one of the actuators for about 4 seconds.

During the four seconds, the actuator speed must increase slowly, then decrease gradually, and then turn in the opposite direction and then stop slowly. The



actuators are running by using PI and STFLPI Controller. Figure 86 represents the speed difference with different controllers.

Table 13: Three-Phase PMSM Parameters

| Parameters | Symbols | Value |
|--|--------------------------|--------------|
| Stator Resistance | R_s (Ω) | 0.12 |
| D-axis inductance | L_d (H) | $8.5e-3$ |
| Q-axis inductance | L_q (H) | $8.5e-3$ |
| Flux Constant | Flux (Φ) | 0.05 |
| Inertia | J (kg.m ²) | 0.002 |
| Friction factor | Fr (N.m.s) | 0.005 |
| Pole pairs | P () | 8 |
| Base sample time | T_{s_base} (s) | $1e-6$ |
| Current controller hysteresis bandwidth | HCC (A) | 0.1 |
| Maximum switching frequency | F_{max} (HZ) | $50e3$ |
| Controller sampling time | T_s (s) | $1e-5$ |
| Base sample time | T_{s_base} | $1e-6$ |

Table 14: PI Controller Parameters

| Controller Parameters | Value |
|-----------------------|-------|
| kp | 5 |
| ki | 100 |

Table 15: STFLPI Controller Parameters

| Controller Parameters | Value |
|-----------------------|-------|
| Ge | 0.2 |
| Gce | 10 |
| Giq | 2 |

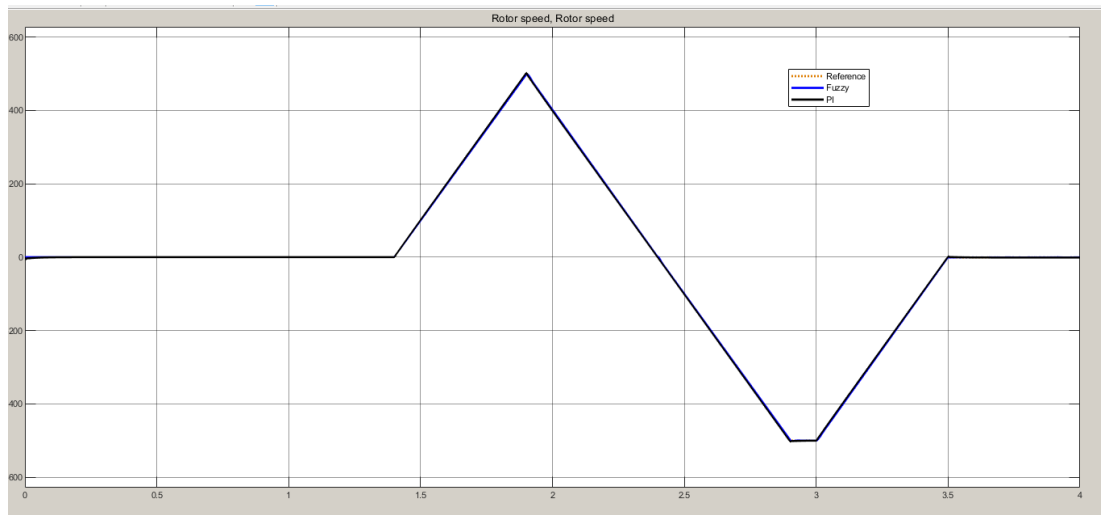


Figure 86: Comparing Actuator Speed Using PI And STFLPI Controller

Through Figure 86, it is not easy to distinguish who is the best controller, but when zooming in more closely, it can be seen that STFLPI is faster than the PI controller.

Within Figure 87, when the figure was enlarged, it represents the speed comparison at a steady state. The speed of the actuator using STFLPI is closer to reference speed than the PI controller.

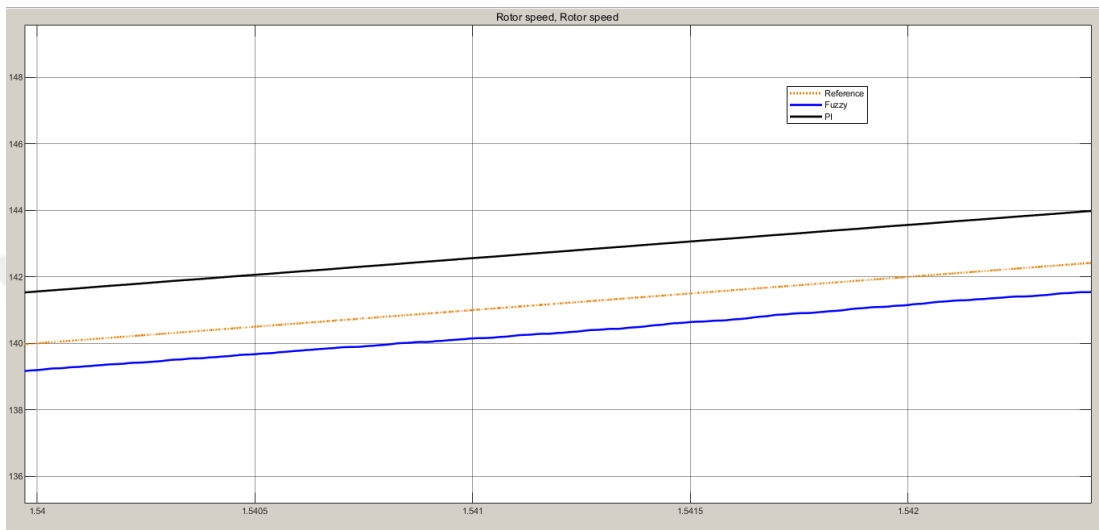


Figure 87: Comparing Actuator Speed Using PI And STFLPI Controller At Steady

VI. CONCLUSION

A. Summary

This thesis aims to reveal a new control method of future aircraft utilizing the fuzzy logic controller for electric motors on MEA. The STFLPI controller was presented in this paper. The STFLPI achieves perfect results in terms of tracking of reference speed, low start torque, and current, and reduce consumption of power. High tracking speed turns the MEA to become more accurate and faster during the operation. Low starting current and torque extend the life of the devices and protect them from damage on MEA. Reducing power leads to reduced use of electrical wires and thus reduce weight on the MEA.

For different conditions, speed responses of PMSM and induction motors have been examined. Implementing the FL controller, the STFLPI controller provides the speed to reach the reference value at a faster rate comparing with the PI controller despite the changing of applied torque and reference speed. During the starting of motors, the overshoot has been eliminated by using the STFLPI. The problems of high starting current in most motors have been reduced.

B. Outlook

For the planned works, the plan is to spread of using the STFLPI, not only on aircraft but also in different systems that require a controller. The MEA is going to be replaced by FEA (Full Electric Aircraft) that depends only on electricity for power generation. That goal will be achieved by improving the controllers to reduce power consumption. The aircraft will be work for a long duration without interruption carrying more payloads

VII. REFERENCES

- [1] **European Commission.** (23 April 2009). Amending Directive 2003/87/EC so as to improve and extend the greenhouse gas emission allowance trading scheme of the Community,". *Official Journal of the European Union*.
- [2] **Commission, E.** (2011). *Flightpath 2050: Europe's Vision for Aviation*. Luxembourg: Publications Office of the European Union,.
- [3] **S.A.S, A.** (2013). *Global Market Forecast*. Blagnac, France: Airbus S.A.S.
- [4] **Kumhof , M., & Muir, D.** (2012). *Oil and the World Economy: Some Possible Futures*. Washington, D.C: International Monetary Fund, Working Paper No. 12/256.
- [5] **Bundesregierung.** (2009). *Nationaler Entwicklungsplan Elektromobilität der Bundesregierung*. Berlin, Germany: Bundesministerium für Bildung und Forschung.
- [6] **Abdelhafez, A. A., & Forsyth, A. J.** (May 2009). A Review of More-Electric Aircraft. *13th International Conference on AEROSPACE SCIENCES & AVIATION TECHNOLOGY*,. Cairo.
- [7] **Provost, M. J.** (2002). THE MORE ELECTRIC AERO-ENGINE: A GENERAL OVERVIEW FROM AN ENGINE. in *International Conference on Power Electronics, Machines and Drives* , 246-251.
- [8] **Moir, I., & Seabridge, A.** (2001). *Aircraft Systems Mechanical, electrical, and avionics subsystems integration*. London:.
- [9] **Rosero, J. A., Ortega, J. A., & Romeral, L.** (march 2007). Moving Towards a More Electric Aircraft. *IEEE A&E SYSTEMS MAGAZINE*, 3-9.
- [10] **Rajashekara, K.** (june 2014). Parallel between More Electric Aircraft and Electric/Hybrid Vehicle Power Conversion Technologies. *IEEE Electrification Magazine*, 2(2), 50-60.
- [11] **Buticchi, G., Bozhko, S., Liserre, M., Wheeler, P., & Al-Haddad, K.** (2018). On-board Microgrids for the More Electric Aircraft – Technology Review. *IEEE TRANSACTIONS ON INDUSTRIAL ELECTRONICS*.
- [12] **Sarlioglu, B., & Morris, C. T.** (June 2015). More Electric Aircraft – Review, Challenges and Opportunities for Commercial Transport Aircraft. *IEEE Transactions on Transportation Electrification*, 1(1).
- [13] **Boucher, J. B.** (1984). History of Solar Flight. *AIAA/SAE/ASME 20th Joint Propulsion*. Cincinnati, Ohio .

- [14] **Masson, P.** (1906). Albert Tissandier. *La Nature*, 1738, 256.
- [15] **Moulton, R.** (1973). An electric aeroplane. *Flight International*, 104(3378), 946.
- [16] **Marzinzik, G.** (october 2003). Flugbericht Antares: Den Sternen schon sehr nah. *Aerokurier*(10), 50-53.
- [17] **Electric Aircraft Corporation.** (april 22, 2020). (ElectraFlyer) april 22, 2020 tarihinde <http://www.electraflyer.com> adresinden alındı
- [18] **Tomazic, T., Plevnik, V., Veble, G., Jure, T., Popit, F., Kolar, S., Langelaan, J. W.** (2011). Pipistrel Taurus G4: on Creation and Evolution of the Winning Aeroplane of. *Journal of Mechanical Engineering*, 57(12), 869-878,.
- [19] **Schumann, L., Geinitz, S., & Nitschmann, R. V.** (2012). e-Genius – Elektroflugzeug in CFK -Bauweise. *Fachtagung Carbon Composites*. Augsburg, Germany.
- [20] **Felder, J. L., Kim, H. D., & Brown, G. V.** (2009). Turboelectric Distributed Propulsion Engine Cycle Analysis for Hybrid-Wing-Body Aircraft. *47th AIAA Aerospace Sciences Meeting Including The New Horizons Forum and Aerospace Exposition*. Orlando, Florida.
- [21] **A. R. Gibson, D. Hall, M. Waters,, B. Schiltgen, T. Foster, J. Keith, & P. Masson.** (2010). The Potential and Challenge of TurboElectric Propulsion for Subsonic Transport Aircraft. *48th AIAA Aerospace Sciences Meeting Including the New Horizons Forum and Aerospace Exposition*. Orlando, Florida.
- [22] **E. M. Greitzer, Hollman, J. S., & Lord, W. K.** (2010). *N3 Aircraft Concept Designs and Trade Studies, Final Report*. Cleveland, Ohio: NASA Glenn Research Center, NASA CR-2010-216794,.
- [23] **L. Lorenz, H. Kuhn, & A. Sizmann.** (2013). *Hybrid Power Trains for Future Mobility*. Stuttgart, Germany: 62. Deutscher Luft- und Raumfahrtkongress.
- [24] **C. Pornet, C. Gologan, P. C. Vratny, A. Seitz, O. Schmitz, A. T. Isikveren, & M. Hornung.** (2013). Methodology for Sizing and Performance Assessment of Hybrid Energy Aircraft. *Aviation Technology, Integration, and Operations Conference*. Los Angeles, California.
- [25] **Pornet, C., Gologan, C., vratny, P. C., Seitz, A., Schmitz, O., Isikveren, A. T., & Hornung, M.** (2015). Methodology for Sizing and Performance Assessment of Hybrid Energy Aircraft. *Journal of Aircraft*, 52(1), 341-351.
- [26] **Droney, & Bradley, M. K.** (2011). *Subsonic Ultra Green Aircraft Research: Phase I Final Report*. Hampton, Virginia: NASA Langley Research Center.
- [27] **Kluge, R.** (September 2013). E-Star, E-Fan, E-Thrust, Auf dem Weg zum Elektrischen Luftverkehr. *FliegerRevue - Special Triebwerke*(9), 30-31.
- [28] **Stuckl, S., Vantoor, J., & Lobentanzer, H.** (2012). *VoltAir – The All Electric Propulsion Concept Platform – A Vision for Atmospheric Friendly*

Flight. Brisbane, Australia: 28th International Congress of the Aeronautical Sciences (ICAS).

- [29] **Andrade, L., & Tenning, C.** (July 1992). Design of Boeing 777 electric system. *IEEE Aerospace and Electronic Systems Magazine* , 7(7), 4-11.
- [30] **Masson, P., & Luongo, C.** (2007). *HTS Machines for Applications in All-Electric Aircraft*. Tampa, Florida: IEEE Power Engineering Society General Meeting.
- [31] **Haldar, P., Ye, H., Efstathiadis, H., Reynolds, J., Hennessy, M. J., Mueller, O. M., & Mueller, E. K.** (June 2005). Improving performance of cryogenic power electronics. *IEEE Transactions on Applied Superconductivity* , 15(2), 2370-2375.
- [32] **Brown, G. V.** (2011). *Weights and Efficiencies of Electric Components of a Turboelectric Aircraft Propulsion System*. Orlando, Florida: 49th AIAA Aerospace Sciences Meeting including the New Horizons Forum and Aerospace Exposition.
- [33] **Balakrishnan, J.** (2007). Fuel cell technology. *IEEE*. Melbourne, VIC, Australia.
- [34] **H. J. Bergveld, W. K.** (2002). *Battery Management Systems: Design by Modelling*. Luxemburg: Springer Netherlands.
- [35] **Wohlfahrt-Mehrens, A. J.** (2007). Overview on current status of lithium-Ion batteries. 2. *International Renewable Energy Storage Conference*. Bonn, Germany.
- [36] **Jossen, A., & Weydanz, W.** (2019). *Moderne Akkumulatoren richtig einsetzen*. German: Cuvillier Verlag.
- [37] **Hufnagel, W.** (1988). *Aluminium-Taschenbuch*. German: Düsseldorf : Aluminium-Verlag.
- [38] **Weber, C., & Farrell, R.** (2009, DOE Cooperative Agreement Number DE-FC36-03GO013301). *High Temperature Superconducting Underground Power Cable [The "Albany Cable Project"]* . New York: SuperPower, Inc.
- [39] **Hofmann, P.** (2010). *Hybrid vehicles An alternative drive system for the future*. Vienna, Austria: Springer .
- [40] **Dudley, M.** (2010). *Promising Electric Aircraft Drive Systems*. Oshkosh, Wisconsin: EAA Electric Aircraft World Symposium.
- [41] **Maamoun, A., Alsayed, Y. M., & Shaltout, A.** (2013). Fuzzy Logic Based Speed Controller for Permanent-Magnet Synchronous Motor Drive. *IEEE International Conference on Mechatronics and Automation*, 1518-1522.
- [42] **Kamel, H. M., Hasanien, H. M., & Ibrahim, H. E.** (2009). Speed Control of Permanent Magnet Synchronous Motor Using Fuzzy Logic Controller. *IEEE International Electric Machines and Drives Conference*, 1587-1591.
- [43] **Karakaya, A., & Karakas, E.** (2007). PERFORMANCE ANALYSIS OF PM SYNCHRONOUS MOTORS USING FUZZY LOGIC AND SELF

- [44] **Kamel, T., Abdelkader, D., & Said, B.** (2015). Vector control of five-phase permanent magnet synchronous motor drive. *4th International Conference on Electrical Engineering (ICEE)*,
- [45] **Xue, S., & Wen, X.** (2005). Simulation analysis of two novel multiphase SVPWM strategies. *IEEE International Conference on Industrial Technology*, 1337-1342.
- [46] **Chen, H.-C., Hsu, C. H., & Chang, D. K.** (2014). Position sensorless control for five-phase permanent-magnet synchronous motors. *IEEE/ASME International Conference on Advanced Intelligent Mechatronics*, 794-799.
- [47] **Hosseyeni, A., Trabelsi, R., & Mimouni, M. F.** (2018). Comparative study of Sliding Mode Control and Vector Control in a Five-Phase Permanent Magnet Synchronous Motor Drive. *15th International Multi-Conference on Systems, Signals & Devices (SSD)*, 1363-1368.
- [48] **Kesraoui, H., Echeikh, H., Iqbal, A., & Mimouni, M. F.** (2019). Five-Phase Permanent Magnetic Synchronous Motor Fed by Fault Tolerant Five Phase Voltage Source Inverter. *International Journal of Electrical and Computer Engineering (IJECE)*, 6(5), 1994-2004.
- [49] **Parsa, L., & Toliyat, H. A.** (2007). Sensorless Direct Torque Control of Five-Phase Interior Permanent Magnet Motor Drives. *IEEE TRANSACTIONS ON INDUSTRY APPLICATIONS*, 43(4), 952-959.
- [50] **Si, X., & Wang, J.** (2010). A Vector-control System Based on Fuzzy Self tuning PID controller for PMSM. *International Conference on E-Product E-Service and E-Entertainment*. Henan, China.
- [51] **El-Sharkawi, M. A., El-Samahy, A. A., & El-Sayed, M. I.** (Jun 1994). High performance drive of DC brushless motors using neural network. *IEEE Transactions on Energy Conversion*, 9(2), 317-322.
- [52] **Saad, B., Salim, C., & Khodja, D. E.** (2018). Application of Hyper-Fuzzy Logic Type -2 in Field Oriented Control of Induction Motor with Broken Bars. *IOSR Journal of Engineering (IOSRJEN)*, 8(5).

RESUME

Name Surname: Abdel Rahman Beyrouti

Place/Date of Birth: Tripoli, Lebanon

Phone: +90 55 2328 6905

Email: abdel.beyrouti@gmail.com

Education:

2015-2018: Bachelor Electrical Engineering from Lebanese International University

2018-2020: Master Degree Electrical and Electronics Engineering from Istanbul Aydin University

Languages:

- Arabic Language: Mother tongue

-English: Advanced

-Turkish: Intermediates

-French: Intermediates

-German: Intermediates

Skills:

Analytical, Collaborating, Optimistic, Hard Working, Well Organized, Confident, Team playing & Interpersonal skills.

Computer skills: MS Office and MS Excel / (ICDL) - International Computer Driving License